UNIVERSITA' DEGLI STUDI DI VERONA

DEPARTMENT OF

BIOTECHNOLOGY

GRADUATE SCHOOL OF

NATURAL SCIENCES AND ENGINEERING

DOCTORAL PROGRAM IN

BIOTECHNOLOGY

Cycle / year **XXXIII /2021**

TITLE OF THE DOCTORAL THESIS

$FePO_4$ NANOPARTILCES AS SOURCE OF NUTRIENTS: EFFECTS ON THE PLANT-SOIL SYSTEM AND EVIDENCE FOR A SAFE AND SUSTAINABLE NANO-FERTILIZATION

S.S.D. AGR/13

Coordinator: Prof. **MATTEO BALLOTTARI**

Tutor: Prof. **ZENO VARANINI**

Doctoral Student: Dott. **ANDREA CIURLI**

FePO4 NANOPARTILCES AS SOURCE OF NUTRIENTS: EFFECTS ON THE PLANT-SOIL SYSTEM AND EVIDENCE FOR A SAFE AND SUSTAINABLE NANO-FERTILIZATION

Andrea Ciurli

Tesi di Dottorato

Verona, 10 Febbraio 2021

ABSTRACT

$FePO_4$ nanoparticles as source of nutrients: effects on the plant-soil system and evidence for a safe and sustainable nano-fertilization

In the last decade, nanotechnology became a consistent part of the technological progress in modern agriculture, with applications in agri-food technology, nano-biosensoring, plant defence and plant nutrition. Nanomaterials which can provide one or more macro/micro-nutrient to the plant are commonly referred as nanofertilizers. Nevertheless, in the scientific literature there are still few evidence of a successful utilization of nanomaterials as fertilizers. In a previous work, it has been shown that iron phosphate ($FePO_4$) nanoparticles (NPs) can provide either iron (Fe) or phosphate (P) to plants grown in hydroponic. The present study is aimed to highlight the effect of $FePO_4$ NPs used as nanofertilizer in the whole plant-soil system, and to determine if they can represent a safe and effective alternative to conventional fertilizers. To investigate the plant early transcriptomic responses to $FePO_4$ NPs exposure, microarray expression analyses have been performed in maize and cucumber roots grown in hydroponic for 24 hours. Responses of the plants treated with $FePO_4$ NPs were shown to be associated mainly to biotic and abiotic stress, cell wall modulation and regulation of transcription, and triggered a different pattern of responses that was dependent on the nano-size. To evaluate the possibility to apply $FePO_4$ NPs to the soil as fertilizer, two different bare soils were treated. Soil enzyme activities, CO_2 respiration and DGGE analyses showed that there was not negative impact of $FePO_4$ NPs onto soil microbial community and metabolic functions, neither toxic effects. Further, $FePO_4$ NPs provided available P in bare soil in respect to triple superphosphate (TSP), even though the efficacy was dependent on the soil characteristics. Moreover, $FePO_4$ NPs represented a source of available P for plant, which grown in soil in controlled condition without significant differences in respect to TSP, although P availability in the bare soil resulted lower for NPs than TSP. Microbial community associated to rhizosphere was not negatively affected by NPs and a stimulatory effect on enzyme activity was observed. In this work it was shown that $FePO_4$ NPs can be applied to the soil without any negative consequence for the environment, enhancing plant growth and providing nutrients. These results encourage the hypothesis that the nanoparticulate nature of fertilizers could contribute to rationalize the chemical inputs in agriculture and increasing nutrient use efficiency.

RIASSUNTO

Impiego di nanoparticelle di $FePO_4$ come fonte di nutrienti: effetto sul sistema suolo-pianta ed evidenze per una nano-concimazione sicura e sostenibile.

Nel corso dell'ultima decade le nanotecnologie sono diventate parte sempre più integrante delle moderne pratiche agricole, trovando applicazione nel settore agroalimentare, nella costruzione di nano-biosensori ambientali, nella difesa e nella nutrizione delle piante. I nanomateriali in grado di fornire alle piante uno o più macro o micronutrienti sono generalmente chiamati nanofertilizzanti, ma in letteratura le evidenze di una loro efficace applicazione in campo sono ancora scarse. In un lavoro precedente è stato dimostrato che le nanoparticelle (NPs) di fosfato ferrico ($FePO_4$) sono in grado di fornire sia fosforo (P) che ferro (Fe) a piante cresciute in idroponica. Il presente studio ha lo scopo di valutare l'effetto del $FePO_4$ in forma nanoparticellare ($FePO_4$ NPs) sul sistema suolo-pianta, e di determinare se esse possano essere utilizzato come alternativa ai fertilizzanti convenzionali in maniera sicura ed efficace. Al fine di valutare la risposta trascrittomica precoce delle piante all'esposizione delle nanoparticelle di $FePO_4$, si sono condotte analisi di espressione genica tramite *microarray* su piantine di mais e cetriolo cresciute in idroponica per 24 ore. I risultati ottenuti hanno evidenziato una risposta prevalentemente associata allo stress biotico e abiotico, rimodulazione della parete cellulare e regolazione della trascrizione, con specificità che dipende dalla forma nanoparticellare o non-nanoparticellare (*bulk*), del $FePO_4$. Per valutare la possibilità di utilizzare le nanoparticelle di $FePO_4$ come fertilizzanti in suolo sono stati trattati due suoli differenti. Le analisi delle attività enzimatiche, dell'evoluzione della CO_2 e della struttura della comunità microbica tramite DGGE non hanno evidenziato alcun effetto negativo o tossico sul microbioma del suolo. Inoltre, si è dimostrato che le nanoparticelle di $FePO_4$ sono una fonte di P disponibile in suolo anche se l'efficacia dipende dalle caratteristiche del suolo utilizzato. Inoltre, le piante cresciute in suolo in vaso con nanoparticelle di $FePO_4$ come fonte di P presentavano una crescita uguale a quelle fertilizzate con perfosfato triplo (TSP), sebbene vi fossero state differenze significative nell'analisi del P disponibile fornito dai due diversi concimi in suolo nudo. La comunità microbica dell'ambiente rizosferico non è stata negativamente influenzata dal trattamento con nanoparticelle, piuttosto si è evidenziato un effetto stimolante su certe attività enzimatiche. Nel presente studio, si è dimostrato che le nanoparticelle di $FePO_4$ possono essere applicate sul suolo senza conseguenze negative, incrementando la crescita delle piante e apportando nutrienti. I risultati ottenuti suggeriscono che la natura nanoparticellare dei fertilizzanti potrà contribuire a razionalizzare il loro impiego in maniera più mirata e ad incrementare l'efficienza di utilizzo dei nutrienti.

INDEX

1. INTRODUCTION

1.1 Introduction: trends in modern agriculture

Since the Green Revolution of the 1960s, the use of fertilizers in modern agriculture became crucial, dramatically increasing the availability of nutrients for crop and generally the food production. The current world population of 7.8 billion is expected to reach 8.5 billion by 2030, 9.7 billion in 2050, and 11.2 billion in 2100 (Marchiol et al., 2020 (Fig 1.1). To face the fast growth of population and the continuous increase in food demand, the use of fertilizers will become more and more indivisible from the modern farming practice in agriculture. The world potential balance of ammonia (NH_3) for nitrogen (N), phosphoric acid (H_3PO_4) for phosphorus (P) and potash (K_2O) for potassium (K) has been calculated by FAO (United Nation, 2015) as maximum achievable production (supply) minus total demand of these compounds (including fertilizer and other uses demands) (Fig.1.2). Forecasts provided by FAO/Fertilizer Outlook Expert Group meeting held in 2019 estimated demand of 200.919 tonnes of

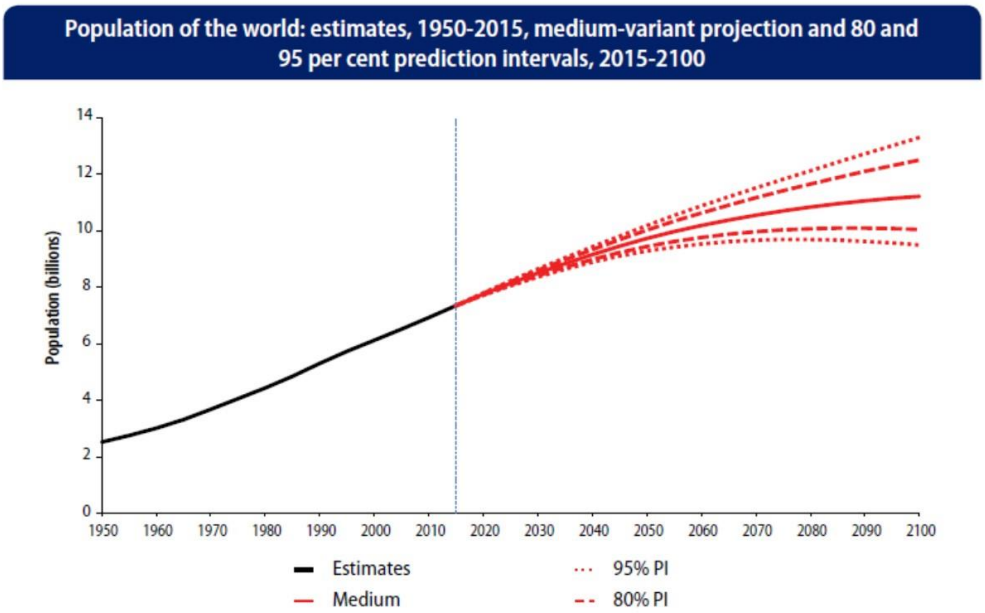

Figure 1.1. World population estimated growth until 2100. Prediction intervals are shown: 95% PI express the uncertainty range that has the 95 percent of probability to occur, as well as 80% PI. (United Nations, Department of Economic and Social Affairs, Population Division, 2015. World Population Prospects 2015 – Data Booklet (ST/ESA/SER.A/377).

N, P and K as fertilizers in 2022 and a maximum achievable production (indicated as supply) of 269.482 tonnes. Potential balance is globally expected to decrease, meaning an ever-greater gap between demand and supply, becoming increasingly difficult to fill. Since early 1900s, the emergence of the large-scale N fertilizer industry based on Haber-Bosch process allowed a virtually unlimited production of ammonia, even if not without consequences on the environment (FAO and IWMI, 2018). Moreover, energy is essential to produce N fertilizers, and the industrial production involves the use of fossil fuels (Mudahar & Hignett, 1985). On the other hand, world resources of P are very limited, consisting of non-renewable sources such as phosphorites; thus, P should

be used as efficiently as possible in order to face the constantly growing demand of P-fertilizers resources and to maintain and increase, where necessary, agricultural productivity (FAO and IWMI, 2018).
Over-application of fertilizers is not only unaffordable because of the limited sources,

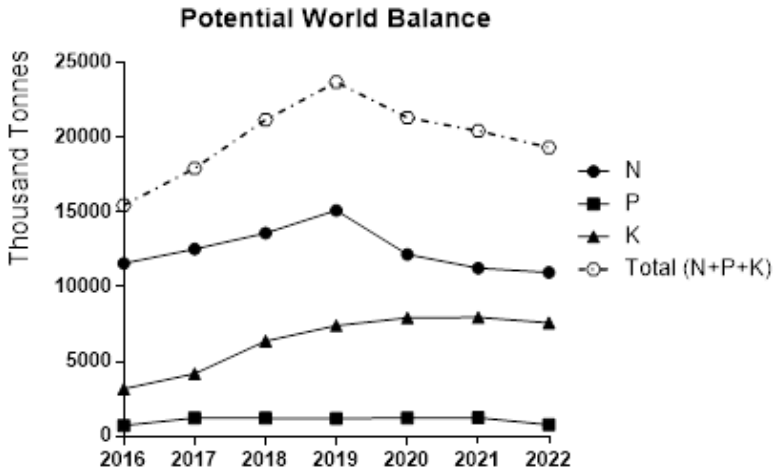

Figure 1.2. Potential world balance of nitrogen, phosphorus, and potassium, calculated as supply (fertilizer uses + other uses demand) in 2016-2022 (thousand tonnes). Data plotted from FAO. 2019. World fertilizer trends and outlook to 2022. Rome

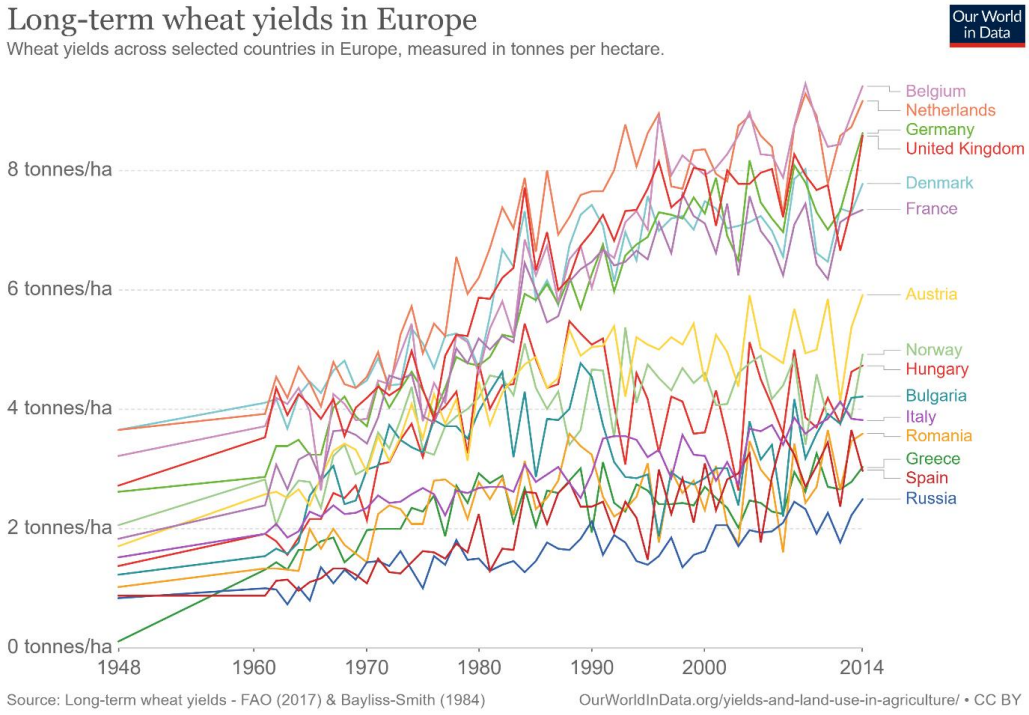

Figure 1.3 Wheat yields in Europe, measured in tonnes per hectare (https://ourworldindata.org/crop-yields). Data from prior to 1961 is sourced from Bayliss-Smith & Wanmali (1984). Understanding Green Revolutions: Agrarian Change and Development Planning in South Asia. Data from 1961 onwards are as reported by the UN Food and Agricultural Organization (FAO) from its FAOstat database.

but such an increase of crop production per land (Fig 1.3) has unmeasurable costs in terms of environmental impact such as water eutrophication and toxicity, groundwater

pollution, air pollution, soil quality degradation, risks to humans, animal and soil health and further, in the long time, the ecosystems change (Kummu et al., 2012). Moreover, intensive agriculture has a tremendous negative impact on water availability. Water shortage in many countries in the world is due to the physical lack of the resource and the worsening of water quality, leading to a reduced quantity of safe and potable water. Human settlements, industries, and agriculture are all sources of water pollution but, in many countries, agriculture is the biggest polluter (Hawkesford et al., 2014). Although livestock remains the most pollutant sector of agriculture, more rational use of fertilizers for crop cultivation will be fundamental to reduce nutrient source depletion, prevent environmental impact from irrigation water and face the challenge of an increasing population and food quantity and quality demand (Baligar et al., 2001). A so high yield obtained in post-Green Revolution agriculture depends, and will ever more depend, on fertilizer additions. Nevertheless, fertilizers applied in excess reflect in an inefficiency that leads to a negative impact for the environment. To outflank environmental effects from agriculture, nutrient use efficiency (NUE) must be increased. NUE is a measure of how well plants use the available mineral nutrients and can be defined as yield (biomass) per unit input (Marschner, 2011). Apart from climate conditions, there are three main factors that concur to NUE and on which we can act to implement it: (i) soil factors, that depend on soil physical and chemical characteristics of the soil; (ii) fertilizers factors, that include source, rate, method of application, and presence of amendments; (iii) plant factors, accounting for specie, variety, genotypes and all the environment conditions that affect the ability of plants to acquire and absorb nutrients (Baligar & Fageria, 2015). Considering fertilizers, elements that are fundamental for plant growth can be distinguished into macro- and micronutrients. Generally, macronutrients (N, P, K, S, Ca, Mg) account for the 0.2%–4.0% of the total dry biomass of the plant, while micronutrients (B, Fe, Mn,Cu, Zn, Mo, Cl) are lower than 0.01% (Monreal et al., 2016). In an agroecosystem, NUE of crop plants for macronutrients is lower than 50% due to physic-chemical soil properties, leaching, gaseous losses and fertilizer characteristics (Chen et al., 2018), while for micronutrient it is frequently lower than 5% (Marchiol et al., 2020). Retarding or even controlling the release of nutrients into soil is one of the strategies to increase NUE. Several innovative fertilizers have been employed in the recent years to achieve this aim: for instance, the use of coating materials to engineer fertilizers permitted a retarded nutrient release and increase fertilizer-use efficiency, while agriculture residues were engineered to be applied in soil as fertilizers and soil improvers, such as biochar (Liu & Lal, 2015). So, crop fertilization efficiency must be improved to avoid nutrient losses and synchronize the release of nutrients with their uptake by crops. Among the emerging technologies of the last decade, the use of nanotechnology in agriculture is regarded as one of the most promising approaches to significantly increase crop production limiting the negative effects on the environment (Duhan et al., 2017).

1.2 Nanotechnology in agriculture

Nanotechnology is often described as a recent promising field of research, but its origin can be accounted to the last century in the occasion of the famous lecture held by Richard Feynman in 1959 "*There's Plenty of Room at the Bottom*", in which he displayed the possibility and potentiality of Nano sized materials (Feynman, 1960). Anyway, through the last years nanotechnology has been successfully used into many fields,

such as chemistry, physics, pharmacology and medicine and the promising results obtained suggested the possibility to extend its application to agriculture (Raliya et al., 2018). Nanotechnology is defined as the science and manipulation of small sized materials in the range of nanometer (nm), typically between 1 and 100 nm for at least one dimension; nanomaterials may exhibit physical properties significantly different from

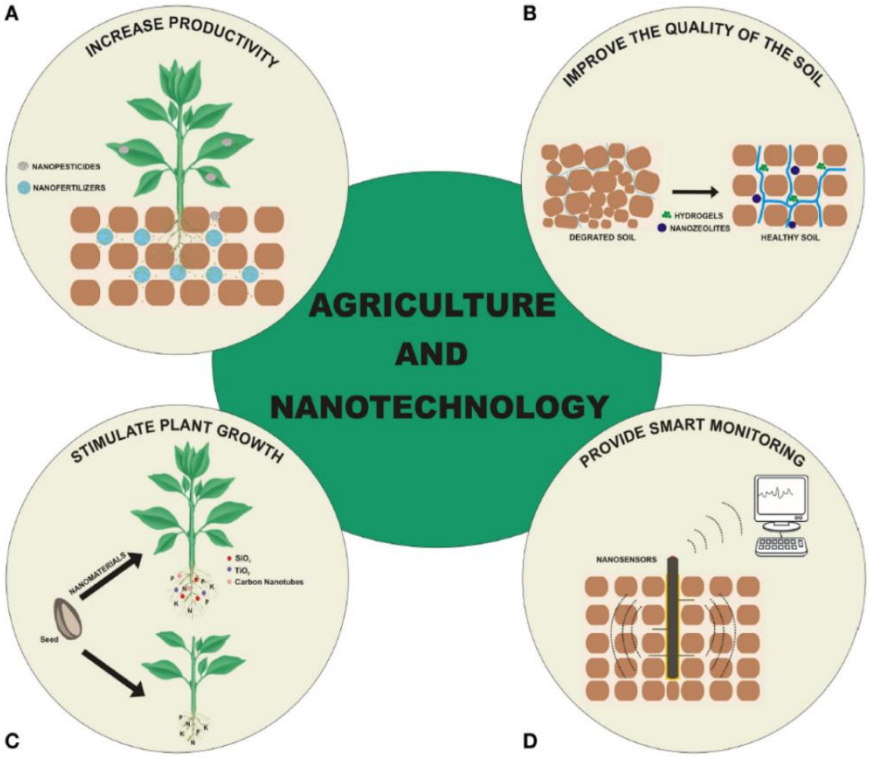

Figure 1.4. Potential roles of nanotechnology in agriculture summarized by L.F. Fraceto et al (2016). Nanotechnology can A) increase productivity being applied in plant nutrition as nanofertilizers and in plant defense as nanopesticides; B) improve and fix the quality of degraded soils by means of nanozeolites or hydrogel that helps to constitute new hydric reservoirs; C) stimulate the plant growth using biostimolant materials (the inclusion of this application among nanofertelization often depends on the literature considered and on the author); D) Provide smart monitoring using nanosensors in communication with digital devices.

that of non-nanomaterial counterpart (bulk) (Fraceto et al., 2016; Khan et al., 2019). Nanomaterials possess a large amount of surface atoms per volume units. The ratio of surface atoms to interior atoms dramatically increases while the diameter of nanoparticles reduces, as well as the total surface energy increases with the overall surface area. Such exponential increase can explain why physical-chemical properties of nanomaterials may be so different to the bulk (Cao, 2004). Peculiar characteristics of nanomaterials make them more reactive in the environment. This is the carrying idea under the use of nanotechnology in precision agriculture, that now a day moves toward the reduction of inputs and wastes in the face of sustainability (Duhan et al., 2017). Nanotechnology in agriculture can find application as (Fig 1.4):

(i) Nanopesticides; nanoparticles or nanoencapsulated active compounds that can protect crops from pathogen and allow higher shelf-life to active ingredients.

(ii) Nanofertilizers: nanomaterials that can provide one or more macro- or micronutrients to the plant, or that improve the capability of plants to uptake other nutrients. In the latter category can be cited also carbon nanotubes or metal oxide nanoparticles

that, in specific sizes and concentration, can act as biostimulants or enhance the uptake of other elements. (iii) Nanosensors: nanotubes, nanowires, or nanocrystals for monitoring physico-chemical properties in difficult spots to reach. They can also be part of sensing elements having similar size. (iv) Nanosized compounds as improvers of soil quality: hydrogels, nanoclays and nanozeolites that can enhance water holding capacity of the soil acting as slow-release source of water, or organic nanopolymers and inorganic and metal oxide that can absorb environmental contaminants from the soil and might be used in soil remediation (Marschner, 2011).

1.2.1 Nanofertilizers

Since this thesis work deals with the use of $FePO_4$ nanoparticles ad nutrient-bearing substances for plants, the following sections of the introduction will be focused on nanofertilizers. As said above, nanomaterials can be more reactive for their higher surface energy, but they can also hold the molecules together more strongly than conventional solid formulations (Liu & Lal, 2015). The efficacy of slow-release nanofertilizers derives from two aspects of the nano form. To uptake nutrients, plants create a water potential gradient between the soil and the plant root surface, because of plant transpiration. Soil solution is gradually depleted of nutrients, so ions can move with the water flux by diffusion toward root surface, moving from a higher concentrated area to a low concentrated one. (Achari & Kowshik, 2018; Christian et al., 2008; Subramanian et al., 2015). Nanoparticles have higher dissolution rate in the soil solution than their non-nano (bulk) forms, therefore in this condition they can dissolve easily and thus become more available for plants (Achari & Kowshik, 2018). On the other hand, nanoparticles' high surface area leads to an increased sorption capacity, so they can be adsorbed onto soil colloids and act as reservoirs of functional ions that can be drew only when plants actively create the water flux to move ions (Kah et al., 2018). Therefore, nanoparticles applied to the soil can undergo biotransformation after interaction with organic materials and root exudates and by means of these being absorbed by the plant (Berendsen et al., 2012). These aspects of nanofertilizers could avoid the conversion of solid low-soluble formulations into biologically unavailable forms and the leaching in the groundwater of nutrients applied to the soil as liquid formulations.
Concerning the role of the nanomaterials and the element provided, we can separate nanofertilizers into three different categories: (i) nanomaterials made of macronutrients, (ii) nanomaterials made of micronutrients, and (iii) nanomaterials acting as carriers for nutrients (Marchiol et al., 2020). The first two categories refer to nanomaterials

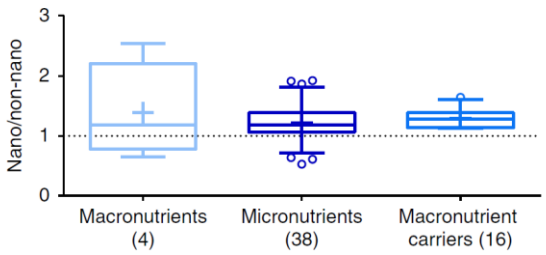

Figure 1.5. Relative efficacy between nanofertilizers and their conventional analogues by selecting one parameter for germination. The numbers in parentheses indicate the number of comparisons considered in each box. (Kah et al., 2018)

as nutrient themselves, while in the third category are often grouped nano-delivered nutrients, where the nanomaterials do not represent the nutrient *per se*. Kah et al (2018) provided a meta-analysis of 29 studies from 16 papers allowing comparisons of efficacy for nanofertilizers and non-nano fertilizers prior to 2018. They compared the relative efficacy between a nanofertilizer and its conventional analogues. Efficacy was calculated by selecting one representing parameter for germination growth or crop yield. The median efficacy gain of nanofertilizers over conventional fertilizers was between 18 and 29% for the examined category (Fig 1.5). This comparison demonstrated that there was an actual increase of efficacy given by the use of nanomaterials in respect to conventional analogues, but also demonstrates that there is still a high variability of obtained results that strongly depends on the experimental design. As the authors underlined, the quality and amount of data on comparisons between nano and conventional fertilizers is still insufficient to support a robust comparative analysis on the true efficacy of the employed nanofertilizers.

1.2.2 Nanomaterials in the soil and ecotoxicology aspects

The soil in which plants live and grow is inhabited by a wide diversity of microorganisms that are commonly referred as microbial community. Soil microbial communities represent the greatest resource of biodiversity known in the world, entailing interactions that make soil a heterogeneous and discontinuous system whose function and ecology are highly dynamic in time and space (Nannipieri et al., 2003) (Fig. 1.6). Soil microorganisms include bacteria, fungi and algae that concur to enzymatic degradation of the complex organic substances to mineral elements, and therefore are responsible, with pros and cons, to plant development. Of particular interest in plant nutrition is the rhizosphere, that is defined as the closest zone to the root, and the area whose ecological conditions in soils influence - and are influenced by - root secretions and plant activity. Rhizosphere is also the region of the soil in which metabolic activity and biological diversity are higher than in the surrounding soil. For this reason, the peculiar conditions observed in the rooting zone are referred as rhizosphere effect (Pastorelli

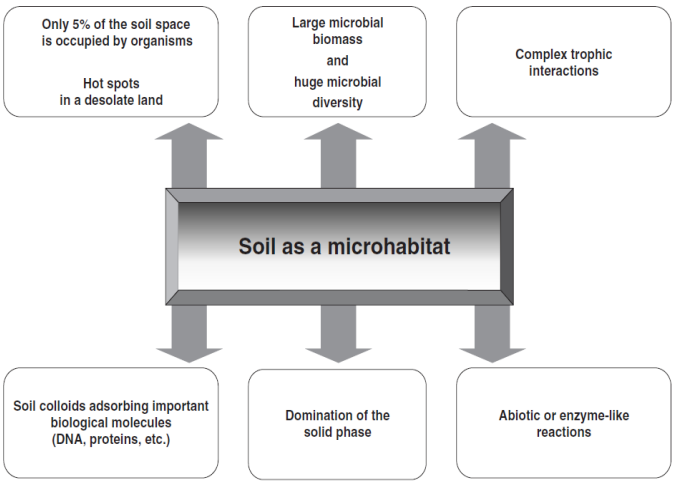

Figure 1.6. Schematic representation of the main characteristics of a soil microhabitat (Nannipieri et. al 2003)

& Landi, 2009). Soil can be defined a 4-dymensional object, that can vary in space (depth, surface) and time. In soil science, revealing the diversity of soil samples is a critical point. The use of DNA as a marker molecule to assess microbial diversity in soil gives a higher resolution in microbial taxonomy than other techniques (Nannipieri et al., 2020), and through molecular fingerprinting techniques, such as Denaturing Gradient Gel Electrophorese (DGGE), is possible to determine the diversity and dynamics of soil microbial communities in space and time (Pastorelli & Landi, 2009).

Nanomaterials in the environment are not novel: natural nanomaterials are commonly present on earth, and they can have interstellar origin, or originate from biogenic, geogenic and atmospheric processes (Pachapur et al., 2015). Studies on ecotoxicity of nanomaterials relatively scarce in number and difficult to compare. Some experiments indicate that certain nanoparticles, for instance metal oxides as zinc oxide (ZnO) and titanium oxide (Ti_2O) and fullerenes, are toxic for a variety of organisms even in low amounts (Rana & Kalaichelvan, 2013). Toxicity of nanoparticles was shown to be linked to their surface area, thus they higher reactivity. Consequently, even small masses of a nanoparticulate compound could have major toxic effects because of their larger overall surface (Handy et al., 2008). Mobility is the ability of a nanoparticle to move from a site to another, for example from a contaminated soil to an uncontaminated one, or from the soil to the ground water, and represent a critical aspect of nanomaterial's toxicity. Mobility is strongly dependent on the stability of a nanoparticulate dispersion (Norwegian Pollution Control Authority 2008). Nanoparticulate dispersion into water has a colloidal state, and nanoparticles can collide with each other by Brownian motion or shear flow, but do not stick together after the collision. Stability of a colloidal suspension, therefore, refers to the kinetic state that can lasts for long, but not to the thermodynamic state, that remains unstable (Norwegian Pollution Control Authority 2008). As result nanoparticles will always tend to separate or aggregate, even if in long time, depending on the surrounding environment and on the chemistry of the nanomaterial. Manufactured nanoparticles are often coated to prevent aggregation (Lin & Xing, 2008), so coating is one of the aspects to consider when evaluating the stability of a nanoparticles. Other aspects are surface charge and point of zero charge (PZC), which together can determine if a nanoparticle would be attached on charged surfaces depending or not to the pH of the solution. Crystallinity grade can also influence the stability of a nanomaterial (Ameen et al., 2021).
Nanotechnology is a fast-growing field of research that can present positive as well as negative aspects for environment. Evaluation from an ecotoxicological point of view of nanomaterials remains difficult to assess. Toxicity of nanoparticles depends on their property, test organism species, and surrounding solution conditions (Ray et al., 2009). Any evaluation will not be complete without considering the chemistry of the nanomaterial, the concentration and the surrounding environment conditions. Therefore, the evaluation risks of the application of nanofertilizers to the environment must be done considering the variables of each specific case.

1.2.3 Behaviour of nanomaterials in the plant

Plant uptake of nanoparticles is affected by different factors that depend on the nature of the nanoparticle itself, but also on the physiology of the plant. Nanoparticles are mostly limited by their size to enter and move inside the plant cells (Achari & Kowshik, 2018), that depends on their chemical-physical nature of the nanoparticles, but also on the surface coating of engineered nanoparticles. Morphology, in terms of shape and crystallinity, and chemical nature of nanoparticles can also influence plant uptake regarding their adhesion on foliar or root surface. Nanoparticles can enter the plant through the leaves or the roots. The primary barrier of leaves is cuticula. Cuticular pores are estimated to have a diameter of around 2 nm (Pérez-de-Luque, 2017) and most nanoparticles have a size range that is way higher than this exclusion limit, so it is unlikely that nanoparticles can significantly use this route. Nanoparticles could enter the leaves through stomata and move via symplastic route if under 50 nm of diameter, or apoplastic route if above 50 nm. Nanoparticles in a range of 20-50 nm can enter the root through root cell wall pores (Achari & Kowshik, 2018; Pérez-de-Luque, 2017). Some nanoparticles, such as metal oxides (ZnO) are known to induce formation of bigger pores into root walls and allow plant to uptake bigger size nanoparticles, hence a reason why phytotoxicity can occur (Navarro et al., 2008). In roots nanoparticles are transported mainly in the extracellular space between epidermal cells until they reach endodermal cells. Nanoparticles can cross the Casparian strip symplastically mainly via endocytosis and pore formation, reaching the central cylinder and loaded into phloem and xylem (Achari & Kowshik, 2018) (Fig. 1.7).

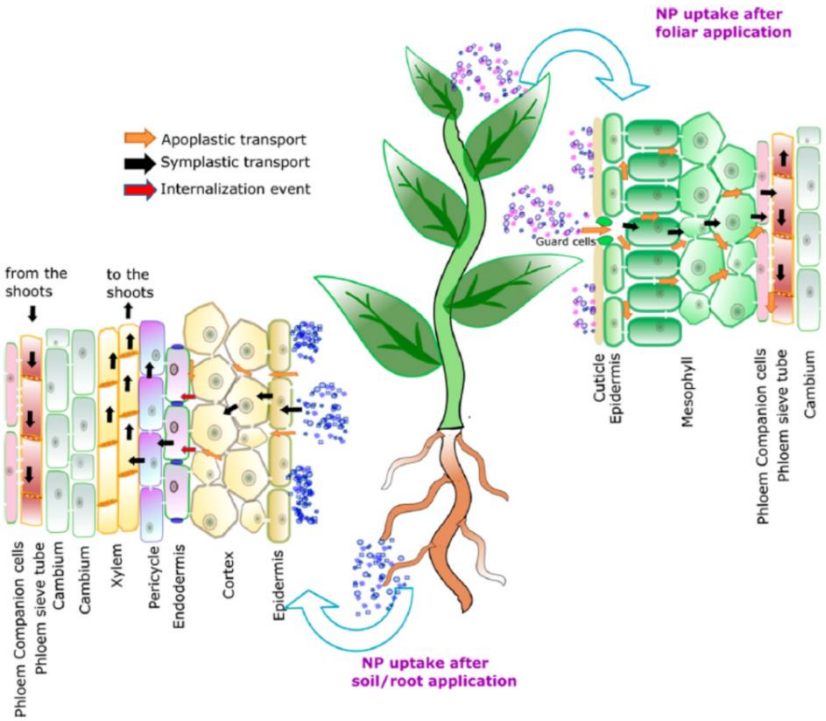

Figure 1.7. Schematic representation of nanoparticles uptake from roots and shoot in a dicotyledon plant. Nanoparticles enter mostly through stomata in leaves and through root pores in soil/root system. Nanoparticles entered in the leaves can move through the apoplastic and symplastic route to enter the phloem and to be transported toward roots and different plant parts. Nanoparticles entered the

epidermal cell roots mainly via the apoplast. When reaching the endodermis, they are first transported unidirectionally to the shoots via the xylem then back to the roots from the shoots via the phloem (Achari and Kowshik, 2018).

Leaf cuticle prevents the entry of most nanoparticles, as well as in root the epidermis and the Casparian strip can limit the penetration of nanoparticles. Thus, it is very likely that delivery efficacies of foliar and root direct application are low, although the efficiency of the foliar application was reported to be higher than that of the root application (Su et al., 2020). Sega et al (2019) showed that $FePO_4$ NPs do not directly enter the plant but remain onto the root surface and probably undergo a progressive dissolution process in order plant can absorb the nutrients. So, dissolution of a concretion of nanoparticles pooled on the root surface could be a mechanism by which nutrients present in nanofertilizers can be available for plant absorption. However, once nanoparticles enter a plant, remains largely unknown which effect the internal environment of the plant could have on their further transformation and transport. The total ionic strength (associated with inorganic ions) of the sap, high salinity and abundant organics are luckily to influence the aggregation, transport, and dissolution of nanoparticles (Su et al., 2020). Nevertheless, further investigations still have to be done in this field because they can give indications about which parts of the plant can be reached by nanoparticles, and where they might be stored.

1.3 Dynamics of nutrients in the plant-soil system

Plants require a wide range of factors to develop properly such as light, water, nutrients, CO_2, and their growth rate is strongly dependent by the availability of all these factors. The supply of any of these components can be increased from the deficiency level by environmental condition or, in case of agriculture, human practices. When a growth factor – or a nutrient – availability increases, response in terms of biomass yield increases too, but the other growth factors or nutrients become limiting for the plant growth. This relationship is mathematically known as the "law of diminishing yield

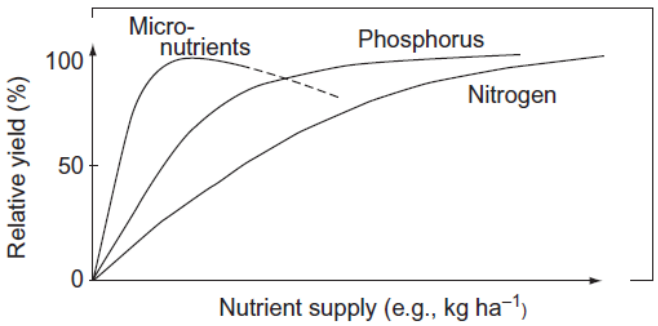

Figure 1.8. Typical yield response curve of Nitrogen, Phosphorus and Micronutrients (Marschner, 2011).

increment". According to this law, in terms of plant biomass yield, the response curve for a nutrient or a growth factor has an asymptotic trend (Marschner, 2011) (Fig. 1.8). However, this relation does not correctly describe the real scenario that occurs in the

soil. Yield response curves are strongly modulated by interactions between nutrients and other growth factors. When there is an abundant supply of nutrients, a point of inversion appears on the curve, as is possible to see in the figure 1.8 for micronutrients. The inversion can be caused by several factors, among which there are direct toxicity effect of an over-supplied nutrient or an induced deficiency of another one. Therefore, yield response curve is valid for low and sufficient concentrations. When concentrations exceed the tolerance and reach the toxicity threshold, relative yield start to decrease, so it is not only important the availability of one nutrient or factor itself, but rather a good balance between growth factor, according to the plant requirements.
Nutrients can be differentiated into two distinct groups: 1) macronutrients, which are required and are present in relatively high concentrations in plants; 2) micronutrients which are equally essential, but present in very much lower concentrations than macronutrients (Fig. 1.9).
According to Mengel and Kirkby (2001), nutrients required by the plant can be further divided into four groups:

1. C, H, O, N, and S that are the major constituents of proteins, enzymes, amino acids and nucleic acids and whose assimilation is linked to oxidation-reduction reactions.
2. P, B and Si that behave biochemically similarly and are uptake from the soil solution as anions or inorganic acids. In the cells they are bound to hydroxyl group of sugars to become esters.
3. K, Na, Ca, Mg, Mn, and Cl taken up by the soil solution as ions as well as they are present in cell compartments. They can have several unspecific functions.
4. Fe, Cu, Zn, and Mo mainly present in plants in chelated form and can serve, among the other functions, as electron transporters.

Element	Chemical symbol	µmol g^{-1} dw	mg kg^{-1}
Molybdenum	Mo	0.001	0.1
Nickel	Ni	0.001	0.1
Copper	Cu	0.1	6
Zinc	Zn	0.3	20
Manganese	Mn	1.0	50
Iron	Fe	2.0	100
Boron	B	2.0	20
Chlorine	Cl	3.0	100
Sulphur	S	30	1,000
Phosphorus	P	60	2,000
Magnesium	Mg	80	2,000
Calcium	Ca	125	5,000
Potassium	K	250	10,000
Nitrogen	N	1,000	15,000

Figure 1.9. List of micro and macro elements and their concentration and ppm content in plant (Marschner, 2011)

1.3.1 Phosphorus (P)

Phosphorus (P) is necessary as structural element, particularly into nucleic acids that compose DNA and RNA, and serves as carrier of energy. Phosphate participates into structuring of nucleic acid macromolecules by creating a bridge between ribonucleoside units. The amount of P in ribonucleic acids in respect to total organic P in the plant differs among tissues: in expanding leaves is higher because of the rapid protein synthesis that requires large amount of ribosomal RNA, whereas it is lower in senescent leaves. P is also a structural component in phospholipids in cellular membranes. In both these macromolecules, P serves as an essential source of charge for its anionic nature in the cellular environment, that for this reason can maintain a high cation concentration. Another critical role of cellular P is in energy transfer. Phosphate esters are intermediates in metabolic pathways of biosynthesis and degradation. The energy required for biosynthetic processes is mostly provided by coenzymes, such as Adenosine triphosphate (ATP). Moreover, the energy liberated by energy producing pathways, such as glycolysis and phase I of photosynthesis, can be transferred in the form of phosphoryl groups by ATP in phosphorylation reactions, playing a critical role into post-translational regulation of enzymes such as PEP carboxylase, mediated by protein kinases (Marschner, 2011). Therefore, due to its ubiquitous role into cellular functions, P availability for plants in their substrate is crucial for an optimal growth and, for crops, to ensure a satisfying biomass yield.

1.3.2 Behaviour of P in the soil-plant system

Phosphorus in the soil exists in inorganic or organic form. Inorganic phosphate can derive from primary P minerals such as apatites, strengite, and variscite. These minerals are very stable, and the release of available P by weathering is generally too slow to meet the crop demand, therefore in agro-ecosystems inorganic phosphate is generally provided through fertilization. Organic phosphate derives from organic matter as part of nucleic acid, phospholipids, inositole phosphates, and therefore, in the bulk soil, depends on the rate of mineralization of organic matter by soil microorganisms. Phosphate in soil has a very low solubility, low mobility, and high fixation by the soil matrix, which make this nutrient unique in its dynamic, so that the P use efficiency for plant has been accounted as the lowest for a macronutrient, often 10-15% of the applied P (Syers et al., 2008). Therefore, the availability of P to plants is mainly controlled by 1) spatial availability in terms of plant root architecture, taking in account the associations with mycorrhizas fungi, and (2) bioavailability based on the rhizosphere chemical and biological processes. Plant roots adapt themselves to their nutritional state by modifying the rhizosphere environment as result of various physiological activities, mostly the exudation of organic compounds such as organic acids, phosphatase enzymes, and specific signalling substances, which are able to trigger various rhizosphere processes. The chemical and biological processes occurring in the rhizosphere determine the mobilization and acquisition of soil nutrients and microbial dynamics, that indirectly reflects onto nutrient availability. Since phosphate has a so low solubility and mobility in soil, the uptake by root soon causes a depletion area in the rhizosphere causing a gradient concentration in a radial direction away from the root surface (Fig. 1.10). For all these reasons, P availability in the rhizosphere is mainly controlled by plant root

growth and physiology, nevertheless also highly related to soil characteristics such as structure, texture and not least the microbiome homeostasis and functions (Roberts & Johnston, 2015).

The concentration of phosphate in the soil solution is the first factor that determines its availability for plant roots. Soil buffering capacity is another important factor to consider when assessing P availability in a soil or another. P-buffer capacity is the rate at which P in soil solution is replenished, therefore the rate of desorption of P from the solid phase of the soil when the one that is in solution is depleted by plant uptake. P concentration in soil solution is estimated to range from 10^{-4} M (very high) to 10^{-6} M (deficient) and finally to as low as 10^{-8} M (in some very low-fertility tropical soils) (Syers et al., 2008). It has been shown that the main process that moves P toward the root surface is diffusion (Degryse & McLaughlin, 2014). Phosphate ions can diffuse when

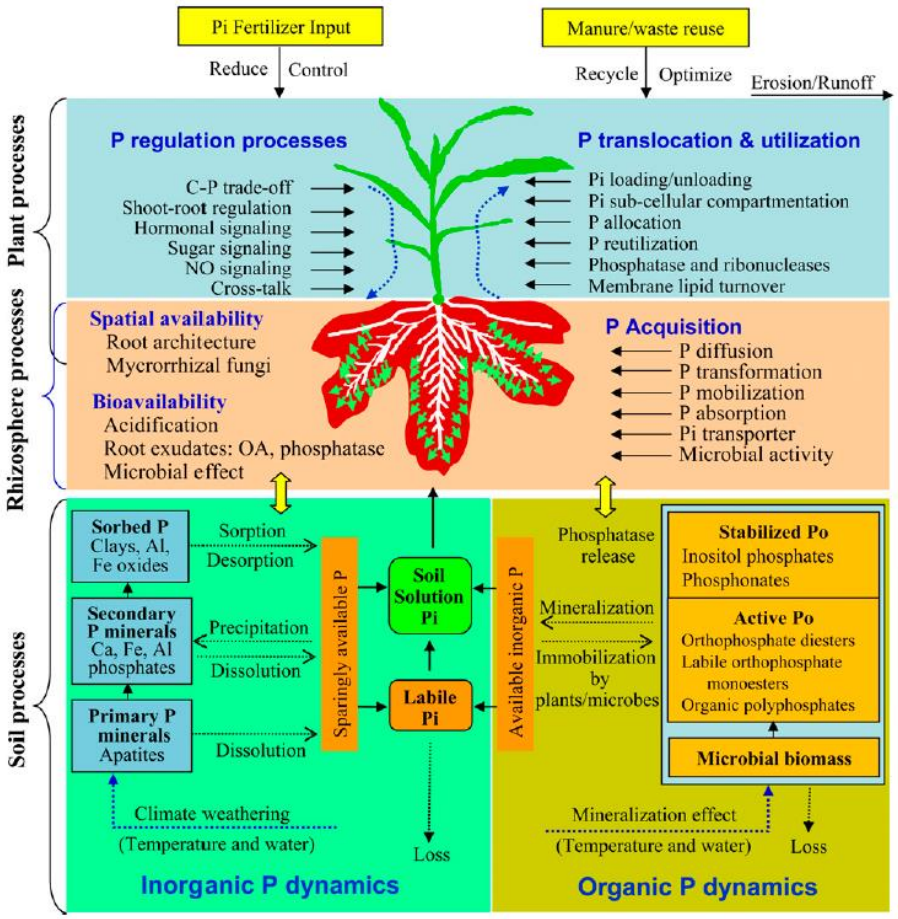

Figure 1.10. Schematic representation of phosphorus dynamic in soil (Shen et al, 2011)

a gradient of P concentration is created by the depletion of P in the rhizosphere caused by plant uptake. Diffusion rate for phosphate is very low, estimated to be at an average value of 1×10^{-13} $m^2 s^{-1}$, against a magnitude of 10^{-7} $m^2 s^{-1}$ for a nutrient such as nitrate (Oyewole et al., 2014; Syers et al., 2008). So, the movement of $H_2PO_4^-$ would be about 0.13 mm per day. Anyway, a variable that upstream of all the process has a deep impact on soil P solubility is pH. Depending on pH, two main "windows" of maximum P solubility occur in the soil at pH around 4.5 and 6.5 (Fig. 1.11). These two values co-incide with the lowest degree of P fixation by Ca, Al, and Fe minerals (Penn &

Camberato, 2019). The exact pH value of maximum phosphate solubility at which would exist the higher P availability for plant can vary depending on the soil characteristics, but in a general view a near-neutral pH is thought to maximize plant P availability. Phosphate in the soil-solution-plant system is often described as constituent of three different generic P-pools: non-labile P; labile P; solution P (Shen et al., 2011). Labile P is defined as the P held by the soil – mostly through anion exchange and sorption onto soil minerals – and available for plants only in relatively short time. P belonging to this pool must be released to solution before a plant root can uptake it, so when labile P-pool supplies solution P, labile P is in equilibrium with non-labile P that supplies the nutrient. Nevertheless, the three forms of P pools have different equilibrium K value, so the rate at which the labile P-pool equilibrates with solution P is faster than the equilibrium between the non-labile and labile soil P pools. The dynamic of these three pools in a soil is dependent by the soil properties and represents the main mechanism that relate P availability to soil pH.

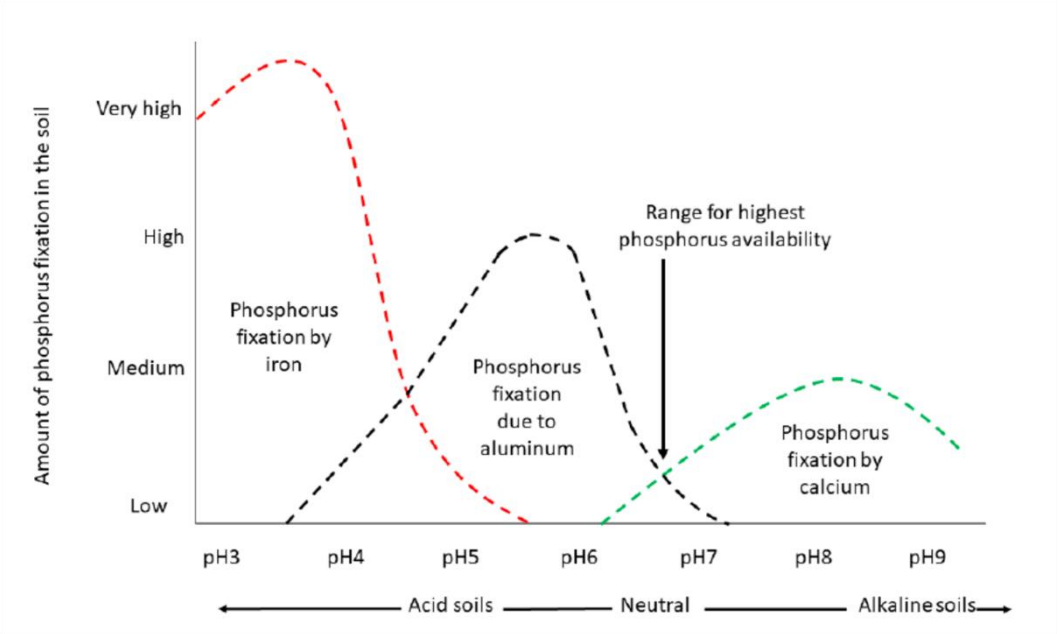

Figure 1.11 Representation of soil phosphorus availability impacted by pH and depending on the fixation of P in the soil by Fe, Al and Ca mineral, from Penn & Camberato (2019).

1.3.3 Mechanisms of P acquisition by plant roots

Plant roots induce chemical and biological adjustments in the rhizosphere environment which play a critical role in enhancing the bioavailability of soil P. These adjustments mostly involve: 1) the acidification of soil solution through proton extrusion by membrane ATPases-driven action; 2) exudation of carboxylate compounds and organic acids to mobilize labile-P by ligand exchange or chelation mechanisms; 3) extracellular secretion of phosphatase and phytase to hydrolyse P from organic matter (Vance et al., 2003). The combined action of these three mechanisms aims to maximize the solubilization of P by increasing soil-buffering capacity. A decrease in soil pH

would move the equilibrium of P fixation-solubilization toward the maximum solubilization. This mechanism is mainly evident into sub-alkaline and calcareous soils. The extrusion of organic acids, such as citrate by white lupin's cluster roots (Shen et al., 2003), can increase the availability of P by increasing the mechanisms of solubilization such as ligand exchange, ligand-promoted dissolution of P-bearing minerals such as Fe/Al oxides and changes in surface charges on clays and Al/Fe oxides. Plants can secrete phosphatase whose activities are up-regulated under P deficiency (Hasan et al., 2016; Cabugao et al., 2017). However, plant phosphatase production do not immediately determinate an higher P uptake in the plant, because the phosphohydrolase activity of microorganisms are crucial. In fact, phosphatases are the most abundant enzyme in the soil, and they are released by both plants and microorganisms to mineralize organic phosphate compounds. These extracellular enzymes are key agents in organic P mineralization, which involves plant and microorganism activity. Therefore, the synergy in the overall phosphatase release depends on the interaction of plants with the rhizospheric microbial community and have a crucial role in plant response to P deficiency, although mechanisms of P mineralization are still not well clarified (Cabugao et al., 2017).

Phosphorus is absorbed by plants roots as orthophosphate ions, principally $H_2PO_4^-$ and to a lesser extent HPO_4^{2-}. P concentration in soil solution is on average in range of micromolar and about three orders of magnitude lower than P in plant tissues (about 10 μM vs. 5 to 20 mM respectively). Therefore, for phosphate uptake high-affinity active transport systems are necessary to overcome a strong chemical potential gradient across the plasma membrane of root cells. There are two different systems which mediate P uptake and transport in plants: the first one is an inducible high-affinity Pi/H^+ symporters synthesized by a member of the PHT1 gene family and having a Km value generally ranging from 10 to 100 μM. The second one is a constitutive low-affinity transport system with a Km value that ranges the concentration of mM (Hasan et al., 2016). PHT genes can be divided in four families in *Arabidopsis*: PHT1; PHT2; PHT3; PHT4. The high affinity-transporters belonging to PHT1 family are expressed mostly in the roots, with 6 members in maize. The transporters of this family are induced by P starvation and is responsible for P uptake from the soil and transport to the shoot. Some members of this family also display a mycorrhiza-specific expression pattern in barley. PHT2 family of high-affinity transporters is expressed in the chloroplast and mediate the allocation of phosphate in the plant tissues. In *Arabidopsis*, these transporters were related to higher phosphate concentrations in the shoot under conditions of phosphorus starvation (Versaw & Harrison, 2002). PHT3 is localized in the mitochondria, whereas PHT4 were found in the Golgi bodies in *Arabidopsis* and contribute to the mobilization of phosphate from the cellular organelles (Hasan et al., 2016). Phosphorus starvation response in plants triggers the overexpression of non-coding small RNAs, such as miR399, which was the first microRNA to be related to phosphate starvation (Bari et al., 2006). The target protein of miR399 is the ubiquitin-conjugating E2 enzyme known as PHOSPHATE 2 (PHO2), which is suppressed by miR399 (Bari et al., 2006). A family of genes induced by phosphate starvation are IPSs (Induced by Phosphate Starvation) (Huang et al., 2011). Several members of this family have been reported to modulate their expression in response to P deficiency conditions and to participate in the P signalling. The regulatory activity of miR399 is quenched by IPS1 which protects PHO2 from miR399-mediated cleavage (Hackenberg et al., 2013).

IPSs genes concur to a fine regulated mechanism in Arabidopsis: AtIPS1 forms an RNA duplex with the microRNA AtmiR399, which inhibits the degradation of AtPHO2 mRNA; AtPHO2 regulates the expression of two PHT members, AtPHT1;8 and AtPHT1;9, and controls the remobilization and translocation of Phosphate, although this mechanism remains still largely unknown (Lauer et al., 1989a; Lauer et al., 1989b; Marschner, 2011). PHR1 (PHOSPHATE STARVATION RESPONSE 1) is a MYB TF plays a central role in the signalling of primary phosphate responses, especially inducing the expression of miR399 (Branscheid et al., 2010); PHR2 in rice, when overexpressed, leads to accumulation of more Pi in the shoot. A lot of other genes are regulated downstream this signalling pathway. WRKY75 is a member of the WRKY transcription factor family that is found to be positively regulate genes involved in phosphorus acquisition and to change root architecture by decreasing lateral root formations (Hasan et al., 2016; Jiang et al., 2007).

1.3.4 Plant responses to P deficiency

P deficiency triggers a wide range of physiologic and metabolic adjustments in plants, aimed at maintaining the Pi, ATP and nucleotide concentrations in their homeostatic range. Nevertheless, under severe P depletion plant growth and crop yield result sensitively decreased. In these conditions, induced-intracellular acid phosphatases are involved in phosphate remobilization and from intracellular reserves. Phosphate in plant cells is stored in vacuoles, in a non-metabolic P pool. At adequate P supply 85–95% of the total cellular P is stored in the vacuoles as inorganic phosphate (Pi). Conversely, when a condition of P deficiency is occurring, most of the Pi can be founded in chloroplasts and cytoplasm, constituting a metabolic P pool, that actively participate to cell reactions (Jiang et al., 2007; Péret et al., 2014). Also, low P concentration in the cells induces de novo synthesis of extra- and intracellular acid phosphatase. An evident effect of P depletion is the over-accumulation of anthocyanin, especially observable in plant leaves, due to the higher expression of genes involved into phenylpropanoid biosynthesis, such as flavone 3' hydroxylase (F3'H), leucoanthocyanidin dioxygenase, PAP1 and UDP-Glc-flavonoid 3-O-glucosyltransferase (Carstensen et al., 2018). PAPs (purple acid phosphatase) are a family of genes whose members concur to the remobilization of P from phytate reserves stored in grains and seeds. Another response to P starvation is the simultaneous reduction in shoot growth and increase in root proliferation, resulting in a lower shoot/root biomass ratio. As result, the P deficient plant will form an increased lateral root system and a contemporary reduced primary root length, (LPR1 was found to have a strong effect on primary root growth arrest in response to P starvation). Phytohormone equilibrium, such as for auxin sensitivity and cytokinin, are also changed when P deficiency occurs, toward the increase of lateral roots and the diminution of primary root elongation. Jiang et al. (2007) suggested the possibility that Pi starvation reduces growth via a reduction in bioactive GA levels, at least partially. Moreover, photosynthetic capacity of plants is affected under P starvation: P deficiency affects ATP synthesis in the stroma, also reducing CO_2 fixation. Anyway, CO_2 assimilation is not completely disrupted as no changes in the photosynthetic apparatus composition or electron transport chain were reported in literature. P-deficient plants typically do not show leaf chlorosis and remain green (Marschner,

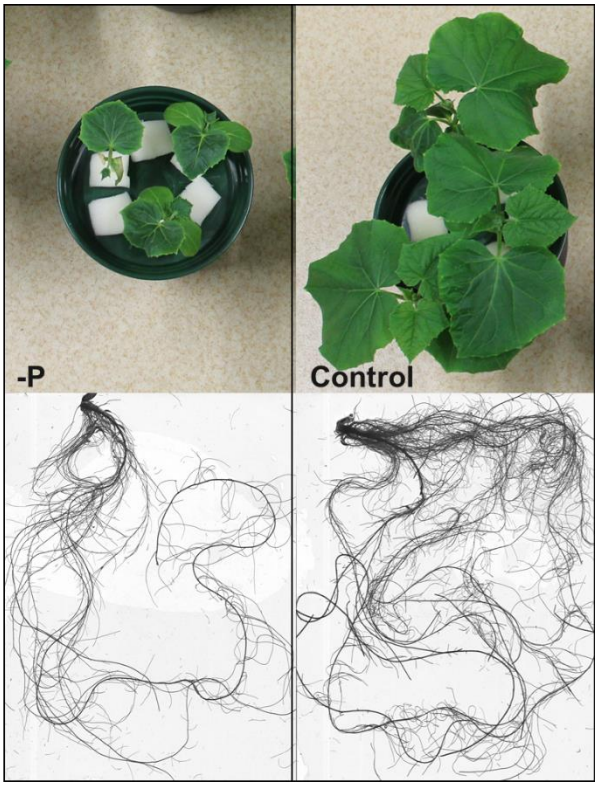

Figure 1.12 Comparison of plants of *Cucumis sativus* grown without P (-P) and with P (Control) in hydroponics in this work. Symptoms of P deficiency, such as a reduced leaves expansion, a darker coloration of the leaves, and the increased root-to-shoot ratio, are evident in -P plants.

2011). The combination of a not reduced chlorophyll production, a reduced leaves expansion and and increased anthocyanin production, would turn in greener/red and smaller leaves in P deficient plants (Carstensen et al., 2018). An example of P a deficient cucumber plant is given in Fig. 1.12. Accumulation of starch and sugars in leaves is another common symptom of P deficiency and it is mainly caused by a lower export of sugars due to lack of ATP. Sucrose can be loaded into the phloem thanks to a proton gradient generated by a membrane ATPase by sucrose-proton cotransport, so a decreased Pi concentration causes a depletion of ATP and therefore the inhibition of triose export from the chloroplast. (Marschner, 2011). Moreover, low cytosolic Pi concentration directly affects triose export, since the triose transporter is a Pi/triose antiporter (Walters et al., 2004).

1.3.5 Limits of P feritilizers

Soluble phosphate fertilizers, such as monoammonium phosphate (MAP), diammonium phosphate (DAP) and triple superphosphate (TSP) have the advantage to provide prompt-use P for plant. On the other hand, water movement can rapidly deplete soluble P and move it away from the rhizosphere, causing immobilization and precipitation and, in a minor part, leaching (Samreen & Kausar, 2019; Syers et al., 2008). Moreover, phosphate fertilizers used in agriculture mostly come from phosphorite rocks, that are a not-renewable sources. This means that at a certain time all the phosphorus would reach the alarming peak condition called "peak phosphorus" (Samreen

& Kausar, 2019). This condition would be calculated based on phosphate rock reserves, but since no consensus was there on the size of these reserves it remains still impossible to precisely estimate when the "peak phosphorus" will occur. FAO (2008) estimated that at the current rate of use, the mostly exploitable reserves could last between 105 and 470 years (Syers et al., 2008). The current annual demand of rock phosphate is of the order of 4 million tons, out of which 95% is consumed in agriculture in P fertilizer industry. Another existing phenomenon regards the rapidly increasing price of soluble P fertilizer (Samreen & Kausar, 2019). To make matters worse, food demand is rising globally, rising the demand of fertilizers too. Reserves of P are finite, even considering the possibility to explore new resources and new methodologies by means of the implementation of future technologies, optimizing P sources efficiently in order to maximize its life span.

1.3.6 Iron (Fe)

Iron can change its oxidation state – switching between Fe^{2+} and Fe^{3+} – with relative ease, as transition element. The redox potential can vary widely depending on the ligand bond to Fe-macromolecules, and this is the main reason why it is so important in biological redox systems (Kappler & Straub, 2005). However, free ionic Fe or low-molecular weight Fe chelates can originate ROS, thus, to prevent oxidative damages to cells Fe must be bound or incorporated into macro-structures (such as heme proteins or Fe-S proteins) to allow reversible redox reactions.

Fe is required as structural component of thylakoid membranes in PSI and PSII (particularly in PSII) and in electron transport chain elements as constituent of heme proteins, such as cytochrome *bf* complex. Moreover, Fe is critical for the biosynthesis of chlorophyll: the precursor of chlorophyll and heme biosynthesis which takes place in plastids by sharing some steps of the chlorophyll biosynthesis pathway (Marschner, 2011), is aminolevulinic acid (ALA). ALA is originated from L-glutamate and the rate of ALA formation is controlled by Fe (Kobayashi & Nishizawa, 2012), tough its role in chlorophyll biosynthesis is still not well clarified. Fe is required as component of ferredoxin, which is involved in both cyclic and non-cyclic photophosphorylation reactions of photosynthesis. Fe is also constituent of the redox chain in nitrate reductase. Catalase and peroxidase are other two enzymes which contain heme group, and therefore are susceptible to Fe deficiency. The activity of these two enzymes decreases in low Fe supply conditions and therefore they can be indicators of the Fe nutritional state of the plant. In Fe-S proteins, Fe is coordinated to the thiol group of cysteine or to inorganic S atoms, or to both. Ferredoxin is a Fe-S protein, which acts as an electron transmitter coenzyme in many metabolic pathways such as nitrate reduction, glutamine synthetase-glutamate synthase pathway and photosynthesis. Another Fe-S protein is Superoxide dismutases (SOD) which detoxifies superoxide anion freeradicals ($O_2\cdot$) by formation of H_2O_2. Fe is also required in ethylene biosynthesis from methionine, in Lipoxygenases which catalyse the peroxidation of linoleic and linolenic acid and it is also component of the leghemoglobin, which can be present in small amounts allowing the formation of root nodules.

1.3.7 Behaviour of Fe in the soil-plant system

Iron (Fe) represents the second most abundant metal in the Earth's crust, just after alluminium (Al). Among the other micronutrients, Fe is required in the largest abundance by plants, although unfortunately its solubility in the soil is extremely low, especially in calcareous ones which account for about 30% of the world's cultivated soils (Mori, 1999). Fe availability depends on the soil redox potential, which is a measure of the electrochemical potential or electron availability within the soil system, and pH. Fe in the soil is ubiquitous as Fe-bearing minerals or as dissolved ions, in the form ferric

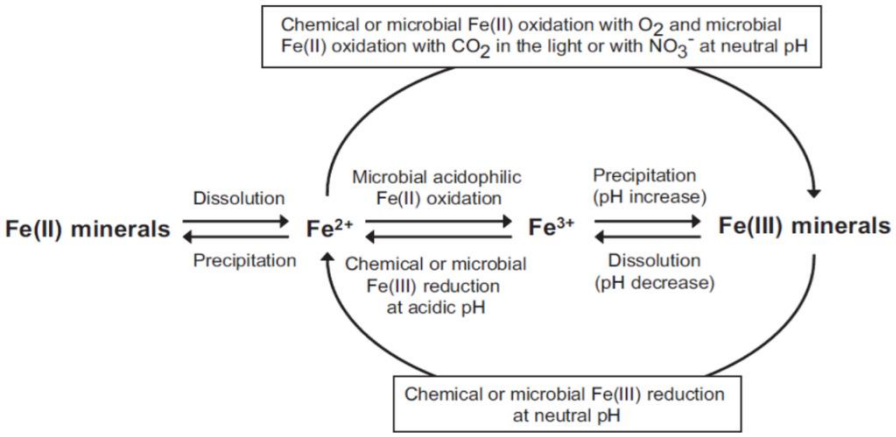

Figure 1.13. Schematical representation of microbial and chemical Fe cycle in a soil system (Kappler and Stoub, 2005).

Fe(III) or ferrous Fe(II) iron. Fe(III) oxides (such as hematite) and hydroxides (such as goethite), have a very low solubility at neutral or close to neutral pH, leading to hardly detectable concentrations present in soil solution, ranging 10^{-9} M of Fe(III) (Kappler and Stoub, 2005). Anyway, if colloid formation or complexation is possible by the presence of organic matter, concentrations of dissolved Fe^{3+} can increase considerably, even at neutral pH. Fe(II) minerals (such as siderite, pyrite, vivianite or ferrous monosulfides) are considerably more soluble at neutral pH. In fact, in soil solution Fe(II) concentration can reach values around 10^{-6} M in acidic environments, but it remains stable at neutral or alkaline pH only in anoxic condition (Colombo et al., 2014). Generally, neutral pH conditions promote the precipitation of low crystallinity of Fe minerals such as ferrihydrite, whereas only reducing and acid conditions promote Fe mobilization. Thus, solubilization of Fe from soil minerals is a slow process regulated by pH and by the dissolution–precipitation equilibrium of ordered forms (Colombo et al., 2014). Microbially-influenced transformations of Fe take place in most soils and sediments and determine the paedogenetic evolution of the soil environment (Fig 1.13). Fe(II) form is preferentially taken up by plants in comparison with Fe(III), even though this preference can vary depending on the plant species (paragraph 1.3.8).

1.3.8 Mechanisms of Fe uptake by plant roots

Fe is essential for plant growth, but chemical properties that make it suitable for redox reactions also facilitate the generation of reactive oxygen species, when Fe exists in a free state. This process is mainly due to the Fenton reaction by which Fe^{2+} reacts with

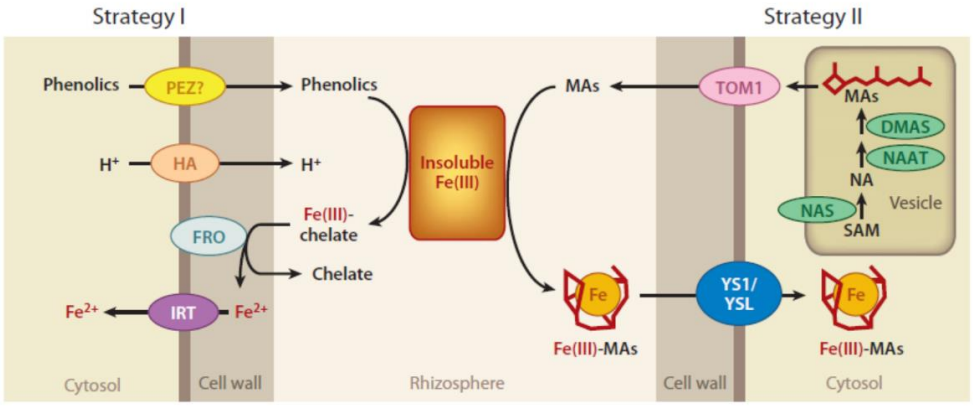

Figure 1.14 Schematic representation of the two strategies used by plants to acquire Fe, Strategy I in nongraminaceous plants and Strategy II in graminaceous plants (Kobayashi & Nishizawa 2012).

H_2O_2 in the cellular environment, causing the production of the ·OH radical reactive specie. Consequently, plants must tightly control Fe homeostasis and finely react to Fe deficiency, as well as to Fe excess. Plants have two different strategies to acquire Fe from the rizosphere: Strategy I in nongraminaceous plants (left) and Strategy II in graminaceous plants (right) (Kobayashi & Nishizawa, 2012) (Fig. 1.14). Strategy I is utilized by all the higher plants except for the graminaceous plants and consists into reduction of Fe^{3+} chelates on the root surface followed by the absorption of the so reduced Fe^{2+} ions across the root plasma membrane. Ferric-chelate reductase oxidase gene *FRO2* codifies the NADPH-dependent reduction of Fe^{3+} to Fe^{2+}. Then, reduced Fe can be transported into the root epidermal cells by the divalent metal transporter *IRT1*, which also transports other divalent metals such as Mn, Zn, and Co (Kobayashi & Nishizawa, 2012; Morrissey & Guerinot, 2009). Other divalent metal transporters in both nongraminaceous and graminaceous plants have found to exist as homologs of Arabidopsis *IRT1*, and belongs to ZIP (zinc-regulated transporter, iron-regulated transporter–like protein) and NRAMP (natural resistance-associated macrophage protein) families (Kobayashi & Nishizawa, 2012). IRT transporters are generally localized to the plasma membrane, whereas NRAMP transporters were found to either intracellular vesicles or the plasma membrane. Non graminaceous Strategy I plants also facilitate Fe acquisition through the extrusion of proton and phenolic compounds from the roots to the rhizosphere. Proton extrusion, similarly to P assimilation strategy, is thought to help increase the solubility of Fe(III) ions via acidification of the soil solution and to support the reducing capacity of Fe^{2+} onto the root surface (Marschner, 2011). H^+-ATPases (AHA) are responsible for the proton extrusion into the rhizosphere and are expressed in the epidermis of root cells. *AHA2* is the primary gene to respond to the Fe deficiency in *Arabidopsis* roots, with its expression found to be higher than the other members of this family, as well as for cucumber *CsHA1* (Santi et al., 2005). In Strategy I plants, genes responsible for the excretion of phenolics compounds have not been identified yet. However, the identification of rice *PHENOLICS*

EFFLUX ZERO 1 (*PEZ*) rises the possibility of the existence of a homologous family in non graminaceous plants that might be responsible for phenolics compounds release (Kobayashi & Nishizawa, 2012). Up to 75% of Fe in the roots is adsorbed to the apoplast due to the negatively charged carboxyl groups present onto the cell wall, which can function as cation sink. It has been shown that when plants go toward Fe deficiency, this pool is rapidly depleted, suggesting mobilization into the symplast (Kobayashi & Nishizawa, 2012). It remains unclear how this Fe is actually taken up. However, in red clover roots, phenolics compounds were shown to be able to strip Fe from purified cell wall, so phenolic compounds release could represent a strategy to acquire Fe once entered into the apoplast of plants roots (Morrissey & Guerinot, 2009). It remains unclear if a Fe-phenolic complex is transported into the root. Anyway, in calcareous soils the presence of high bicarbonate and calcium carbonates concentrations (and therefore a high pH) impair the effectivity of the membrane-bound reductase. Thus, preventing acidification of the soil solution, can be a limiting factor for the effectivity of Strategy I in Fe acquisition in calcareous soils (Marschner & Römheld, 1994).

Strategy II is a chelation-based strategy for Fe acquiring and it is used by plants belonging to graminaceous group (Poaceae family). Graminaceous plants synthesize and secrete phytosiderophores (PS), which are natural chelators belonging to the family of mugineic acids (MAs) (Suzuki et al., 2021). MAs are a large family of compounds derived from S-adenosyl-L-methionine via a conserved pathway. In MAs pathway three sequential enzymatic reactions occur, and they are mediated by nicotianamine synthase (NAS), nicotianamine aminotransferase (NAAT), and deoxymugineic acid synthase (DMAS). These subsequential reactions generate 2'- deoxymugineic acid (DMA), the precursor of all other MAs. Secretion of MAs follow a circadian rhythm, reporting a peak in the morning, and it was proved that MAs synthesis occurs in vescicles, whose production was observed during Fe deficiency in root (Beasley et al., 2017; Kobayashi & Nishizawa, 2012). A transporter of mugineic acid family phytosiderophores TOM1 was recently identified to be responsible for MA secretion. Once MAs have been secreted and released into the rhizosphere, they can chelate and therefore solubilize Fe(III) due to the high affinity of the ligand for the metal even at high pH soils. The resulting Fe(III)-MA complexes are absorbed by root cells through the *YELLOW STRIPE 1 (YS1)* and *YELLOW STRIPE 1–like (YSL)* transporters. There is a strong correlation between the volume of PS released and the resistance to Fe deficiency in certain soils. For instance, barley is well adapted to alkaline soils and releases a much greater amount of PS than most rice species (Morrissey & Guerinot, 2009). Although rice is a graminaceous plant, a cross-mechanism was identified: OsIRT1 allows to take up Fe^{2+} in addition to the chelation–based strategy, by which complexation of Fe(III)-DMA is possible, followed by the uptake process through the OsYSL15 transporter However, rice has very low ferric-chelate reductase activity, suggesting that this mechanism represent an adaptation to the direct uptake of Fe^{2+} which is abundant in submerged and anaerobic conditions (Wairich et al., 2019; Morrissey & Guerinot, 2009).

Low solubility and high reactivity of Fe make necessary the existence of a tuned mechanism of chelating molecules and proper control of its redox state. Some principal chelators inside the plant are citrate, nicotianamine (NA), and MAs. *PEZ1* is thought to be responsible for xylem loading of phenolic compunds, which might facilitate the remobilization of precipitated apoplastic Fe inside the plant. YSL family

members are involved in Fe translocation, since they have been found in nongraminaceous plants too, which do not synthesize MAs. Moreover, YSL transporters were found to be involved in the translocation of metals chelated with NA, which is a precursor and chemical analogue of MAs. Anyway, most of the pattern of Fe translocation in the plant remains still unclarified.

1.3.9 Plant responses to Fe deficiency

Iron deficiency occurs frequently in many crops, especially when cultivated in alkaline soils. The critical concentration of Fe under which plants present the symptoms of deficiency is in the range of 50–150 mg Fe kg^{-1} (dry weight) in leaves (Kobayashi & Nishizawa, 2012; P. Marschner, 2011). The most visible symptom of Fe deficiency is a decreased chlorophyll concentration (internerval chlorosis) (Fig. 1.15). Fe is required as structural component of the photosynthetic apparatus, as cofactor in photosynthesis and for the formation of ALA, as mentioned above. Iron chlorosis is particularly evident in young leaves, since Fe is a very low movable element into the plant tissues (Kobayashi & Nishizawa, 2012; Marschner, 2011). Responses to scarcity of Fe availability are accompanied by morphological changes in root architecture. A general inhi-

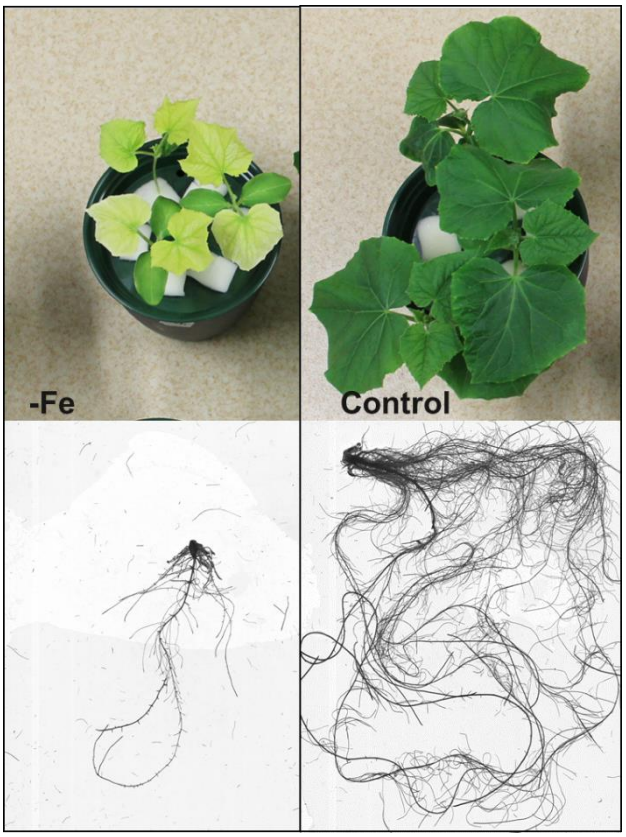

Figure 1.15. Comparison of plants of *Cucumis sativus* grown without Fe (-Fe) and with Fe (Control) in hydroponics in this work. Symptoms of Fe deficiency, such as a leaves chlorosis and reduced root growth are evident in -Fe plants.

bition of root elongation, an increase in the diameter of apical root zones, and abundant root hair formation are observed in Fe-deficient plants (Müller et al., 2015). Fe deficiency root morphological changes are coupled with the formation of transfer cells.

Transfer cells are specialized parenchyma cells that possess an increased surface area due to the higher level of folding of cell membrane. In Strategy I plants, transfer cells are thought to be the major site of excretion of protons and release of phenolic compounds.

Plants modulate the expression of various genes related to Fe homeostasis in condition of Fe deficiency or excess (Figure 1.16). Important role of several transcription factors (TFs) in regulating Fe transporters was recently clarified. In non-graminaceous plants, basic helix-loop-helix (bHLH) transcriptional regulator FER was identified in tomato, together with its ortholog FIT in *Arabidopsis* (Hsieh & Waters, 2016). These TFs regulate various Fe responses genes such as IRT1 and FRO. Other bHLH genes, such as *At*bHLH38, *At*bHLH39, *At*bHLH100, *At*bHLH101 are strongly induced under Fe deficiency in root and shoot (Wang et al., 2007). In some plants, such as in tobacco, orthologs of *At*bHLH38 and *At*bHLH39 overexpression enhance riboflavin secretion (Vorwieger et al., 2007), which is another typical response to Fe deficiency in some strategy I plants, as well as for phenolic and flavin compounds. In cucumber, an overexpression of genes involved in riboflavin biosynthesis was found in alkaline condition (Hsieh & Waters, 2016). Ethylene insensitive 3 (EIN3) and ethylene insensitive 3-like1 (EIL1) are TFs that play central roles in ethylene signaling and have been found to interact with FIT TFs (Dolgikh et al., 2019), suggesting a linkage between ethylene biosynthesis and Fe deficiency. Another bHLH TF, POPEYE (PYE), is critically involved in root growth during Fe deficiency and might negatively regulate Fe homeo-

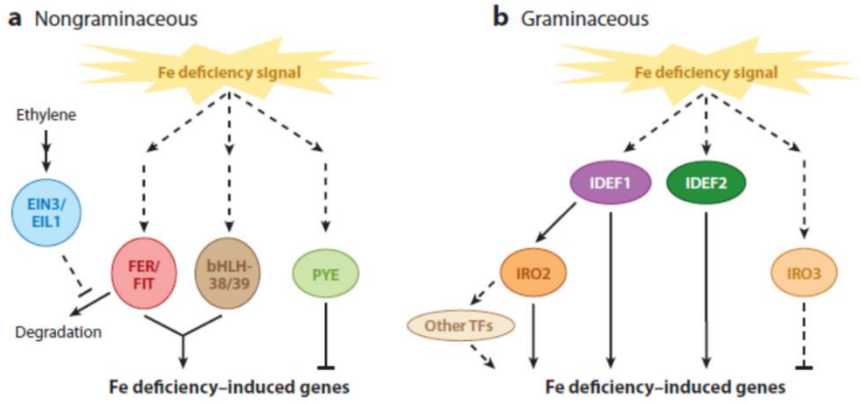

Figure 1.16. Schematic involvement of transcription factors in Fe deficiency responses in a) nongraminaceous and b) graminaceous plants. Dashed lines: putative or unverified pathways. Circles: Principal transcription factors involved in regulation of Fe deficiency responses (from Kobayashi and Nishizawa, 2012)

stasis-related genes. In graminaceous plants iron deficiency–responsive element 1 (IDE1) and 2 (IDE2), were identified to synergistically induce Fe deficiency responses genes in tobacco roots and in rice roots and leaves. Two TFs named IDE-binding factors (IDEFs) were identified to bind to IDE1 (IDEF1) and to IDE2 (IDEF2). IDEF1 and IDEF2 are constitutively expressed in plant vegetative and reproductive tissues, independently by an induction in Fe deficiency, suggesting a direct role into perception of Fe deficiency signal (Kobayashi and Nishizawa, 2012). These two TFs regulate two different sets of target genes. Late embryogenesis abundant (LEA) genes, which are involved in water stress during seed maturation, are regulated by IDEF1

during the early stage of Fe deficiency condition. Whereas IDEF1 positively regulates *Os*YSL2 in rice, to allow redistribution of Fe in the whole plant. An overexpression of the bHLH *Os*IRO2 is strongly induced under Fe deficiency and positively regulated by IDEF1 TF. IRO2 in turn positively regulates several Fe-responses genes related to strategy II, such as NAS, TOM and YSL (Liang et al., 2020). *Os*IRO3 is another bHLH TF, which is essential for maintaining Fe homeostasis in rice under Fe deficiency. It was demonstrated that OsIRO3 negatively regulates the expression of various Fe deficiency-inducible genes, mainly under conditions of Fe sufficiency and early Fe deficiency (Wang et al., 2020b). Through sequence comparisons, it was found that IRO2 has significant similarity to *At*bHLH38, -39, -100, and -101 TFs present in nongraminaceous plants, whereas IRO3 has similarity to PYE. A graminaceous ortholog of FER/FIT *Os*FIT was recently identified (Liang et al., 2020). An interaction between *Os*FIT and *Os*IRO2 to form a functional transcription activation complex which initiate the expression of Fe-uptake genes was demonstrated (Liang et al., 2020). Thus, molecular components of Fe deficiency responses appear to be, at least partially, conserved between strategy I and strategy II Fe deficiency-responses.

1.3.10 Limits of Fe fertilizers

Concerning the widely diffused problems of insufficient Fe supply for crops, a solution is to apply synthetic chelated Fe-fertilizers in the soil or as foliar spray. The use of these Fe-bearing fertilizers can rapidly increase Fe content in the soil and prevent Fe deficiency of crops. However, only a small amount of the Fe added with these fertilizers can be absorbed and utilized by plants in soil, due to rapid nutrient loss. In fact, the negative charged Fe-chelates are not retained by soil particles and easily prone to leaching (Lucena, 2003). Moreover, Fe-fertilizers are generally expensive and difficult to produce, easily leachable and therefore risk to cause environmental pollution. Leachable Fe-chelates are commonly not easily degradable and can persist in the ground water when leached. Natural polymer-based fertilizers are employing in order to promote eco-sustainability of Fe fertilization (Pérez-Labrada et al., 2020). Synthetic Fe(III)-chelates used as fertilizers are generally derivatives from the family of ethylenediaminecarboxylic acids, such as Fe(III)-chelates of ethylenediamine tetraacetic acid (Fe-EDTA), containing 13% of soluble Fe; Fe(III)-diethylenetriamine pentaacetic acid (Fe-DTPA) containing 0.3% of soluble Fe; ethylenediamine-N-N bis acid (Fe-EDDHA), containing 6% of soluble Fe (Álvarez-Fernández et al., 2007). The effectiveness of these Fe-chelates is mainly based on their ability to provide Fe in soluble forms in aerobic environments, promptly adsorbable by the plants. Other Fe complexes can be used in Fe-fertilization, such as organic acid complexed with Fe. Citrate, salicylic acid, oxalic acid or their mixture could restore Fe nutrition in tomato (Pérez-Labrada et al., 2020), as well as the use of humic complexes combined with Fe-chelates. Anyway, still remains the needing to develop new sustainable fertilizers able to provide Fe in an available form for plants and less leachable as possible.

2. AIM OF THE THESIS

In plant nutrition, nanofertilizers represent a promising tool to increase nutrient use efficiency (NUE) being more reactive and, perhaps, more available to plants. This would limit the dispersion in the environment that normally affects conventional fertilizers when applied to the soil (Marchiol et al., 2020). Nevertheless, little is known about their effects on plants, soil microbial community and rhizosphere in particular if molecular aspects are concerned.

The present work is aimed to evaluate the effect of $FePO_4$ nanoparticles (NPs) on the plant-soil system when used as source of nutrients, focusing on: i) the early transcriptomic responses of plants to $FePO_4$ NPs treatment in hydroponic, which may be assessed as a highly controlled system without the influence of other organisms as in the soil; ii) the possibility to apply $FePO_4$ NPs directly on the soil without negative consequences for the microbial community and, therefore, the environment; iii) the efficacy of $FePO_4$ NPs as fertilizer in a controlled system but in the soil environment, focusing both on plant responses and on the rhizosphere environment, thus on soil microbiome. To achieve these objectives, microarray analyses were carried out using RNA extracted from roots of cucumber and maize seedlings grown for 24 hours in a nutrient solution added with $FePO_4$ NPs or non-nano $FePO_4$ (bulk) as source of P or Fe. Differentially expressed transcripts were then identified comparing the transcriptomic profiles of plants after each treatment to the ones grown without the corresponding nutrient. The effect of the size of $FePO_4$ (NPs or bulk) on the transcriptome of plants was investigated. Then, $FePO_4$ NPs were provided to two different bare soils to evaluate the impact on soil microbial community and to determine if any toxic effect would be observed. A comparison of $FePO_4$ NPs and triple superphosphate (TSP) was done in terms of Olsen-extractable P in order to assess the availability of the element in comparison of a commercial and large-used fertilizer. With the aim to study the effects of $FePO_4$ NPs on a plant-soil microcosm, cucumber plants were grown in pots in a growth chamber. Physiological parameters of plants were acquired to evaluate the differences of plants grown with $FePO_4$ NPs or with TSP and, therefore compare the efficacy of the two fertilizers. Finally, the impact on the rhizosphere environment in terms of microbial community structure and enzyme activity after the plant growth was evaluated consequentially to the treatment with NPs or TSP.

SECTION I

3. MATERIALS AND METHODS OF SECTION I

3.1 $FePO_4$ nanoparticles synthesis

$FePO_4$ NPs were synthesized through co-precipitation adding 25 mL of 0,6 M K_2HPO_4 drop by drop to 25 mL of 0,6 M $Fe(NO_3)_3$ continuously stirred at room temperature (25°C). The solution partially precipitated was centrifuged for 20 minutes at 4500 rcf at room temperature, then the supernatant was precipitated warming at 85°C for 1 hour. The suspension obtained was then let cool at room temperature under continuous stirring, then purified through dialysis using membranes with Molecular Weight Cut-Off (MWCO) of 14 kDa against H_2O for 24 hours. The retentate:water ratio was 1:40 and water was changed four times. Then 50 mL of the obtained solution were citrate-capped with 5.55mL of 1M tribasic potassium citrate and vortexing for 2 minutes. The solution was then purified from excess citrate through further dialysis. The method is described in major detail by Sega et al., 2019.
Size distribution of $FePO_4$ NPs was determined through DLS (Dynamic Light Scattering) analysis with a Malvern Zetasizer ZS instrument. The sample was diluted at the final concentration equal 1:20 in deionized water and analysed by the instrument set onto size mode, measuring 173° backscatter.
To determine Fe and P concentration in the solution, 2.5 mL of the solution were dissolved in 2,5 mL of 37% HCl. The obtained solution was diluted to be included into the calibration curve to quantify Fe and P. Calibration curves were prepared using a 0.1M $FePO_4$ in 6 M HCl solution. Fe quantification was based on Stookey (1970) and calibration curve points were 2.5, 5, 10, 15 ,20, 30, 50 µM. The assay was set up directly in cuvettes, adding the following components: 800 µL of sample or $FePO_4$ standard, 10 µL 10% (w/v) of 5 mM NH_2OH, 40 µL of PDT disulfonate (3-(2-Pyridyl)-5,6-diphenyl-1,2,4-triazine-4',4"-disulfonic acid sodium salt), and 150 µL of deionized H_2O to a final volume of 1 mL. Absorbance of coloured solution was read at 562 nm after 10 minutes on Agilent Cary 60 CV2 2.20 spectrophotometer.
The quantification of P was based on Riley and Murphy (1962). The calibration curve points used were 25 µM, 50, 100, 150, 200 and 300 µM. Riley and Murphy reagent was prepared by mixing 50 mL of 2.5 M H_2SO_4, 15 mL of 4% (w/v) ammoniummolybdate, 30 mL of 1.76% (w/v) L- ascorbic acid and 5 mL of 2.74 g/L potassium antimonyl(III) tartrate hydrate. Then, the assay was set up directly in cuvettes, adding the following components: 100 µL of sample or standard, 160 µL of Murphy and Riley reagent and 740 µL of deionized H_2O to a final volume of 1 mL. Absorbance of coloured solution was read at 720 nm after 10 minutes by an Agilent Cary 60 CV2 2.20 spectrophotometer. The average concentration of the solution of $FePO_4$ NPs produced ranged from 0,1 M to 0,13 M with a ratio Fe/P of approximately 1:1.

3.2 Hydroponic plant growth

Seeds of *Cucumis sativus* Viridis F1 hybrid (Franchi Sementi S.p.A.) and of *Zea mays* L. inbred line PR33T56 (Pioneer Hybrid Italia S.p.A.) were germinated on paper soaked with 1 mM $CaSO_4$ in dark at 25°C. Six seedlings have been transferred into each pot per condition filled with 1,8 L of nutrient solution. Nutrient solution was maintained continuously aerated. Plants were grown into a 16/8 day/light photoperiod at 25°C and at 200 μmol m^{-2} sec^{-1} PPFD (Photosynthetic Photon Flux Density) as PAR (Photosynthetically Active Radiation). The control (C) nutrient solution composition was: 0.7 mM K_2SO_4, 2mM $Ca(NO_3)_2$, 0.5mM $MgSO_4$, 0.1 mM KH_2PO_4, 0.1 mM KCl, 100 μM FeNaEDTA, 10 μM H_3BO_3, 0.5 μM $MnSO_4$, 0.5 μM $ZnSO_4$, 0.2 μM $CuSO_4$ and 0.01 μM $(NH_4)_6Mo_7O_{24}$. In addition to the C condition, other six conditions were set up: plants grown without P (-P); plants grown without Fe (-Fe); plants grown without P and with $FePO_4$ NPs as P source (-P+NPs); plants grown without Fe and with $FePO_4$ NPs as Fe source (-Fe+NPs); plants grown without P and with non-nano $FePO_4$ (bulk) as source of P (-P+bulk); plants grown without Fe and with bulk $FePO_4$ as source of Fe (-Fe+bulk). $FePO_4$ bulk and NPs were used in a concentration equivalent to the 100 μM of the control solution. Solutions without KH_2PO_4 were balanced in K^+ cations using 0,2 mM KCl instead of 0,1 mM. The nutrient solution was changed twice a week. The experiment was repeated three times. Three out of 6 seedlings each pot were sampled after 24 hours, stored in liquid nitrogen and used for RNA extraction. The remained 3 seedlings of maize and cucumber plants were grown for 10 and 13 days respectively, in accordance with the evidence of the symptoms of nutrient deficiency.

3.3 RNA extraction and cDNA synthesis

Total RNA extractions were performed from 80 mg of plant tissue previously homogenized in liquid nitrogen using the Spectrum™ Plant Total RNA kit (Sigma-Aldrich) and following "protocol A". 1 μg of total RNA was treated with 10 U of DNAse RQ1 (Promega®). The mix used, according to the manufacturer's protocol, was: 1 μg Total RNA; RQ1 1 μL DNAse 10X buffer; 1 μL RQ1 DNAse; H_2O up to 10 μL. The reaction was incubated for 30 minutes at 37 °C. 1 μL of "stop solution" (Promega®) was added to stop the reaction, which was then incubated at 65°C for 10 minutes. cDNA was then synthesized: 1 μL of oligodT (20 pmol/μL) was added to 10 μL of treated RNA. The mixture was incubated at 70 °C for 5 minutes and transferred in ice for 5 minutes, then the following mix was added to each sample: 4 μL 5X buffer (Promega®); 2.4 μL MgCl2 (25 mM); 1 μL dNTPs (0.5 mM); 1 μL RNAse inhibitor (50 u/μL, Promega®); 1 μL ImProm-II Reverse Transcriptase (Promega®); Final volume was 9.4 μL. The reverse transcription reaction thermal cycle was: 5 minutes at 25°C, 1 hour at 42°C, and 15 minutes at 70°C using a Gene Pro TC-E-48D thermal

cycler (BIOER). The quality of obtained cDNA was checked through PCR using couples of primers of housekeeping genes.

3.4 Microarray expression analysis

The total RNA quantity was determined using Nanodrop whilst the quality was analysed with Bioanalyzer 2100 using a Bioanalyzer Chip RNA 6000 Nano kit (Agilent). The cRNA was synthesized, labelled and hybridized using 200 ng of total RNA of each sample and the Low Input Quick Amp Labeling Kit, according to "One-Color Microarray-Based Gene Expression Analysis For microarray analyses" protocol (www.agilent.com). For each sample 1.65 µg of Cy3-labeled cRNA was used to carry out the hybridization reactions. Three independent biological replicates were used for each condition, for a total of 21 samples for each plant species. The cy3-labeled cRNA samples of maize and cumber were hybridized on two different 4x44k Agilent arrays according to manufacturer's manual for 17 h at 65° C and scanned on Agilent G2565CA Microarray Scanner System (Agilent). In the case of maize was used the same chip reported by Santi et al (2017). The complete descriptions of this chip is available at the Gene Expression Omnibus (http://www.ncbi.nlm.nih.gov/geo) under the following series entry: GPL22578. For cucumber, a new chip was developed using the eArray software (https://earray.chem.agilent.com/earray/) and the sequence information of the predicted transcripts of the cucumber (Gy14) v1 genome (http://cucurbitgenomics.org/organism/7). Feature intensities were extracted using Agilent's Feature Extraction Software 12.0 (www.agilent.com). The hybridization data all samples were normalized using the value of the 75th percentile. Differentially expressed transcripts between -P+NPs vs -P; -P+Bulk vs P; -Fe+NPs vs -Fe; -Fe+Bulk vs -Fe were identified through t-test using MeV software (http://mev.tm4.org/#/welcome) setting with p-value based on permutation with critical value of 0.05 without any correction. Differentially expressed transcripts were then filtered basing on fold changes value ($|FC| \geq 2$).

3.5 Real Time RT-PCR analysis

Real-Time RT-PCR analyses were performed to confirm microarray expression analyses on StepOnePlus™ (Applied Biosystems) system using the FastSYBR® Green Master Mix. 2 primers per condition were designed. Primers concentration was 0.350 mM and 1 ul diluted template cDNA 1:3 was used. Reaction conditions were: 20seconds at 95°C for initial denaturation, then 3 seconds at 95°C and 30 seconds at 60°C for 40 cycles. Primers used are reported in Tables 1 and 2.

Table 1 Primers used in Real-time RT-PCR experiments in cucumber. Transcript ID, sequence forward and reverse and protein name are reported.

Transcript ID	Name	Verse	Sequence
Cucsa.133230.1	ENT1	FW	GTTGTTGACTTGTTTGATGGG
		RV	GCTATTTCCGCCTGTTGTAAT
Cucsa.146940.1	THC	FW	CGTGACTATCGTTTTGGTCG
		RV	GGGTTTCAGTTTAGGAGTTCT
Cucsa.106380.1	DEHY	FW	CGCTGTGATCTTAGAAGGGA
		RV	AACACATCAACCAAGCTAGTC
Cucsa.038100.1	POLY	FW	ACTTCCATCTACGTTAGCCTA
		RV	CACAAACTCGTTATTTTCCGC
Cucsa.066810.1	TAU8	FW	ATAGACCACCTGCGTTATGTA
		RV	GAAAATGATTGCTGGGAAGGA
Cucsa.092390.1	NAS4	FW	AGGGATTGTATTTGTGTGTCG
		RV	CTTCCAGAATGAGCAAAGTAC
Cucsa.122170.1	UNK12	FW	ACGATGAGATCGAGAGGTTTT
		RV	TAGAGAAGAGGCATTTCCAGT

Table 2 Primers used in Real-time RT-PCR experiments in *Zea mays*. Transcript ID, sequence forward and reverse and protein name are reported.

Transcript ID	Name	Verse	Sequence
GRMZM2G703077_T01	DHS2	FW	GTCTATCTCTTAGCTCGTTT
		RV	TGTTCTCGTACACACAAGTT
GRMZM2G036631_T01	HMT	FW	GATTTTGTTGGCTGTGGGTT
		RV	CATCTGTCCGTGGTTATTCC
GRMZM2G361475_T01	PER12	FW	CAGTAGCACTGGACGGCAT
		RV	GAAGATTGGTTGCGGTAGATT
GRMZM2G092780_T01	PHT2.1	FW	TTAAGTGGTACAGCCCATTGT
		RV	TCTGGTGGAACTTGTGGAATC
GRMZM2G068557_T01	FRO7	FW	GAAGCACGAAGGTTAAATGCT
		RV	TTTGACGTACTCACAAACGCA
GRMZM2G045699_T01	NotAnn	FW	GAGTGCGATGGAGGAATAATT
		RV	GCAACTCTCGTTACAAACATC
GRMZM2G053639_T01	ACP	FW	CGTCAGGGATCTGAAGAGCA
		RV	GAGGAAACTTCGTTCCACAATA
GRMZM2G125196_T01	ZDH	FW	GCGGCTCTAATCGGGTTGT
		RV	GCATTGATAGTTCCTGCTTCA

Mean Normalized Expression (MNE) (Simon, 2003) was calculated for every sample through the equation

$$MNE = \frac{(E_{ref})^{CTref}}{(E_{target})^{CTtarget}}$$

where E_{ref} is the mean amplification efficiency of the housekeeping gene; E_{target} is the mean amplification efficiency of the target gene; CT_{ref} is the mean of threshold cycle of housekeeping gene for the sample; CT_{target} is the mean of threshold cycle of target gene for the sample.

$$MNEmean = \sqrt{MNEa \times MNEb}$$

Housekeeping genes used and primer for cucumber and maize are listed in Table 3.

Table 3 Housekeeping genes and primers used in Real-time RT-PCR experiments in *Cucumis sativus* and *Zea mays*. Transcript ID, sequence forward and reverse and protein name are reported.

Species	Transcript ID	Name	Verse	Sequence
C. sativus	Cucsa.313280.1	AP-2	FW	ATTTCTTCTGGGCTGCCTGT
			RV	CACAAGCCAACATCGAAGGA
	Cucsa.219360.1	TIP41-like	FW	TGCAGAAGACCCAAAAGCTTA
			RV	CAGCACCAACATACACGAGA
Z. mays	*GRMZM2G047204*	UNKN	FW	TGCCTGTTCTGTGTGATGGA
			RV	CAAGCAAACAAGGGACGGG
	GRMZM2G149286	CDK	FW	CACGAAGAGGAAAACTGAAGA
			RV	AAGAGCCTGCCTTACGGAAT

The determination of each CT was carried out using StepOne™ software (Applied Biosystems). The efficiency of each reaction was calculated using LinRegPCR software (Ramakers et al., 2003) basing on fluorescence raw data. MNE was calculated against each one of the two housekeeping genes, and the geometric mean of MNE values was calculated as below:
The mean MNE of every condition (-P+NPs; -P+Bulk; -Fe+NPs; -Fe+Bulk) was divided by the mean MNE of their respective control (-P and -Fe) obtaining the corresponding fold change value.

3.6 MapMan pathway analysis

MapMan is a software that displays large datasets, such as gene or transcript expression profiles, using diagrams of metabolic pathways or other processes. Analysis is based on a mapping file that assigns a bincode number to every transcript or gene. Bincodes represent the metabolic pathways and allow the software to collocate genes or transcripts with their fold change value into different table and displayed image of pathways. Visualization of differentially expressed transcripts within the treatments was carried out using MapManv.3.6.0RC1 (Usadel et al.,2009). Mapping files used were provided by the MapMan homepage (Zmays_181; http://mapman.gabipd.org/). We used the homology of the transcripts found in cucumber with the *Arabidopsis* sequences of predicted protein to use the mapping file (Ath_AGI_MODELS_TAIR9_Jan09; http://mapman.gabipd.org/).

4. RESULTS OF SECTION I

4.1 DLS (Dynamic Light Scattering) analysis of synthesized $FePO_4$ NPs

Dynamic light scattering technique was used to determine the size distribution of the suspension of $FePO_4$ NPs obtained. Figure 4.1 shows the average of three measurements performed through DLS on one of the $FePO_4$ NPs batches synthesized during the experiment. The graph indicates that the higher number of the NPs produced are present in a dimensional range of 100-200 nm.

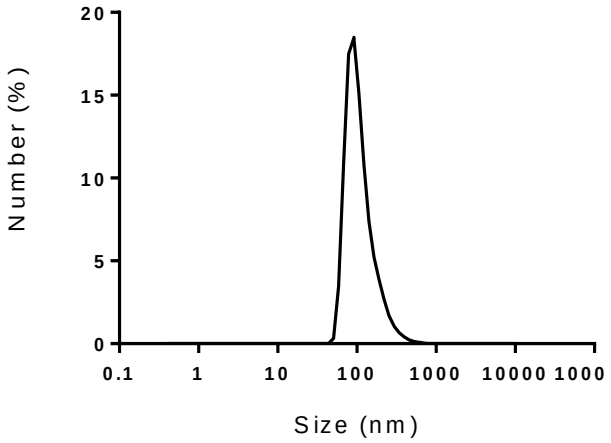

Figure 4.1 Size distribution of $FePO_4$ NPs by number percentage. The analysis was performed through DLS technique.

4.2 Hydroponic growth of maize and cucumber

To evaluate plant responses to $FePO_4$ NP, two different plant species were grown in hydroponic system: *Cucumis sativus* (dicotyledon and strategy I plant for Fe acquisition) and *Zea mays* (monocotyledon and strategy II plant for Fe acquisition). Plant nutritional conditions set-up were the following: control plants (C), to which every macro and micronutrient was supplied; P deficient (-P) and Fe deficient (-Fe) plants grown without any source of P or Fe respectively; nanoparticle-supplied plants (-P+NPs and -Fe+NPs) grown with $FePO_4$ NPs as source of P or Fe; bulk-supplied plants (-P+Bulk and -Fe+Bulk) grown with bulk $FePO_4$ as source of P or Fe. Bulk refers to the non-nano form of $FePO_4$ salt.

4.2.1 Cucumber

4.2.1.1 Dry weight

Cucumber plants were grown in hydroponics for 13 days. Plants grown with $FePO_4$ NPs as source of P (-P+NPs) showed a lower dry weight to control plants, but higher if compared to that of plants grown with bulk $FePO_4$ as P source (-P+Bulk) (Fig. 4.2A). The -P+Bulk plants did not show any significant difference if compared to -P plants,

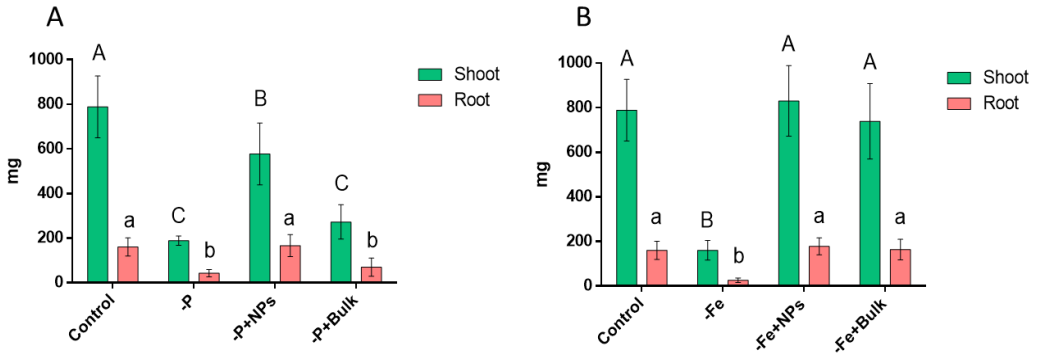

Figure 4.2. Dry weight of cucumber plants after 13 days of growth in hydroponics. A: control plants (Control); plants grown without P (-P); plants grown with $FePO_4$ NPs as source of P (-P+NPs); plants grown with bulk $FePO_4$ as source of P (-P+Bulk). B: control plants (Control); plants grown without Fe (-Fe); plants grown with $FePO_4$ NPs as source of Fe (-Fe+NPs); plants grown with bulk $FePO_4$ as source of Fe (-Fe+Bulk). Data are means ± SD of three independent experiments with three plants each one (One-way ANOVA with Turkey's test, $p<0.05$). Significant differences are indicated by different letters, capital letters are related to shoot data, whereas lowercase letters are related to root data.

indicating that bulk $FePO_4$ did not deliver a sufficient quantity of P to sustain plant growth, while nanosized $FePO_4$ could. Conversely, plants grown with $FePO_4$ NPs as source of Fe (-Fe+NPs) did not show any significant difference in comparison to control and bulk-supplied plants (-Fe+Bulk). Taken together these results show that at least in hydroponic $FePO_4$ NPs could represent a more available source of P than bulk for cucumber. (Fig. 4.2 B).

4.2.1.2 SPAD index

SPAD index of cucumber plants was evaluated after 13 days of growth in hydroponic condition. Measures were performed on the first leaf of each plant because the typical insurgence of P deficiency involves old leaves, since P is a movable element in the plant tissues (Marschner, 2011). SPAD index did not show the existence of statistical significant differences among-P+NPs, -P+Bulk and -P plants. (Fig. 4.3 A). One of the symptoms of P deficiency is the intensification of the leaf colour due to the

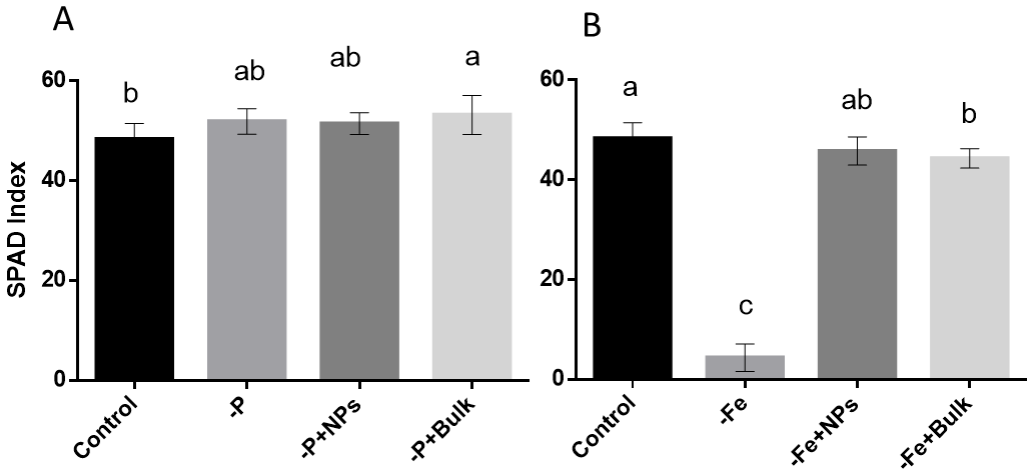

Figure 4.3. SPAD index of cucumber plants after 13 days of growth in hydroponics. A: control plants (C); plants grown without P (-P); plants grown with $FePO_4$ NPs as source of P (-P+NPs); plants grown with bulk $FePO_4$ as source of P (-P+Bulk). B: control plants (C); plants grown without Fe (-Fe); plants grown with $FePO_4$ NPs as source of Fe (-Fe+NPs); plants grown with bulk $FePO_4$ as source of Fe (-Fe+Bulk). Data are means ± SD of three independent experiments with three plants each one (One-way ANOVA with Turkey's test, $p<0.05$). Significant differences are indicated by different letters.

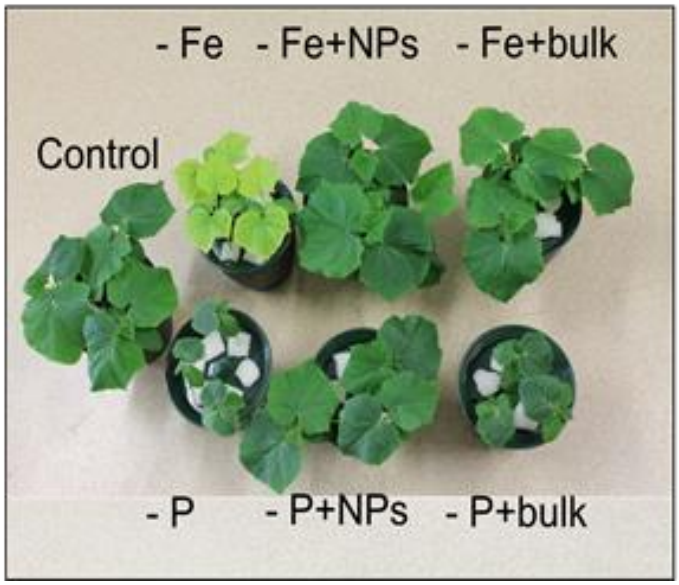

Figure 4.4. Picture of cucumber plants grown in hydroponics for 13 days. Control plants (Control); plants grown without P (-P); plants grown with $FePO_4$ NPs as source of P (-P+NPs); plants grown with bulk $FePO_4$ as source of P (-P+Bulk); plants grown without Fe (-Fe); plants grown with $FePO_4$ NPs as source of Fe (-Fe+NPs); plants grown with bulk $FePO_4$ as source of Fe (-Fe+Bulk).

concentration of chlorophyll and an overaccumulation of antocyanins (Carstensen et al., 2018), and -P+bulk leaves showed higher values of SPAD and a small size (Fig. 4.4), remarking that bulk was not a good source of P. When NPs and bulk were used as source of Fe, the greater difference in this parameter was observed between C and -Fe plants, demonstrating that Fe deficiency was occurring (Fig. 4.3B). Anyway, significant lower levels of this parameter in comparison to C was also observed for -Fe+bulk plants.

4.2.1.3 Root analysis

Root system of cucumber plants was analysed with the software WinRHIZO™ after 13 days. Total length (Fig. 4.5 A; D), surface area (Fig. 4.5 B; E) and volume (Fig. 4.5 C; F) were measured in scanned root pictures. The trend exhibited by the three parameters was the same and remarked the pattern of dry weight results. The three parameters measured for -P+NPs plants showed similar values to the control whilst plants supplied with bulk $FePO_4$ exhibited similar root parameters to P-deficient ones, in particular concerning length and volume (Fig. 4.5).

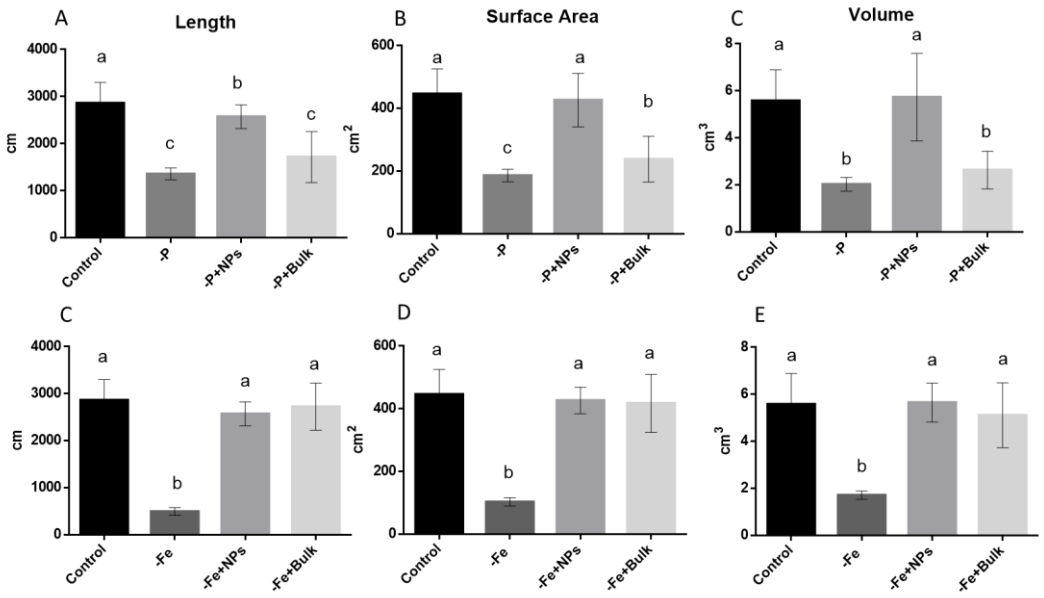

Figure 4.5. Winrhizo™ root analyses of cucumber plants after 13 days of growth in hydroponics. A, D: total root length. B, E: total root surface area. C, F: total root volume. A-C: control plants (Control); plants grown without P (-P); plants grown with $FePO_4$ NPs as source of P (-P+NPs); plants grown with bulk $FePO_4$ as source of P (-P+Bulk). D-E: control plants (Control); plants grown without Fe (-Fe); plants grown with $FePO_4$ NPs as source of Fe (-Fe+NPs); plants grown with bulk $FePO_4$ as source of Fe (-Fe+Bulk). Data are means ± SD of three independent experiments with three plants each one (One-way ANOVA with Turkey's test, $p<0.05$). Significant differences are indicated by different letters.

4.2.2 Maize

4.2.2.1 Dry weight

Maize plants were grown in hydroponic condition for 10 days. The dry weight of -P+NPs plants did not show appreciable differences with respect to -P+Bulk plants (Fig. 4.6 A). indicating that in these experimental conditions both NPs and bulk $FePO_4$ represented a good source of P for maize. Dry weight of -Fe+NPs plants showed significant difference with -Fe+Bulk (Fig 4.6 B), indicating that $FePO_4$ NPs were a good source of Fe instead of bulk $FePO_4$.

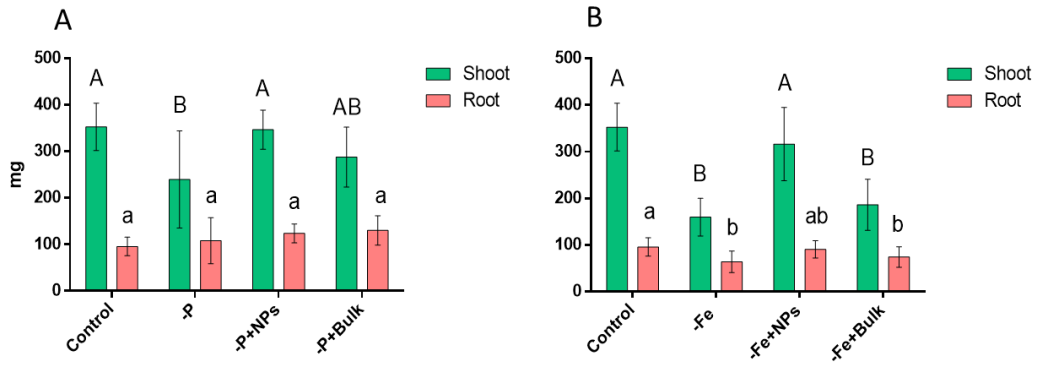

Figure 4.6. Dry weight of maize plants after 10 days of growth in hydroponics. A: control plants (C); plants grown without P (-P); plants grown with $FePO_4$ NPs as source of P (-P+NPs); plants grown with bulk $FePO_4$ as source of P (-P+Bulk). B: control plants (C); plants grown without Fe (-Fe); plants grown with $FePO_4$ NPs as source of Fe (-Fe+NPs); plants grown with bulk $FePO_4$ as source of Fe (-Fe+Bulk). Data are means ± SD of three independent experiments with three plants each one (One-way ANOVA with Turkey's test, $p<0.05$). Significant differences are indicated by different letters, capital letters are related to shoot data, whereas lowercase letters are related to root data.

4.2.2.2 SPAD index

SPAD index of maize plants was measured after 10 days of growth on the third leaf since significant differences were more evident (Fig. 4.7 A). On the other hand, SPAD index of Fe deficient plants (-Fe) was greatly lower than SPAD of control (C) plants, as expected as result of Fe deficiency. Moreover, despite -Fe+NPs plants showed lower leaf SPAD index than C, these levels were significantly higher if compared to those measured for -Fe+bulk and -Fe plants (Fig. 4.7). Figure 4.8 remarks the trend observed in SPAD results.

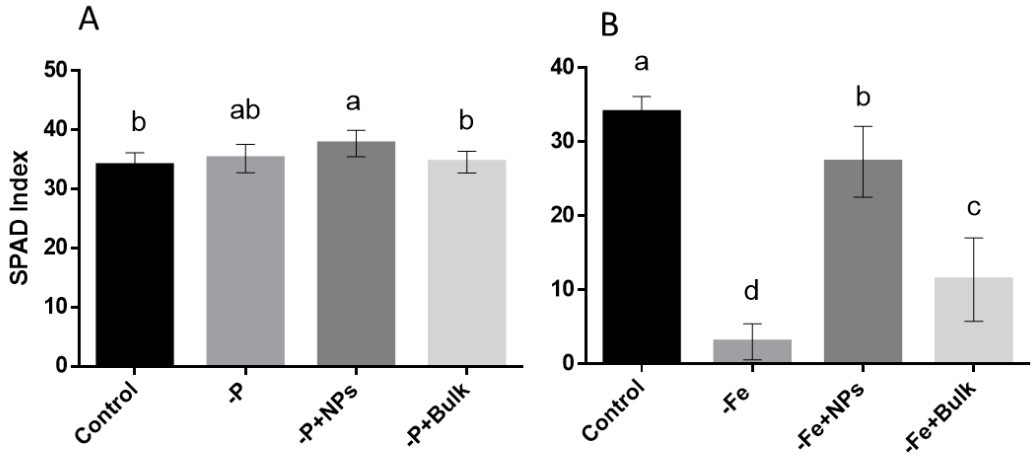

Figure 4.7. SPAD index of maize plants after 10 days of growth in hydroponics. A: control plants (C); plants grown without P (-P); plants grown with $FePO_4$ NPs as source of P (-P+NPs); plants grown with bulk $FePO_4$ as source of P (-P+Bulk). B: control plants (C); plants grown without Fe (-Fe); plants grown with $FePO_4$ NPs as source of Fe (-Fe+NPs); plants grown with bulk $FePO_4$ as source of Fe (-Fe+Bulk). Data are means ± SD of three independent experiments with three plants each one (One-way ANOVA with Turkey's test, $p<0.05$). Significant differences are indicated by different letters.

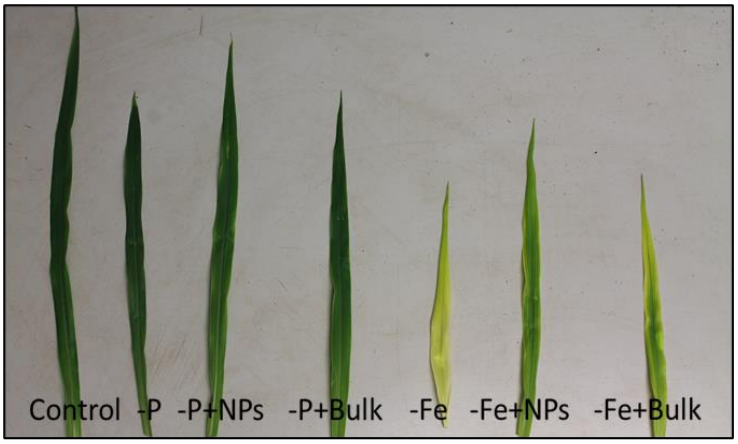

Figure 4.8. Picture of maize plants grown in hydroponics for 10 days. Control plants (Control); plants grown without P (-P); plants grown with $FePO_4$ NPs as source of P (-P+NPs); plants grown with bulk $FePO_4$ as source of P (-P+Bulk); plants grown without Fe (-Fe); plants grown with $FePO_4$ NPs as source of Fe (-Fe+NPs); plants grown with bulk $FePO_4$ as source of Fe (-Fe+Bulk).

4.2.2.3 Root analysis

In the case of roots parameters analysed with the software WinRHIZO™, as for cucumber we observed differences only in length and surface area considering the P nutrition (Fig. 4.9 A; B; C). In particular, these two parameters were significantly different between -P+NPs and control plants, with higher values recorded for the NP-treated

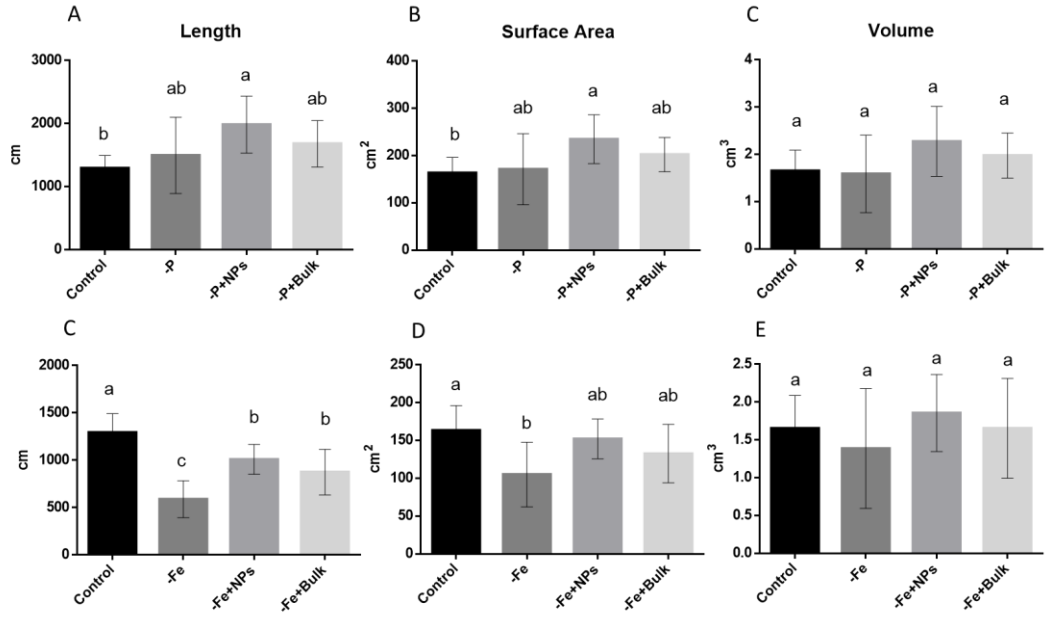

Figure 4.9. WinRHIZO™ Root analysis of maize plants after 10 days of growth in hydroponics. Root length (A; D), root surface area (B; E) and root volume (C; F). A-C: control plants (C); plants grown without P (-P); plants grown with $FePO_4$ NPs as source of P (-P+NPs); plants grown with bulk $FePO_4$ as source of P (-P+Bulk). D-E: control plants (C); plants grown without Fe (-Fe); plants grown with $FePO_4$ NPs as source of Fe (-Fe+NPs); plants grown with bulk $FePO_4$ as source of Fe (-Fe+Bulk). Data are means ± SD of three independent experiments with three plants each one (One-way ANOVA with Turkey's test, $p<0.05$).

ones. In the case of Fe supply, both NPs and bulk exhibited a similar root development as suggested by values of length, surface area and volume (Fig. 4.9 D; E; F). Anyway, the levels of length and surface area were significantly lower than control plants (Fig. 4.9 D; E).

4.3 Microarray expression analysis

To evaluate the early transcriptomic responses in plants treated with $FePO_4$ NPs, microarray expression analyses on seedlings' roots grown in hydroponics for 24 hours were made. Roots were chosen as target of the analysis because the aim was to investigate the early responses of plants after the first contact with NPs, which occurs at root level. Cucumber and maize plants were grown in the same conditions described in paragraph 4.1 and sampled one day after. We performed the microarray analyses of cucumber root using a new Agilent chip developed on the basis of the sequence information of the predicted transcripts of the cucumber Gy14 v1 genome, while maize analyses were carried out using an Agilent chip based on transcripts of the maize B73 genome (release 5b) (Santi et al. 2017). Differentially expressed transcripts were identified comparing the transcriptional profiles obtained for roots of plant grown in different nutritional conditions. The differential expression of some transcripts was also analysed by Real-time RT-PCR (par 4.3.2).

4.3.1 Differentially expression of transcripts in maize and cucumber

Differentially expressed transcripts in roots of both cucumber and maize plants were identified comparing the transcriptional profiles of NP- and bulk-treated plants as source of P or Fe with the transcriptional profiles of roots of plants grown in absence

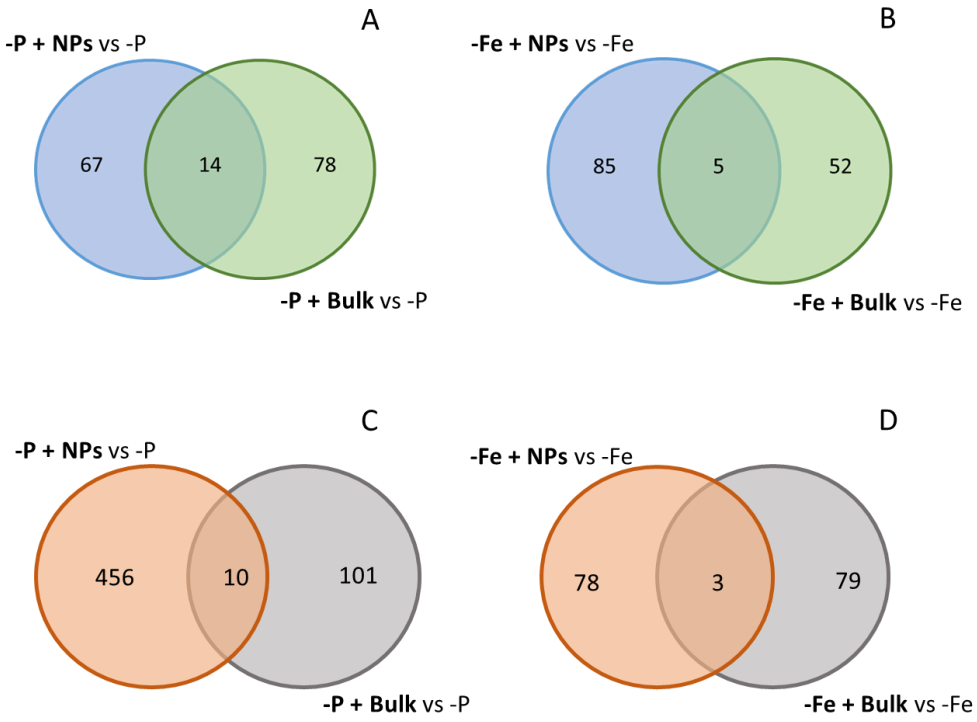

Figure 4.10. Venn diagrams showing the common and the specific differentially regulated transcripts in the different comparisons (adjusted p-value ≤ 0.05, (|FC| ≥ 2). A; B cucumber. C; D maize.

of the corresponding nutrient (-P and -Fe). These comparisons were subjected to a series of t-test (adjusted p-value≤ 0.05). The identified differentially expressed transcripts were then filtered selecting those that were upregulated and downregulated at least twice.

In cucumber, $FePO_4$ NPs and $FePO_4$ bulk specifically modulated 67 and 78 transcripts respectively in comparison to -P (Fig. 4.10A) whilst 14 transcripts were differentially expressed in both conditions. The same approach was carried out for Fe, identifying 85 and 52 transcripts differentially expressed specifically between -Fe+NPs *vs* -Fe and -Fe+bulk *vs* -Fe (Fig. 4.10B). Five transcripts were identified in both comparison (Fig. 4.10B). In maize, when NPs were used as P specifically modulated 456 transcripts while bulk 101 (Fig. 4.10 C). Ten transcripts were commonly modulated in both comparisons (Fig. 4.10 C). Concerning Fe, $FePO_4$ NPs specifically modulated 78 transcripts while bulk modulated 79. Only three transcripts were differently expressed in both comparisons (Fig. 4.10 D). Globally, the analyses revealed that plant roots had highly different transcriptional profiles depending on the form of $FePO_4$ in both cucumber and maize. Moreover, maize reported a wider transcriptomic response to $FePO_4$ NPs as source of P in comparison to cucumber (456 specific transcripts in maize and 67 in cucumber).

The percentage of downregulated and upregulated transcripts was similar in all the conditions, even though in cucumber there always were more downregulated than upregulated, especially in -Fe+Bulk vs -Fe, while in maize the comparisons identified more upregulated transcripts than downregulated. Tables of detailed differentially expressed transcripts are reported in Appendix I, II and III.
In addition, through other Venn diagram analyses, we identified the transcripts specifically modulated by NPs regardless of their use as a P or Fe source (Fig. 4.11). In particular, we used the sets of differentially expressed transcripts identified in the comparisons -P+NPs *vs* -P and -Fe+NPs *vs* -Fe. Eight and 9 transcripts resulted commonly modulated by NPs in both nutritional conditions in cucumber and maize respectively (Fig. 4.11). The same analyses showed that 72 and 81 transcripts resulted specifically modulated by NPs as source of P and Fe respectively in cucumber (Fig. 4.11A) whilst in maize were 457 and 72 (Fig. 4.11 B).

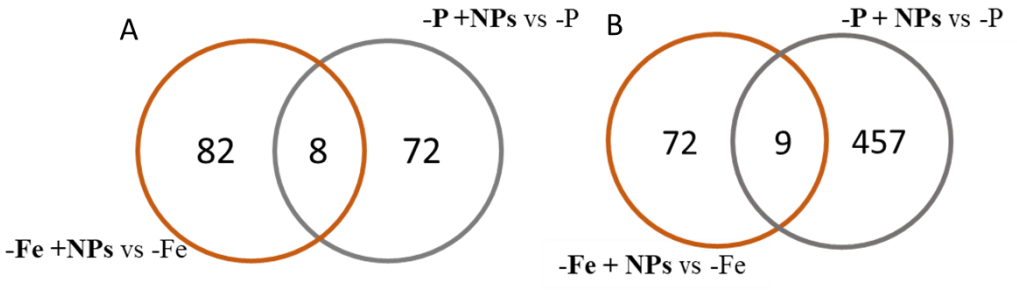

Figure 4.11. Venn diagrams showing specific and common differentially regulated transcripts by $FePO_4$ NPs regardless of their use as P or Fe source (adjusted p-value ≤ 0.05, |FC| ≥ 2). A cucumber, B maize.

In Table 4 transcripts commonly modulated by $FePO_4$ NPs in cucumber are listed. It is interesting to observe that their modulation is mainly opposite between the two transcriptional comparisons. The transcripts modulated by NPs in both nutritional conditions in maize are presented in Table 5.

Table 4. List of transcripts commonly modulated in the two comparisons -Fe+NPs vs -Fe and -P+NPs vs -P. Cucumber Gy14 v1 genome http://cucurbitgenomics.org/organism/7 FC: Fold Change value.

Transcript ID	ID *Arabidopsis*	Description	FC -Fe+NPs *vs* -Fe	FC -P+NPs *vs* -P
Cucsa.133230.1	AT1G70330.1	equilibrative nucleotide transporter 1 (ENT1)	4.6	-2.7
Cucsa.090660.1	AT1G56430.1	nicotianamine synthase 4 (NAS4)	7.2	-2.8
Cucsa.092390.1	AT1G56430.1	nicotianamine synthase 4 (NAS4)	9.0	-2.2
Cucsa.398260.2	AT5G64300.1	GTP cyclohydrolase II (GCH2)	3.4	-2.9
Cucsa.398260.1	AT5G64300.1	GTP cyclohydrolase II (GCH2)	3.3	-2.5
Cucsa.204430.1	AT2G01050.1	zinc ion binding; nucleic acid binding	-2.8	-2.5
Cucsa.166810.1	AT5G44440.1	FAD-binding Berberine family protein	11.1	-3.5
Cucsa.121580.1	AT1G68390.1	Core-2/I-branching beta-1.6-N-acetylglucosaminyltransferase family protein	3.4	5.2

Table 5. List of transcripts commonly modulated in the two comparisons -Fe+NPs vs -Fe and -P+NPs vs -P. Maize B73 genome ftp://ftp.gramene.org/pub/gramene/maizesequence.org/release-5b/; FC, fold change value.

Transcript ID	ID *Arabidopsis*	Description	FC - Fe+NPs vs -Fe	FC - P+NPs vs -P
GRMZM2G106511_T01	AT4G10270.1	Wound-responsive family protein (WIP4)	3,2	2,8
GRMZM2G106393_T01	AT4G10265.1	Wound-responsive family protein (WIP3)	3,3	2,0
GRMZM2G011636_T01	AT1G11890.1	Synaptobrevin family protein (SEC22)	3,4	2,2
GRMZM2G361475_T01	AT1G71695.1	Peroxidase superfamily protein (PER12)	2,0	-3,0
GRMZM5G829897_T01	AT5G45920.1	SGNH hydrolase-type esterase superfamily protein	2,1	2,2
GRMZM2G148374_T01	AT3G42640.1	H(+)-ATPase 8 (AHA8) catalytics;transferases;[acyl-carrier-protein] S-malonyltransferases;binding	4,2	3,4
GRMZM2G053639_T01	AT2G30200.2	(EMB3147)	3,1	3,2
GRMZM5G801307_T01		No hits found	2.5	-3.5
GRMZM5G851266_T01		No hits found	3.4	4.6

In cucumber (Table 4) most of the transcripts (7/8) were downregulated in case of $FePO_4$ NPs used as source of P, while they were mostly upregulated (7/8) in case of $FePO_4$ NPs used as source of Fe. On the contrary, in maize (Table 5) transcripts were mostly upregulated both when NPs are used as P or Fe source, with two exceptions: GRMZM5G801307_T01 and GRMZM2G361475_T01 (PER12) were downregulated in case of $FePO_4$ NPs used as source of P.

4.3.2 Real Time RT-PCR

Real time RT-PCR analyses were performed to validate the microarray expression analysis results. Table 6 indicates the transcripts utilized for the validation. Transcripts were chosen basing on the availability of a 3'-UTR sequence in the databases (http://cucurbitgenomics.org/organism/7; https://ensembl.gramene.org/Zea_mays/Info/Index) long enough to design good primers, and on the specificity of the primers. Table 6 reports the fold change value of microarray analysis and real time RT-PCR, indicating that the values correlated and showed the same verse of modulation. Most of the transcripts chosen were related to P or Fe homeostasis processes in the plant (such as PHT2.1 and FRO7 in *Z. mays* and ENT1 and NAS4 in *C. sativus*), with the exception of some not annotated transcripts (NotAn in *Z. mays* and UNK12 in *C. sativus*).

Table 6. Real time RT-PCR and microarray fold change comparison

Maize		Fold Change		
Transcript ID	**Name**	**Microarray**	**Real time**	**comparison**
GRMZM2G361475_T01	PER12	-3,01	-5,09	-P+NPs vs -P
GRMZM2G092780_T01	PHT2.1	-3,57	-5,11	-P+NPs vs -P
GRMZM2G703077_T01	DHS2	-2,98	-9,57	-Fe+NPs vs -Fe
GRMZM2G053639_T01	ACP	3,12	1,10	-Fe+NPs vs -Fe
GRMZM2G045699_T01	NotAn	-9,06	-2,32	-P+bulk vs -P
GRMZM2G068557_T01	FRO7	-2,03	-6,37	-P+bulk vs -P
GRMZM2G036631_T01	HMT	10,24	4,83	-Fe+bulk vs -Fe
GRMZM2G125196_T01	ZDH	5,40	2,31	-Fe+bulk vs -Fe
Transcript ID	**Name**	**Microarray**	**Real time**	**comparison**
Cucsa.133230.1	ENT1	-2,70	-1,75	-P+NPs vs -P
Cucsa.092390.1	NAS4	-2,21	-2,07	-P+NPs vs -P
Cucsa.133230.1	ENT1	4,58	3,10	-Fe+NPs vs -Fe
Cucsa.038100.1	POL	26,67	32,47	-Fe+NPs vs -Fe
Cucsa.106380.1	DEHY	-4,06	-1,75	-P+bulk vs -P
Cucsa.146940.1	THC	3,82	1,40	-P+bulk vs -P
Cucsa.066810.1	TAU	-3,27	-1,68	-Fe+bulk vs -Fe
Cucsa.122170.1	UNK12	-2,49	-2,00	-Fe+bulk vs -Fe

4.3.3 MapMan pathway analysis

The MapaMan analysis was performed on the four lists of differentially expressed transcripts identified both in cucumber in maize through the following comparisons: -P+NPs *vs* -P; -Fe+NPs *vs* -Fe; -P+Bulk *vs* -P; -Fe+Bulk *vs* -Fe. The Fig. 4.12 shows the percentage of transcripts assigned to each biological process for the four sets of differentially expressed transcripts of cucumber (Fig. 4.12) and maize (Fig. 4.13). In cucumber (Fig 4.12), the most represented categories in all the conditions was "RNA regulation", followed by "protein degradation". The "Cell wall" categories, which includes transcripts that concur to cell wall modifications, was more abundant in the transcriptional comparison carried out for the Fe nutrition (Fig 4.12 C; D). The "Stress" category displayed similar values of abundance both when NPs was supplied as source of P and Fe (Fig. 4.12 A, C). In the case of bulk, only when it was supplied as P source can caused a modulation of transcripts belonging to this category (Fig. 4.12 B, D). The category "Transport" was more abundant in the transcriptional comparisons involving NPs (Fig. 4.12 A, C). In maize (Fig. 4.13) around the fifty percent of the total modulated transcripts were not assigned to biological process categories in all transcriptional comparison. Similarly to cucumber, the categories "RNA process and regulation" and "Protein degradation" were the mostly represented in all the conditions. The "Cell wall" category is mainly abundant in the transcriptional comparisons concerning the P nutrition (Fig. 4.13 A, B). The "Stress" category showed similar

abundances considering the comparisons involving NPs (Fig. 4.13 A, C) whilst it was mainly abundant when bulk was supplied as Fe source (Fig. 4.13 D).

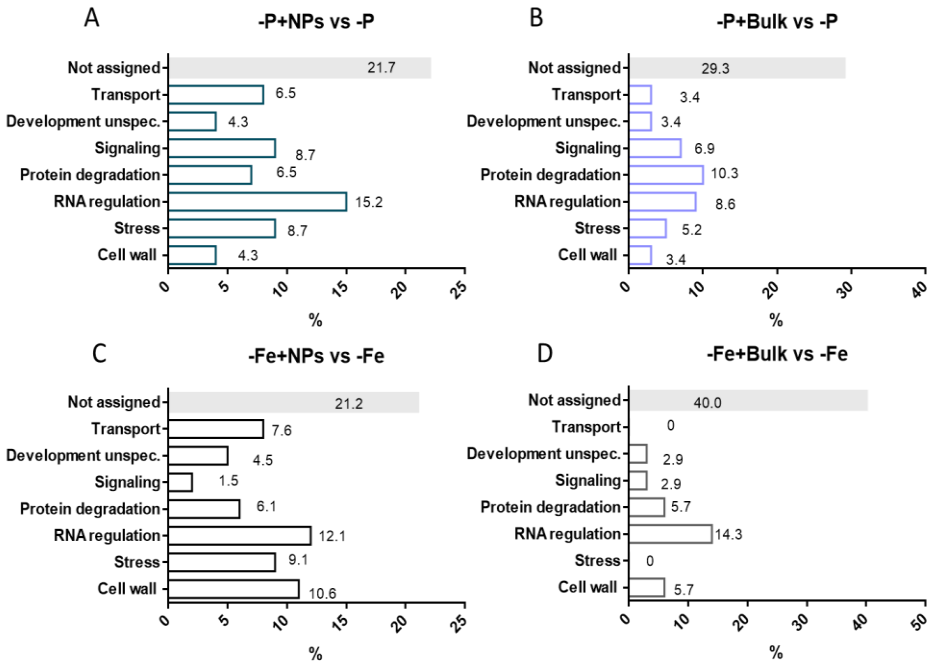

Figure 4.12. Percentage of transcripts distributed in main biological process categories according to MapMan analysis for the four transcriptional comparison carried out for cucumber roots. (A) -P+NPs *vs* -P. B) -P+Bulk *vs* -P. C) -Fe+NPs *vs* -Fe. D) -Fe+Bulk *vs* -Fe.

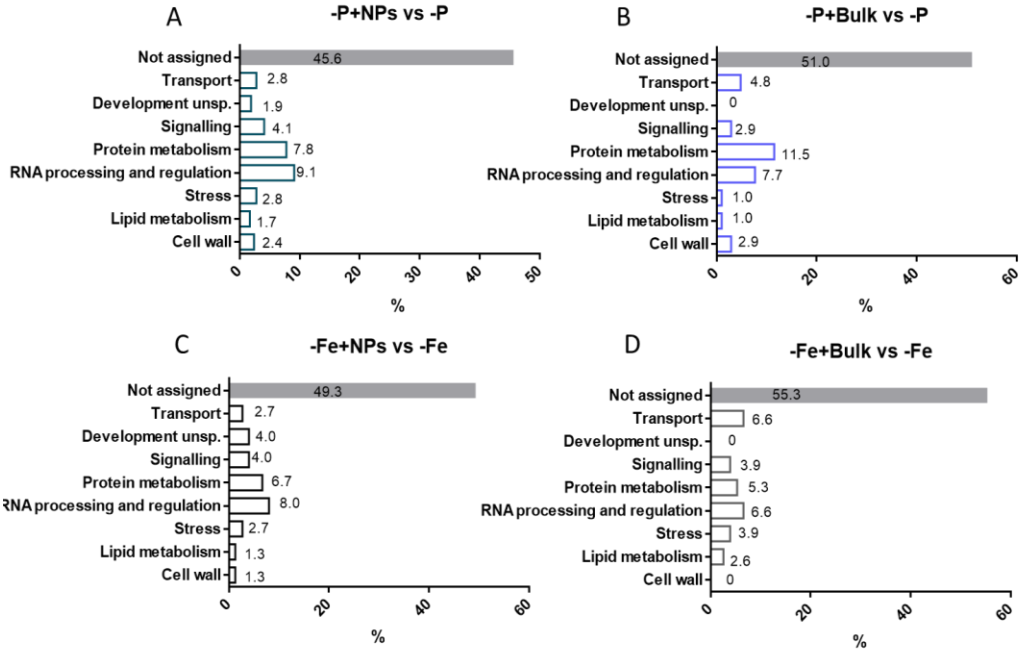

Figure 4.13. Percentage of transcripts distributed in main biological process categories according to MapMan analysis for the four transcriptional comparison carried out for maize roots. (A) -P+NPs vs -P. B) -P+Bulk vs -P. C) -Fe+NPs vs -Fe. D) -Fe+Bulk vs -Fe.

SECTION II

5. MATERIALS AND METHODS OF SECTION II

5.1 Soil samples preparation

In experiments on bare soils, two different soils were collected in two different areas of Tuscany, Cesa (AR) and La Romola (FI). Soils (named as CESA and ROMOLA) were analysed by Vassanelli Lab s.r.l (VR, Italy) and their characteristics are listed in Table 7. Soils have been hydrated to rise a humidity equal to the 55% of Water Holding Capacity (WHC) of each one, that accounted for the 31% for ROMOLA and the 47% for CESA. Control soil samples were hydrated with deionized water, treated soil samples where hydrated with a solution of $FePO_4$ NPs whose volume was calculated in order to apply 34 mg P per kg of dry soil. Control and treated soil were sampled at time zero, then incubated and sampled after one, four and seven days. Each sample was prepared in triplicate.

Table 7. Results of analysed Cesa and Romola soils.

ROMOLA

Analysis	Unit of measure	Value	Rating
Total $CaCO_3$	% w/w dry soil	1.1	
Active CaCO3	% w/w dry soil	0.3	Low
Organic C	% w/w dry soil	1.7	
Soil organic matter	% w/w dry soil	2.95	Medium
Total N (Kjeldahl)	% w/w dry soil	0.11	Medium
Assimilable P	mg/kg dry soil	3	Very low
Soluble B	mg/kg dry soil	0.3	Medium
C/N		16.1	Relative deficiency of N
Soil skeleton	% w/w dry soil	5.7	
Texture		**sand**	
Sand	% w/w dry soil	74.4	
Silt	% w/w dry soil	18.1	
Clay	% w/w dry soil	7.5	
pH (H_2O)		5.4	
Cation-exchange capacity (CEC)	mEq/100g	12.9	Deficiency - risk of nutrient leaching
Exchangeable CaO	mg/kg dry soil	2603	
Exchangeable calcium	mg/kg dry soil	1860	
Exchangeable MgO	mg/kg dry soil	672	
Exchangeable Mg	mg/kg dry soil	406	
Exchangeable K_2O	mg/kg dry soil	83	
Exchangeable K	mg/kg dry soil	69	
Exchangeable Na	mg/kg dry soil	14	
Mg/K		18.9	Relative excess of Mg
Ca/K		52.7	
Ca/Mg		2.8	

CESA

Analysis	Unit of measure	Value	Rating
Total $CaCO_3$	% w/w dry soil	3	
Active CaCO3	% w/w dry soil	2.4	Medium
Organic C	% w/w dry soil	0.78	
Soil organic matter	% w/w dry soil	1.35	Low
Total N (Kjeldahl)	% w/w dry soil	0.1	Medium
Assimilable P	mg/kg dry soil	8	Low
Soluble B	mg/kg dry soil	0.12	Low
C/N		7.6	Relative deficiency of carbon compounds
Soil skeleton	% w/w dry soil	1.5	
Texture		**Silt-Loam**	
Sand	% w/w dry soil	18.7	
Silt	% w/w dry soil	66.3	
Clay	% w/w dry soil	15	
pH (H_2O)		7.1	
Cation-exchange capacity (CEC)	mEq/100g	27.8	Excess- risk of plant/soil competition
Exchangeable CaO	mg/kg dry soil	7233	
Exchangeable calcium	mg/kg dry soil	5170	
Exchangeable MgO	mg/kg dry soil	305	
Exchangeable Mg	mg/kg dry soil	184	
Exchangeable K_2O	mg/kg dry soil	179	
Exchangeable K	mg/kg dry soil	148	
Exchangeable Na	mg/kg dry soil	10	
Mg/K		4	Equilibrated
Ca/K		68.1	
Ca/Mg		17.1	

5.2 Soil CO_2 respiration by titration (Isermeyer 1952, modified by Jaggi 1976)

To measure CO_2 emitted from soil, 50g of each soil were moistened with deionized water and then incubated at 25°C in 300 ml glass containers closed with rubber stoppers. A beacker containing 4 mL of 0,05 M NaOH was placed open into the same container of each sample to trap the evolved CO_2. After the incubation times (0, 1, 4,

7 days) 8 mL of 0,75 N $BaCl_2$ and 3 drops of phenolphtalein indicator were added to the beacker with 0,05 M NaOH. Carbonates precipitated with the $BaCl_2$, then the solution was titrated with 0,1 N HCl (Schinner et al., 1996). Results, expressed as mg CO_2 g^{-1} dry matter · $24h^{-1}$, were calculated with the formula: (C-S) · 2.2 · 100 / Soil Weight · % dry matter, where C is the mean volume of HCl consumed by controls (mL), S is the mean volume of HCl consumed by samples (mL) and 2.2 a conversion factor (l mL of 0.1 M HCI corresponds to 2.2mg CO_2).

5.3 BioTox™ test

Soil toxicity was evaluated by the BioTox test™ Flash Test (Aboatox Oy, Turku, Finland) according to the standard method (ISO 21338) (Lappalainen et al., 1999) BioTox™ is based on the inhibition of the luciferase activity and consequent emission of bioluminescence as indicator of toxicity of soil pollutants. The soil is considered as affected by toxicity if the inhibition percentage (INH%) is higher than 20% in comparison to the *V. fischeri* not in contact with soil. The soil samples used were air-dried for 72 hours after treatment with seven different doses of $FePO_4$ NPs corresponding to 3.4, 7.1, 13.1, 26.3, 52.5, 78.8 and 105 mg P/kg dry soil. The last dose is intended as 10 times a conventional agronomic dose for P, simulating an accidental spillage in field.

5.4 Soil enzyme activity

Enzyme assays were adapted from Schinner et al (1996)(Schinner et al., 1996). On sampled soils the activities of acid-alkaline phosphatases, arylsulphatases, β-glucosydases and proteases were determined. The used substrates are the following: 115 mM 4-nitrophenyl-P disodium salt for acid and alkaline phosphatases (phosphomonoesterases), 25 mM 4-nytrophenil sulfate for arylsulphatase, 25 mM 4-nytrophenil beta-glucopyranoside for β-glucosidase and 1% (w/v) casein in 0.1 M Tris-HCl (pH 8.1) for protease. As media, Modified Universal Buffer (MUB) was used for alkaline phosphatase, acid phopsphatase, and β-glucosydase at pH of 11, 6.5, 6 respectively. The 0.5 M acetate buffer was used as media for arylsulphatase and 0.1 M Tris-HCl (pH 8.1) was used as media for protease. For the first four enzyme activities, 0.5 g of soil were weighted in 13 mL tubes, 2 mL of medias and 0.5 mL of substrates were added, then tubes were incubated at 37°C in shaking bath for 1 hour. Reactions were blocked by adding 2 mL of 0.5 M NaOH and 0.5 mL of 0.5 M $CaCl_2$ to each tube. Five millilitres of deionized water were added, then the tubes were centrifuged using a Beckman J2-HS centrifuge at 4425 rcf (5000 rpm with JA-10 rotor) for 10 minutes. The p-nitrophenol (pNP) released from the substrates by the action of enzymes was determined by reading absorbance at 400 nm on the spectrophotometer. The concentration of pNP expressed as mg/g soil was calculated for each sample using a calibration curve (0, 20, 40, 80 and 160 mg/L of pNP) and values were normalized on the water content

of each sample. Blank samples were prepared in the same manner of test tubes, but substrates were added only after the incubation. Values of blanks were subtracted from values of test samples. For protease, 1 g of soil was weighted. Two millilitres of 0.1 M Tris-HCl (pH 8.1) were added in blank tubes, while 2 mL of 1% (w/v) casein in Tris-HCl were added into test tubes. Samples were incubated in shaking bath at 50°C for 2 hours, after incubation 2 mL of Tris-HCl were added to test tubes, and 2 mL of casein in Tris-HCl were added to blank tubes. One millilitre of 17% (w/v) trichloroacetic acid (TCA) was added then tubes were centrifuged at 5000 rpm for 10 minutes. Then, 3.5 mL of 3,7% (w/v) Na_2CO_3 and 0.5 mL of 0,06% (w/v) $CuSO_4$ were added to 2.5 mL of supernatant. After 30 minutes of incubation at room temperature, 2.5 mL of 1:4 Folin & Ciocalteu reagent were added, and absorbance at 700 nm was read after 20 and 40 minutes. The concentration of L-tyrosine (mg/g soil) were calculated basing on a calibration curve (0, 1.25, 2.5, 3.75, 5 and 6.25 mg/L of L-tyrosine) and values were normalized on the ratio water/dry soil of each sample. Values of blanks were subtracted from values of test samples.

5.5 Soil DNA extraction and amplification

Genomic DNA was extracted from soil using DNeasy® PowerLyzer® PowerSoil® Kit (QIAGEN) according to the producer's manual. Homogenization of the samples were done through FastPrep-24™ set at speed of 6 m/s for 40 seconds. DNA successful extraction was verified through a 0.8% (w/v) agarose gel electrophoresis with TAE buffer (40 mM Tris, 20 mM acetic acid and 1 mM EDTA) and ethidium bromide 1:10000. Four microliters of the solution of extracted DNA per sample were loaded with 2 µL of 5X Green GoTaq® Flexi Buffer. Soil DNA is highly degraded, therefore when DNA extraction was successful, on the agarose gel was visible as smears.

PCR reactions were performed using specific primers to amplify the small subunit rRNA of Bacteria, Fungi and Archaea. Amplifications were carried out using 5 ng of DNA in a 25-µL volume containing 1X Flexi PCR buffer (Promega, Madison, WI), 1.5mM $MgCl_2$, 250 µM deoxynucleotide triphosphates (dNTPs), 400 nM each primer, 0.4 ng/µl BSA, and 1U GoTaq®Flexi DNA polymerase (Promega). PCR reaction for the bacterial 16S rDNA V6-V8 region was performed using the GC986f/UNI1401r primer pair (Felske et al., 1998); PCR reaction for fungal 18S rDNA V7-V8 region was performed using the EF390/GCFR1 primer pair (Eeva J. VAINIO & Jarkko HANTULA, 2000); archaeal 16S rDNA amplicons were obtaining using GC1106F/1378R primer pair(Watanabe et al., 2006). The PCR conditions were the following: 95 °C for 3 minutes, 95 °C for 30 seconds, 55 °C (48 °C for fungi) for 30 seconds, and 72 °C for 45 seconds (34 cycles), followed by 5 minutes at 72 °C. PCR products were analysed on a 1% (w/v) agarose gel in TAE buffer and yields were estimated by comparing amplified DNA to Low DNA mass ladder (Invitrogen) using the Chemidoc system (Bio-Rad). To minimize the effect of PCR bias, three independent PCR amplifications

for each sample were conducted and mixed prior to DGGE analyses (Pastorelli et al., 2020).

5.6 DGGE microbial community analyses

DGGE is an electrophoretic separation method based on differences in melting behaviour of double stranded DNA fragments (Felske et al., 1998). DGGE gels were prepared using the Protean® II system (Protean II xi 2-D Cell) by BIORAD as described by (Zwart & Bok, 2004). DGGEs were carried out in an 8% (w/v) polyacrylamide gel with a 38–74% denaturing gradient for Archaea, an 8% (w/v) polyacrylamide gel with a 35–65% denaturing gradient for Fungi and a 6% (w/v) polyacrylamide gel with a 45–65% denaturing gradient for Bacteria. Thirty microliters of each amplification reaction were loaded on a polyacrylamide gel (40% acrylamide/bis 37.5:1; Fisher Scientific, Geel, Belgium). Denaturant gradient was obtained using a stirred gradient maker with the two solutions corresponding to the higher and the lower denaturing percentage for each type of gel. As stock solutions were used a 100% denaturant solution and a 0% one. The 100% denaturant solution consisted of 250 mL of 40% (v/v) deionized formamide (VWR, West Chester, PA, USA), 7M Urea (Promega, Madison, WI, USA) and TAE 1X, and a 0% denaturing solution without Urea and formamide. Stacking gels were prepared in 5 mL 0% stock solution including 130 mL of APS and 45 mL of tetrametiletilendiammina (TEMED). Gels were run in a 1X TAE buffer for 17 hours at 60 °C and constant voltage (90 V) and an electric current intensity of 100 mA. After DGGEs gels were stained with SYBR®Gold (Molecular Probes, Eurogene, OR, USA) 1:1000 in 1X TAE buffer, and images were captured under UV light (λ=302 nm) using the ChemiDoc XRS apparatus (Bio-Rad). Evaluation of band migration distance and intensity within each lane of the DGGEs was performed using GelCompar II software v. 4.6. Multivariate analyses were performed in Past software version 3.22 (Hammer et al., 2001). Non-metric multidimensional scaling (nMDS) was used to visualize differences of DGGE profiles in two-dimensional space; the accuracy of the nMDS plots was determined by calculating a 2D stress value. One-way analysis of similarity (ANOSIM) using Bray-Curtis distance measure and permutational multivariate analysis of variance (PERMANOVA) with 9999 permutational tests were performed to determine whether DGGE profiles were significantly different from each other and if the differences can be observed among the different populations of data (Pastorelli et al., 2020; Ramette, 2007).

5.7 P Availability (Olsen method, 1982)

Available phosphorus was assayed in bare soil and rhizospheric soil samples. Two grams of dry soil were used for each condition. To these, 0.5 g of active charcoal washed with 0.5 M $NaHCO_3$ (pH 8.5) were added to avoid interferences of organic matter into results. P was extracted by shaking soil aliquots in 40 mL of 0.5 M $NaHCO_3$ (pH 8.5) for 30 minutes. Solution was filtered on Whattman filter paper 42 (11 cm).

The pH of the filtered solution was neutralized adding 2.5 M H_2SO_4 drop by drop until the yellow indicator 0.1% (w/v) pNP became clear. Eight millilitres of solphomolybdic reagent were added and volume raised to 50 mL then absorbance at 720 nm was read at spectrophotometer (Olsen & Sommers, 1982). The P concentration was determined basing on a calibration curve (0, 0.2, 0.4, 0.6, 0.8, 1 mg/L of P, KH_2PO_4 was used as standard).

6. RESULTS OF SECTION II

6.1 Impact on soil microbiome

To evaluate the impact of $FePO_4$ nanoparticles fertilization on the soil system, analyses of soil biochemical parameters and of microbial communities after the treatment with $FePO_4$ NPs were done. For these analyses, a sandy (Romola) and a silty (Cesa) soil were chosen. The physic-chemical characteristics are listed in Table 7. Each soil was treated with a suspension of $FePO_4$ NPs in deionized water in a dose of 34 mg/kg (ppm) of P, a dosage estimated to correspond to 300 kg/ha of P (2,5 times the agronomic dosage of 120 kg/ha). Control samples were prepared for each soil by a treatment with deionized water. On the two soils, BioTox™ test was performed to evaluate a putative toxic effect of $FePO_4$ NPs. In addition, soil CO_2 respiration and soil enzyme activities were analysed to evaluate the metabolic activity of microorganisms after the treatment. Furthermore, DGGE was performed on DNA extracted from the soils to investigate the eventual changes in the structure of the microbial community after the treatment.

6.1.1 BioTox™ test

BioTox™ test was performed on Romola (sandy) and Cesa (silty) soils. The test reports the existence of toxicity when a dose/response curve exceeding the 20% of luminescence inhibition of *Vibrio fischeri* (INH) is observed. Curve fitting of INH did not show a growing trend and never exceed the 20% threshold, except for the second dosage of 7,1 mg/kg of P in Romola soil (Fig 6.1 A). Since this is the only point that oversteps the threshold, it can be considered as a stochastic variation that, anyway, did not affect the curve fitting. In Cesa soil, all the points remained below the threshold and showed a good fitting (R^2=0,0274) (Fig. 6.1 B), so the treatment with $FePO_4$ NPs can be considered not toxic for the two soils at the tested doses.

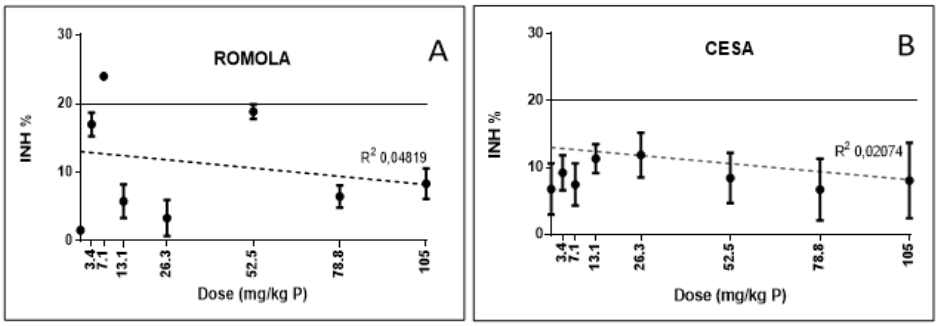

Fig. 6.1. BioTox™ test of Romola (A) and Cesa (B) soil samples after treatment with $FePO_4$ NPs in doses of 0, 3.4, 7.1, 13.1, 26.3, 52.5, 78.8, 105 mg/kg P. Dashed lines represent the non-linear regression analyses. R square values are reported on each graph. Data are means ± SD of three independent experiments Error bars represent the higher and the lower values.

6.1.2 Soil CO_2 respiration

As index of metabolic activity, measurements of evolved CO_2 at time zero, after 1, 4 and 7 days were performed (Fig. 6.2). Romola (R) and Cesa (C) soils showed two different trends of CO_2 respiration, due to their different nature. As expected for a sandy

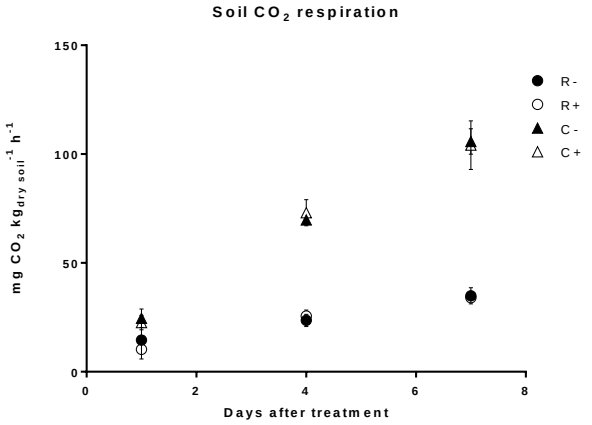

Figure 6.2. mg of CO_2 evolved per kg of dry soil per hour, after the treatment (+) with $FePO_4$ nanoparticles of the Romola (R) and Cesa (C) soils, compared with the control (-) treated with deionized water. Analysis have been performed after 0,1,4 and 7 days of incubation. Data are means ± SD of three three biological replicates (unpaired t test between each condition for each sampling time, $p<0.05$)..

soil, which possess a lower organic matter content (Lohila et al., 2003), Romola had a lower overall CO_2 evolution, but no statistical differences were detected between control (-) and treated (+) samples in all the four sample times for each soil, indicating that $FePO_4$ nanoparticles did not impact this index of metabolic activity of the microbial community.

6.1.3 Soil enzyme activities

The activity of five soil enzymes (alkaline phosphatase; acid phosphatase; arylsulfatase; beta-glucosydase; protease) were tested in order to evaluate the metabolic activity of soil microbial communities. Soil enzyme activities mirror the ability of soils to perform biogeochemical reactions (Nannipieri et al. 2018) considering both actively secreted enzymes and extracellular soil particles-adsorbed enzymes.

6.1.3.1 Acid and alkaline phospho-monoesterases

Phosphorus uptake by plants depends on the mineralization of the organic P into orthophosphate (PO_4^{3-}) catalysed by phosphatases. Phosphatases are enzymes whose production is induced in several organisms under conditions of low phosphorus availability. Phosphomonoesterase (generally so-called phosphatases in *sensu latu*) are commonly used as an index of phosphatase activity, plus they differ from pH optimum, so it is possible to differentiate in acid (Fig. 6.3 A; B) and alkaline (Fig. 6.3 B; C) phosphomonoesterases. Phosphatase activity of Cesa (A; C) and Romola (B; D) soils did not evidence any significant difference after the treatment with $FePO_4$ NPs at time zero and after 1, 4 and 7 days of incubation.

6.1.3.2 Arylsulfatase

Sulphatases are enzymes that hydrolyze the S-O bond present in organic sulfates and provide available sulfur in form of anionic sulfate (SO_4^{2-}) to plants. Arylsulphatases were the first class of sulphatases to be described and thus the most investigated. As well as for phosphomonoesterases, arylsulphatase did not show any significant difference after the treatment with $FePO_4$ NPs at time zero and after 1, 4 and 7 days of incubation both in Cesa (Fig. 6.3 A) and Romola (Fig. 6.3 B) soils.

6.1.3.3 β-Glucosydase

β-Glucosidases are a class of enzymes involved into carbon metabolism. They hydrolyse carbohydrates with a β-D-glycoside bond and play an important role in total degradation of cellulose to glucose. In cellulose catabolism, endo- and exo- β -I,4-glucanases hydrolyse cellulose to cellobiose, which is converted to glucose by β-Glucosidases. As well as phosphomonoesterases and arylsulphatase, β-Glucosidases did not show any significant difference after the treatment with $FePO_4$ NPs at time zero and after 1, 4 and 7 days of incubation in Cesa (Fig. 6.4 A) and Romola (Fig. 6.4 B) soils.

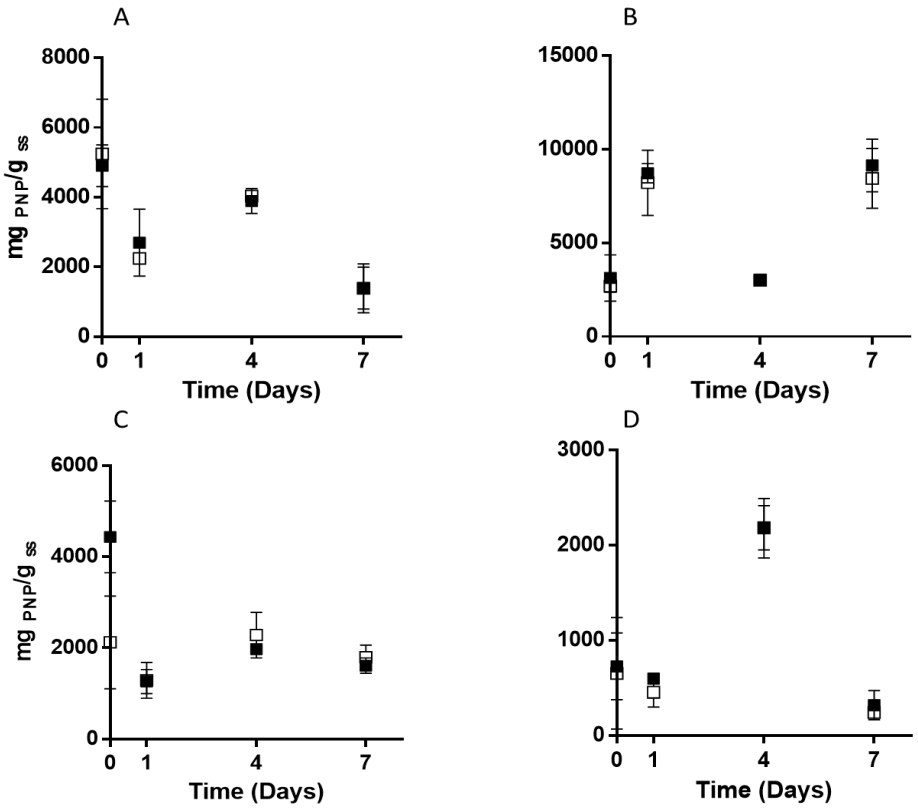

Figure 6.3 Acid (A; B) and alkaline (C; D) Phosphomonoesterases activities, after 0; 1; 4; 7 days of incubation of Cesa (A; C) and Romola (B; D) treated with $FePO_4$ NPs. Control samples have been treated with deionized water. Full squares: NPs treatment. Empty squares: Control. Data are means ± SD of three three biological replicates (unpaired t test between each condition for each sampling time, $p<0.05$).

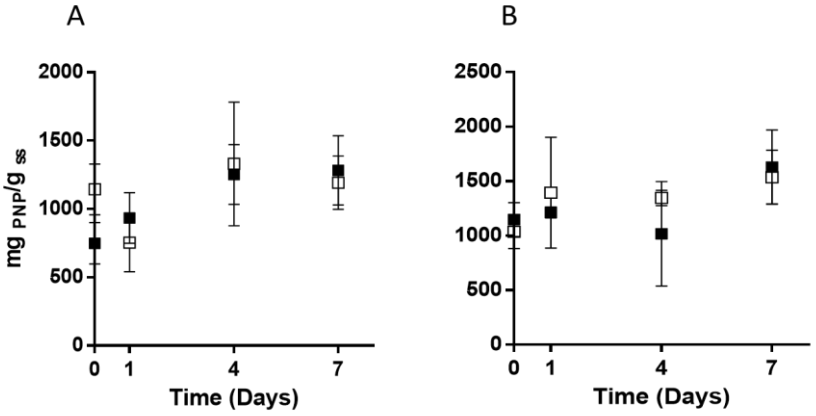

Figure 6.4. Arylsulphatase activity, after 0; 1; 4; 7 days of incubation of Cesa (A) and Romola (B) treated with $FePO_4$ NPs. Control samples have been treated with deionized water. Full squares: NPs treatment. Empty squares: Control. Data are means ± SD of three three biological replicates (unpaired t test between each condition for each sampling time, $p<0.05$).

6.1.3.4 Protease

Proteases are a group of enzymes produced by many bacteria and fungi. Their functions are relevant since while proteins represent a third of the total nitrogen in soil (Ladd & Butler, 1972). Extracellular secreted proteases degrade proteins, releasing ol-

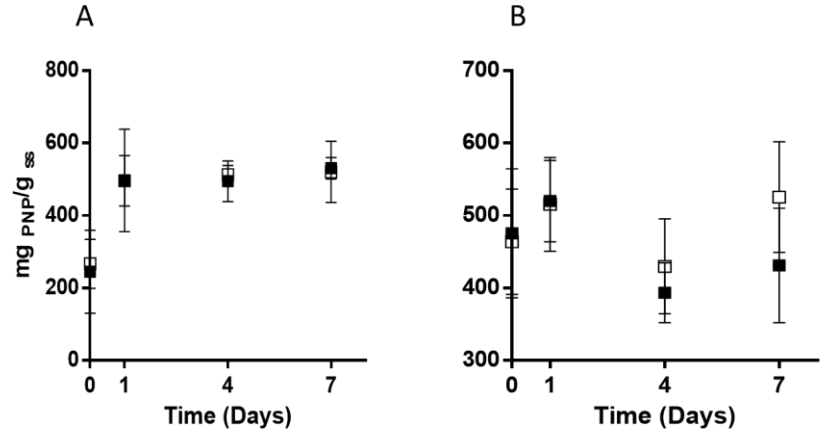

Figure 6.5. β-Glucosidase activity, after 0; 1; 4; 7 days of incubation of Cesa (A) and Romola (B) treated with $FePO_4$ NPs. Control samples have been treated with deionized water. Full squares: NPs treatment. Empty squares: Control. Data are means ± SD of three three biological replicates (unpaired t test between each condition for each sampling time, $p<0.05$).

igopeptides and low molecular weight compounds which are assimilated by microorganisms. Released proteases can be physically adsorbed onto soil colloids or covalently bound to soil organic matter, resulting in an immobilization of these enzymes that can resist proteolysis for long time. T-test of data from protease enzyme activity of Cesa soil (Fig. 6.5 A) evidenced lower values in treated sample than in control sample after 1 and 4 days of incubation. At the 7th day, protease did not show any significant difference between control and treated samples, as well as at time zero. Protease in Romola soil (Fig. 6.5 B) did not show any significant difference after the treatment with $FePO_4$ NPs at time zero and after 1, 4 and 7 days of incubation.

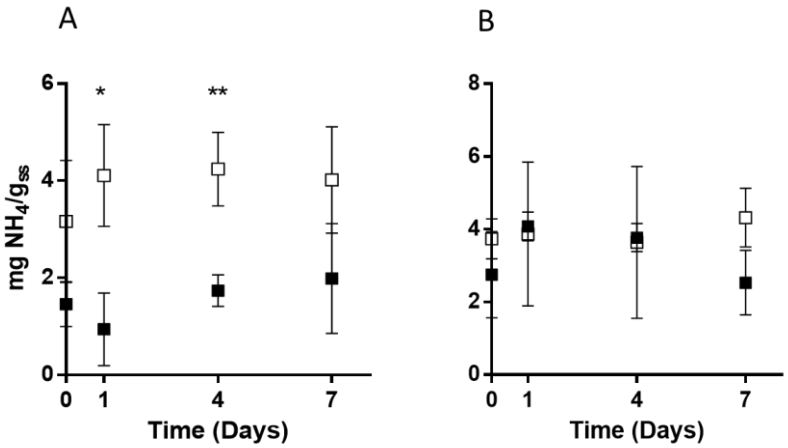

Figure 6.6. Protease activity, after 0; 1; 4; 7 days of incubation of Cesa (A) and Romola (B) treated with $FePO_4$ NPs. Control samples have been treated with deionized water. Full squares: NPs treatment. Empty squares: Control Data are means ± SD of three three biological replicates (unpaired t test between each condition for each sampling time, $p<0.05$). Asterisks indicate significant differences.

6.1.4 DGGE pattern analysis of soil microbial communities

To investigate the effects of a treatment on the structure of a microbial community is fundamental to understand which selection among bacteria, fungi, or archaea species the treatment could trigger. In a view of environmental risk evaluation, it is important to assess whether a nanofertilizer can cause an increase of some microbe species and/or a decrease of some others. Figures 6.6 and 6.7 show the NMDS similarity analysis of quantitative matrixes from DGGE gel patterns for Bacteria 16S rDNA (A; D), Fungi 18S rDNA (B; E) and Archaea 16S rDNA (C; F). The absence of a clusterization of the replicates within to the treatment at time zero (Fig. 6.6) and after 1, 4 and 7 days of incubation (Fig. 6.7), demonstrates that matrixes coming from gel pattern analysis did not show any significant differences caused by the treatment with $FePO_4$ NPs. Moreover, ANOSIM statistical analyses (Table 8) showed that the slight differences among the microbial communities did not depend on the treatment.

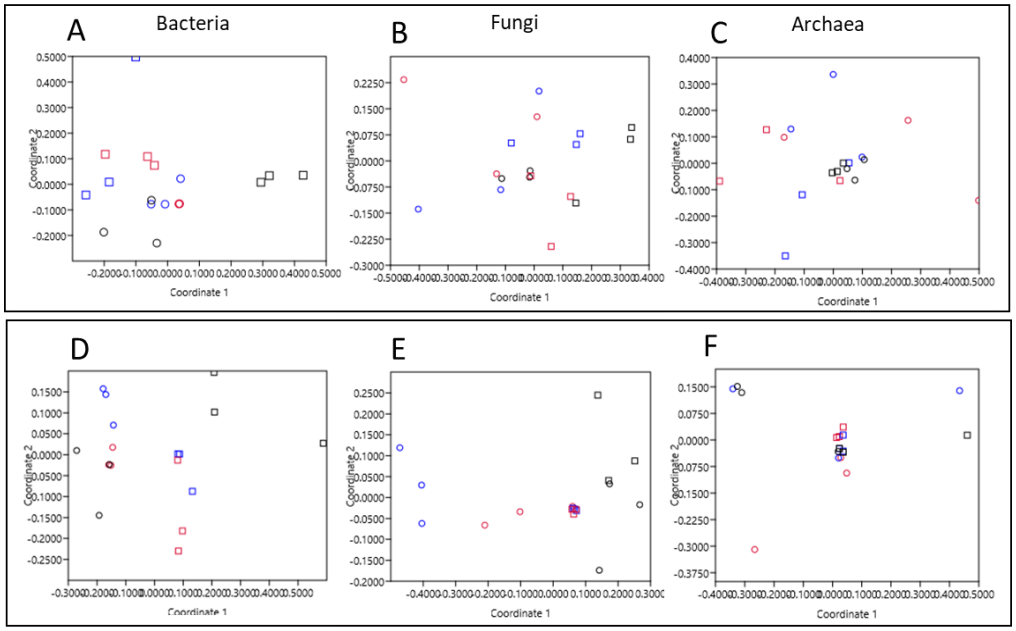

Figure 6.7 Two-dimensional plots of nMDS analyses of quantitative matrixes from DGGE gel patterns for Bacteria 16S rDNA (A; D), Fungi 18S rDNA (B; E) and Archaea 16S rDNA (C; F). A, B and C represent the graphs of Cesa soil, whereas D, E and F represent the graphs of Romola soil. Circles represent control samples, whereas squares represent treated samples. Stress values of NMDS analysis were: A=0.09837; B=0; C=0; D=0; E=0; F=0.

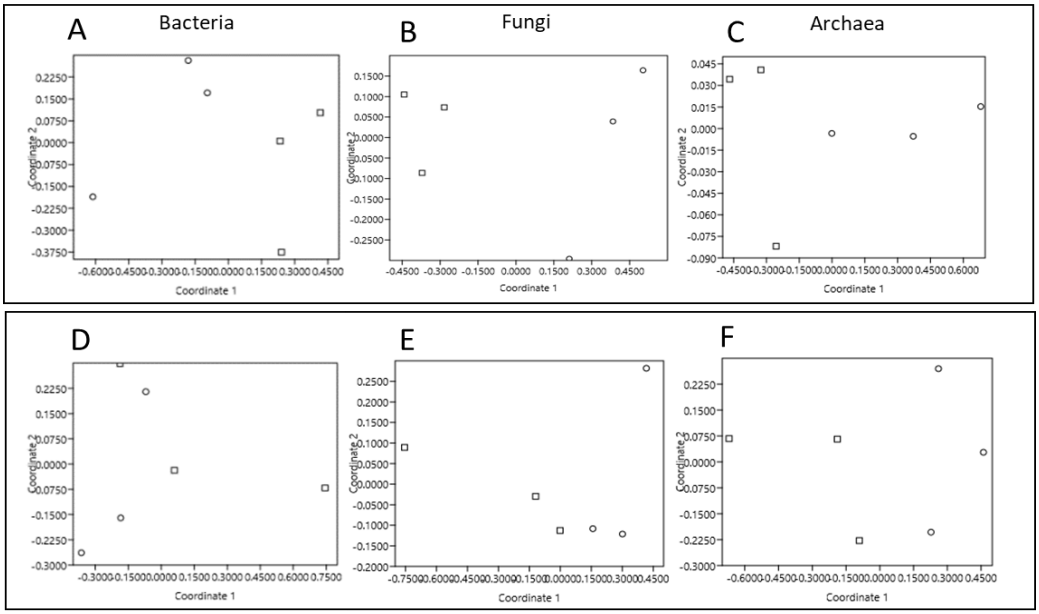

Figure 6.8. Two-dimensional plots of nMDS analyses of quantitative matrixes from DGGE gel patterns for Bacteria 16S rDNA (A; D), Fungi 18S rDNA (B; E) and Archaea 16S rDNA (C; F). A, B and C represent the graphs of Cesa soil, whereas D, E and F represent the graphs of Romola soil. Circles represent control samples, whereas squares represent treated samples. Blue represent samples after 1 day of incubation, red after 4 days, black after 7 days. Stress values of NMDS analysis were: A= 0.1545; B=0.117; C=0.09233; D= 0.1224 E= 0.06245; F= 0.1577.

Table 8. ANOSIM global test based on Bray-Curtis similarity index of Bacteria 16S, Fungi 18S and Archaea 16S rDNA-DGGE profiles analysed by treatment or time (two-way ANOSIM) or by control vs treatment in time zero soil samples (one-way ANOSIM). Values presented are the R-value (R) and the P statistic (P) of significance (Clarke, 1993). R=0 means samples are not different. R=1 means sample are different. R=0,75 means samples are different but overlapping.

Soil	**DGGE gel**	Two-way ANOSIM			
		Factor Treatment		Factor Time	
		R	*P*	R	*P*
Cesa	Fungi 18S	0.43827	0.0165	0.072016	0.2527
	Bacteria 16 S	0.60494	0.002	0.45267	0.0005
	Archaea 16 S	0.23457	0.0549	0.107	0.131
Romola	Fungi 18S	0.5679	0.0008	0.69136	0.0001
	Bacteria 16 S	0.96296	0.0015	0.40329	0.0002
	Archaea 16 S	0.32099	0.007	0.1893	0.0671
Time Zero samples					
Soil	**DGGE gel**	One-way ANOSIM (Control vs Treatment)			
		R	*P*		
Cesa	Fungi 18S	1	0.1012		
	Bacteria 16 S	0.5926	0.098		
	Archaea 16 S	0.7407	0.1017		
Romola	Fungi 18S	0.2963	0.1014		
	Bacteria 16 S	0.03704	0.5065		
	Archaea 16 S	0.7037	0.0994		

6.2 Availability of P after the application of $FePO_4$ NPs on bare soil

To assess if fertilization with $FePO_4$ NPs would be as effective as a commercial non nano-fertilizer, chemical analysis of available P through Olsen method was performed. As a comparison, triple superphosphate (TSP) was used as positive control. Test samples were treated with a suspension of $FePO_4$ NPs (NPs) in a dose of 34 mg/kg (ppm) of P. Deionized water was used to hydrate soil negative control sample (Control) at time zero and after 1, 4 and 7 days of incubation.

6.2.1 Olsen available Phosphorus

The Romola soil displayed different levels of extractable P as a function of the treatment all over the incubation experiment (7 days) (Fig. 4.21 A). Control samples always showed the lower values; NPs samples had lower available P content than TSP samples at almost all the incubation times, indicating that the "chemical" availability of P is lower in soils fertilized with $FePO_4$ NPs. Conversely, Cesa bare soil samples (Fig. 4.21 B) showed no significant differences among all the three conditions in available P, except for the 7^{th} day of sampling in which NPs provided slightly higher level of P.

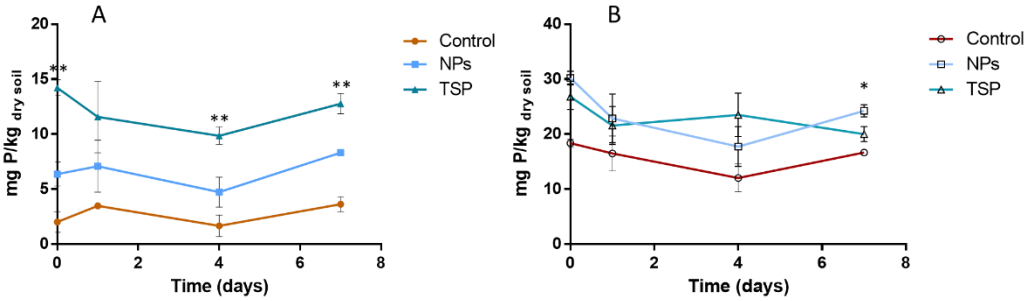

Figure 6.9. Phosphorus availability measured through Olsen method in soil samples (A: Romola, B: Cesa) treated with $FePO_4$ NPs (NPs), with triple superphosphate (TSP) and with deionized water (control). Analyses have been performed on sampled incubated for 0, 1, 4 and 7 days after treatment. Data are means ± SD of three three biological replicates asterisks indicate the existence of significant statistical differences in unpaired t test between NPs and TSP for each sampling time, $p<0.05$).

SECTION III

7. MATERIALS AND METHOD OF SECTION III

7.1 Plant growth in pots

After germination of seeds of *Cucumis sativus* Viridis F1 hybrid (Franchi Sementi S.p.A.) on paper soaked with 1 mM $CaSO_4$ in dark at 25°C and one seedling per condition were transferred into 0.5 kg pot containing 350 g of Romola soil sieved at 0.5 cm. Five different pots were set-up. Plants were grown for 28 days in 16/8 light photoperiod; 25 °C ± 1; 50% ± 5 humidity; light irradiance of 70-100 μmol m^{-2} s^{-1} of PPFD as PAR. Measurement of SPAD index and leaves area were taken after 9, 14, 21 and 28 days. Pots where periodically hydrated with deionized water to maintain a constant soil humidity. Plants were fertilized at day 1^{st}, 7^{th}, 14^{th} and 21^{st} with 100 mL of nutrient solution in order to reach the amount of 80 mg/kg dry soil of $Ca(NO_3)_2$ and 34 mg/kg dry soil of P for each replicate after four fertilizations. $Ca(NO_3)_2$ is provided to limit the relative deficiency of N in Romola soil concerning the C/N ratio of 16.1 (see Table 3). Conditions were plants grown without P (-P); plants grown with $FePO_4$ NPs as P source (NPs); plants grown with triple superphosphate as P source (TSP). After 28 days, plants were sampled and dry weight was taken, roots analysed with WinRHIZO™ software, photosynthetic parameters acquired with PhotosynQ™. Rhizospheric soil was sampled to perform enzyme assays, DGGE, P availability (Olsen). Experiment was reproduced into three technical replicates.

7.2 Dry weight

Dry weight of samples was measured with analytical weight scale after 72 hours of drying in a 60°C oven. Root and shoot samples were measured separately.

7.3 SPAD index measurement

SPAD index was expressed as the average of all the leaves of each plant. For each leaf, the average value of five measurements performed using SPAD-502 Plus Chlorophyll meter® (Konica Minolta) was calculated. For maize and cucumber plants grown in hydroponics SPAD index was determined after 10 days and 13 days of growth respectively. P deficiency symptoms are more evident on older leaves, while Fe deficiency is more evident on young leaves, as consequence of the relative mobility of the nutrients in the plant (Marschner, 2011). Therefore, SPAD index was determined on second leaves for maize plants, that in this experimental setup showed a more marked Fe deficiency symptomatology, whereas first leaf was measured in cucumber, that showed a more marked P deficiency symptomatology.

7.4 Leaves area measurement

Pictures of plants were taken weekly, and images were analysed with ImageJ® software (http://imagej.nih.gov/ij/download.html). Leaves aera was calculated scaling the

measurements on a marker of 1 cm present in each picture and previously positioned on each pot in order to reach the highest point of the canopy of each plant.

7.5 Root analysis

At the last day of sampling, images of roots of three plants per condition for hydroponic experiments and five per condition for soil experiment, were acquired with EpsonV700 perfection. Images were then analysed with WinRHIZO™ software 2015a Pro version (Regent Instruments Inc.) using the "root morphology" mode. By means of this analysis, root volume, length and surface area were estimated to determine the effect of the treatments on the roots.

7.6 Elemental analyses using ICP-MS

ICP-MS analysis needs samples to be digested before to be analysed. Shoot and root plant tissues were dried in an oven at 60°C for 72 hours. Milled tissues (about 10-20 mg) were digested with a solution of 250 µL of 68% HNO_3 ultra-pure (Romil LTD) in a 3-mL TFM microsampling insert (Milestone Srl). Three inserts were placed inside a 100-mL TFM vessel with 11 mL Milli-Q water and 1 mL of ultrapure grade H_2O_2 (30% Romil LTD). and 1 mL of 30% H_2O_2 at in a StartD® microwave digestion system (Milestone Srl). The digestion was performed at 180 °C for 20 minutes in a StartD (Milestone Srl) microwave digestor. Digested samples were diluted with ultra-pure grade water (18.2MΩ·cm at 25 °C) in order to reach the 2% of HNO_3 then analysed with Agilent 7500ce ICP-MS detection system (Agilent technologies).

A calibration curve was achieved diluting a custom multielement standard solution (Romil LTD). Measurement accuracy and matrix effect errors were checked using NIST standard reference material 1515 (Apple leaves)

7.7 Rhizospheric soil experiments.

Materials and methods of the experiment on rhizospheric soil were performed as already described in the materials and methods of section II.

8. RESULTS OF SECTION III

Data acquired from plants grown in hydroponic condition in the case of $FePO_4$ NPs used as source of P, reported more evident results for cucumber, whereas maize reported more evident results in the case of $FePO_4$ NPs used as source of Fe. Hydroponic results are not easily transposable to those that could be obtained in the case of plant grown in soil, due to the wider range of variables to account, such as soil composition, plant adaptation, microbial community etc. Therefore, to better describe the effect of fertilization with $FePO_4$ NPs the experiments on P fertilization in cucumber plants grown in soil were carried out. The choice of the soil fell on Romola soil that, in the case of Olsen P availability, showed important differences between each treatment. Experiments were set up using the same three conditions described in section II: negative control plants in P deficiency (-P), positive control plants fertilized with triple superphosphate (TSP) and test plants fertilized with $FePO_4$ NPs in the same dosage of the previously described experiments (34 mg/kg P) (paragraph 4.3).

8.1 Plant: *Cucumis sativus*

8.1.1 Dry weight

After 28 day of growth shoot and root dry weight of $FePO_4$ NPs fertilized plants and triple superphosphate (TSP) fertilized plants cultivated in Romola soil did not show significant differences between each other. Nevertheless, both the two conditions produced more root and shoot biomass that P deficient plants (-P) (Fig. 8.1).

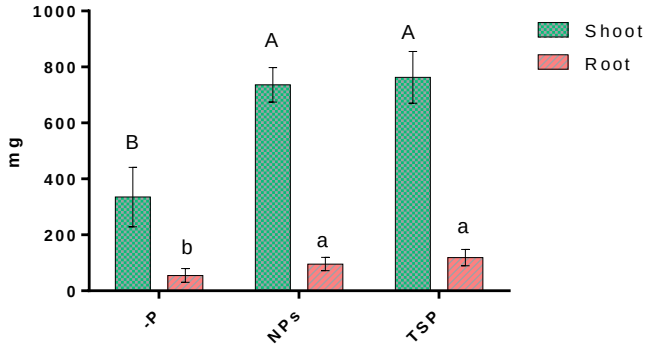

Figure 8.1. Dry weight of cucumber plants after 28 days of growth in Romola soil in pot. Plants grown without P (-P); plants grown with $FePO_4$ NPs as source of P (NPs); plants grown with triple superphosphate as source of P (TSP). Data are means ± SD of three independent experiments with five biological replicates each one (One-way ANOVA with Turkey's test, $p<0.05$). Significant differences are indicated by different letters, capital letters are related to shoot data, whereas lowercase letters are related to root data.

8.1.2 Leaves Area

Scarce P supply causes a reduced availability of assimilates that are used by the plant to expand the leaves, thus in turn limiting the total activity of the photosynthetical

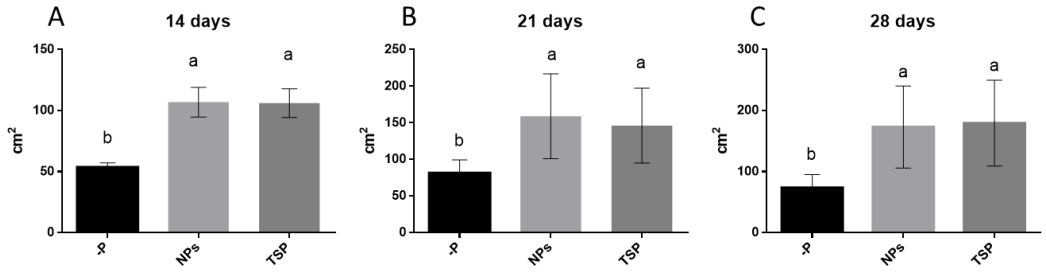

Figure 8.2. Leaves area of cucumber plants after 14, 21 and 28 days of growth in Romola soil in pot. Plants grown without P (-P); plants grown with $FePO_4$ NPs as source of P (NPs); plants grown with triple superphosphate as source of P (TSP). Data are means ± SD of three independent experiments with five biological replicates each one (One-way ANOVA with Turkey's test, $p<0.05$). Significant differences are indicated by different letters.

apparatus. For this reason, it was important to assess the rate of leaves expansion in order to obtain a comprehensive interpretation of all the data. Leaves area were measured with a non-destructive method based on the ImageJ software analysis of plant pictures at three different times, 14 days (Fig. 8.2 A), 21 days (Fig. 8.2 B) and 28 days (Fig. 8.2 C). Data were consistent with those concerning dry weight: in each time point NPs plants and TSP plants did not show significant difference in leaves area indicating no differences in the supplying of P by the two materials. Further, both mterials determined an expansion of leaf apparatus much higher than that of -P plants.

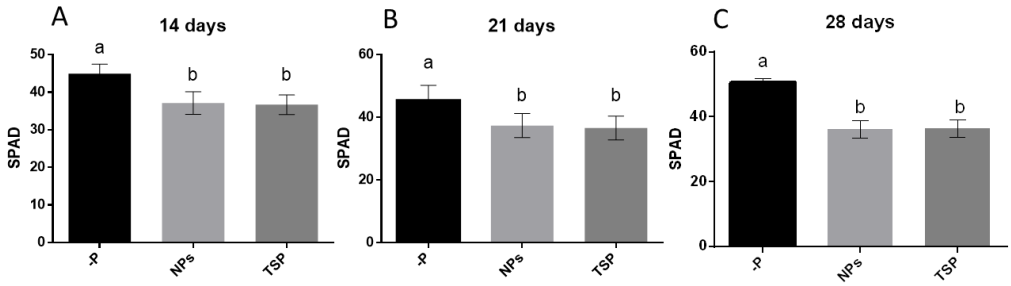

Figure 8.3. SPAD index of cucumber plants after 14, 21 and 28 days of growth in Romola soil in pot. Plants grown without P (-P); plants grown with $FePO_4$ NPs as source of P (NPs); plants grown with triple superphosphate as source of P (TSP). Data are means ± SD of three independent experiments with five biological replicates each one (One-way ANOVA with Turkey's test, $p<0.05$). Significant differences are indicated by different letters.

8.1.3 SPAD index

Data showed that -P plants exhibited the highest values of SPAD index for each of the measurement times, while NPs- and TSP-treated plants were not significantly different (Fig. 8.3 A, B, C, Fig. 8.4). As well as for dry weight and leaves area, $FePO_4$ NPs

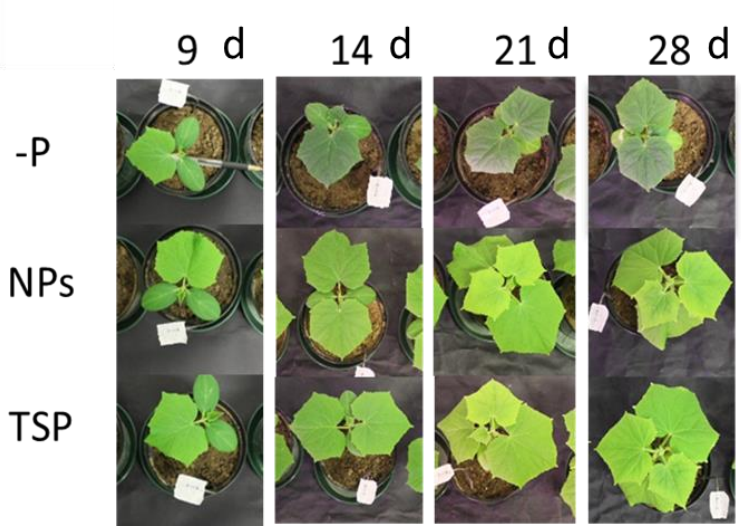

Figure 8.4. Picture of cucumber plants grown in Romola soil in pot after 9, 14, 21 and 28 days. Plants grown without P (-P); plants grown with $FePO_4$ NPs as source of P (NPs); plants grown with triple superphosphate as source of P (TSP).

did not affect SPAD index, confirming that there was not symptoms of P deficiency related to the leaf growth.

8.1.4 Root analysis

Pictures of root apparatus analysed with winRHIZO™ software remarked the results obtained in the case of dry weight, leaves area and SPAD index. In fact, root length (Fig 8.5 A), surface area (Fig. 8.5 B) and volume (Fig. 8.5 C) evidenced that root morphology of NPs plants and TSP plants was not different after 28 days of growth in pot. Taken together, the above-described results showed that plants grown with $FePO_4$ NPs and plants grown with triple superphosphate as source of P in Romola soil in pot did not show measurable differences in the phenotype related to P deficiency symptomatology.

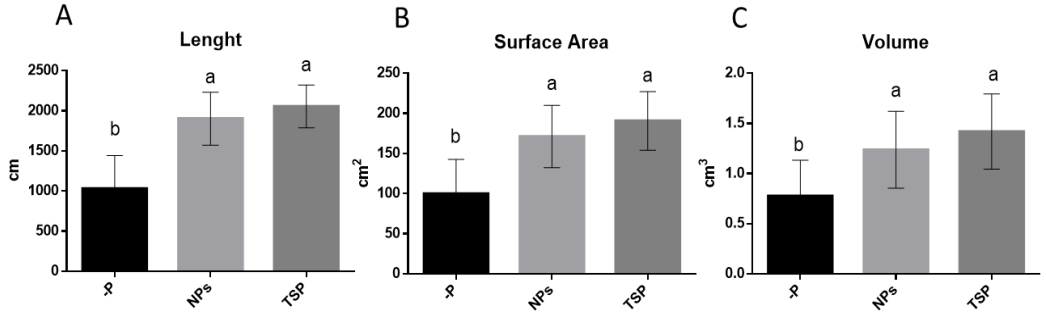

Figure 8.5. Root analysis of cucumber plants after 28 days of growth in Romola soil in pot. A) Root total length. B) Root total surface area. C) Root total volume. Plants grown without P (-P); plants grown with $FePO_4$ NPs as source of P (NPs); plants grown with triple superphosphate as source of P (TSP). Data are means ± SD of three independent experiments with five biological replicates each one (One-way ANOVA with Turkey's test, $p<0.05$). Significant differences are indicated by different letters.

8.1.5 ICP-MS elemental analysis

The concentrations of mineral nutrients, P, Fe, Mg, K, Mn, Ca, Cu and Zn in shoot and root of cucumber plants grown for 28 days in the Romola soil were analysed through ICP-MS elemental analysis. P content in shoot and root of cucumber plants

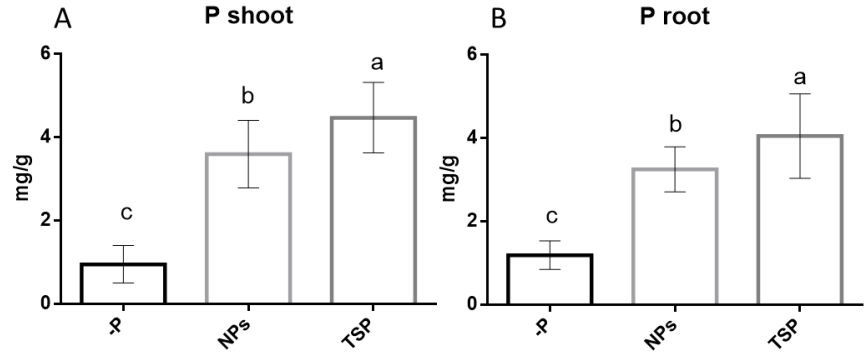

Figure 8.6. P concentration in cucumber plants after 28 days of growth in Romola soil in pot. A) Shoot. B) Root. Plants grown without P (-P); plants grown with $FePO_4$ NPs as source of P (NPs); plants grown with triple superphosphate as source of P (TSP). Data are means ± SD of three independent experiments with five biological replicates each one (One-way ANOVA with Turkey's test, $p<0.05$). Significant differences are indicated by different letters.

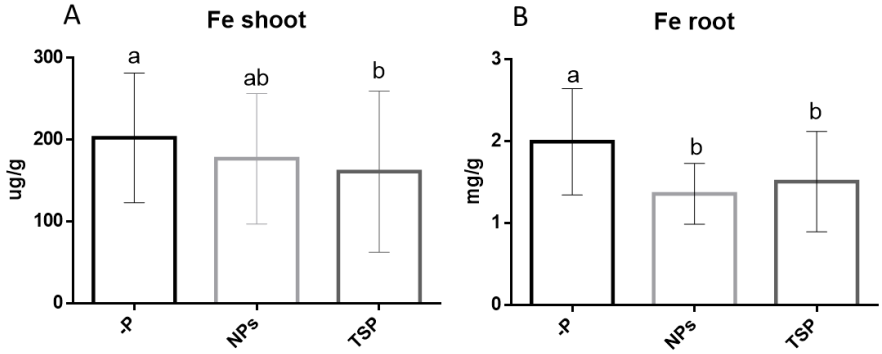

Figure 8.7. Fe concentration in cucumber plants after 28 days of growth in Romola soil in pot. A) Shoot. B) Root. Plants grown without P (-P); plants grown with $FePO_4$ NPs as source of P (NPs); plants grown with triple superphosphate as source of P (TSP). Data are means ± SD of three independent experiments with five biological replicates each one (One-way ANOVA with Turkey's test, $p<0.05$). Significant differences are indicated by different letters.

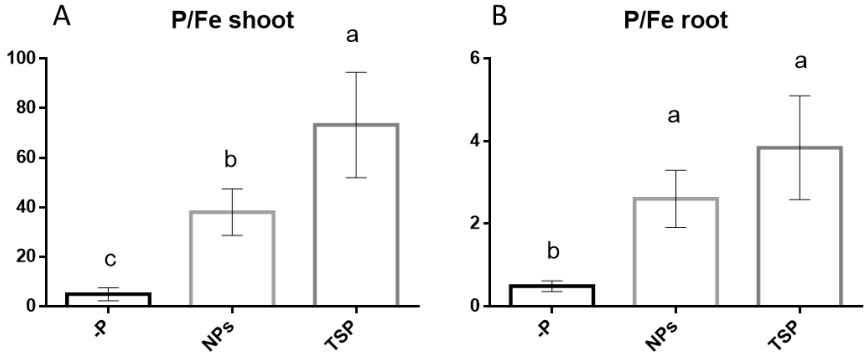

Figure 8.8. P/Fe ratio in cucumber plants after 28 days of growth in Romola soil in pot. A) Shoot. B) Root. Plants grown without P (-P); plants grown with $FePO_4$ NPs as source of P (NPs); plants grown with triple superphosphate as source of P (TSP). Data are means ± SD of three independent experiments with five biological replicates each one (One-way ANOVA with Turkey's test, $p<0.05$). Significant differences are indicated by different letters.

is displayed in fig 8.6. The trend in root and shoot was the same of those observed for the other results: P deficient plants showed the lowest tissues concentration of P. Those fertilized with $FePO_4$ NPs had a significantly different intermediate value while the highest concentrations were detected for plants fertilized with TSP. The concentration of Fe displayed significant differences between -P and TSP plants in the shoot, but NPs plants did not show significant differences with the other two conditions (Fig. 8.7). Conversely, in root was significantly higher in P deficient plants than in plants fertilized with $FePO_4$ NPs or TSP, in accordance with what expected for P deficiency. Ratios between P and Fe showed a trend that remarks the one regarding the accumulation of P (Fig. 8.8): In both shoot and root, P/Fe ratio was the lower in P deficient plant and the highest in triple superphosphate fertilized plants, remarking the interdependence and competition of these two elements to be absorbed by plants (Zanin et al., 2017). The other nutrients analysed did not show great variations in shoot or root concentration, but a slight tendency for divalent ions to be more absorbed by P deficient plants. These results are listed in Appendix IV.

8.2 Rhizospheric soil

Rhizospheric soil is expected to be strongly different from bare soil, because it is influenced by both by the exudates of roots "*per se*" and by their interactions with soil microbiome. When plants are present, availability of nutrient can also be roughly different from that measured in the bare soil. In this work, we defined as rhizospheric all the soil present in the small pots where plants grew. This assumption is justified by the fact that after 28 days plant roots expanded enough to colonize the soil present in the pot entirely, therefore all the soil was in contact with the roots.

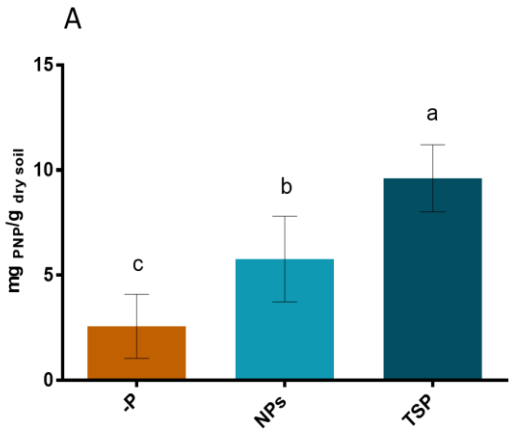

Figure 8.9. Olsen available P in Romola rhizospheric soil after 28 days of growth of cucumber plants in pots. Soil where plants were grown without P (-P); soil where plants were grown with $FePO_4$ NPs as source of P (NPs); soils where plants were grown with triple superphosphate as source of P (TSP). Data are means ± SD of two independent experiments with three biological replicates each one (One-way ANOVA with Turkey's test, $p<0.05$). Significant differences are indicated by different letters.

8.2.1 Olsen available Phosphorus

After 28 days of contact with plants, rhizospheric soil sampled from P deficient plants' pot had the lowest value for available P. Conversely, rhizospheric soil from pots with plants fertilized with TSP had the highest value of available P. Rhizospheric soils from plants fertilized with $FePO_4$ NPs reported a middle significant value between the other two conditions (Fig. 8.9). This trend is not consistent with that observed for plant physiological and growth data (no differences between NPs- and TPS-treated plants), however it is consistent with the results of P elemental analyses. Moreover, this trend is also very similar to that observed for bare soil available P of Romola (Fig. 6.8).

8.2.2 Enzyme activities

As well as for nutrient availability, the activity of microorganism can vary due to the presence of the plants in the soil. Thus, the same enzyme activities performed on bare soils, were performed again on rhizospheric soils, to evaluate the effect caused by the plants grown in the different nutritional conditions on microbiome metabolic activity. A time zero (T0) was also included to compare the analyses to the untreated soil without any plant grown on it.

8.2.2.1 Acid and alkaline phospho-monoesterases

Acid phosphatase (Fig. 8.10 A) showed the higher values in P deficient soil (-P) than in the triple superphosphate fertilized soil (TSP). Time zero (T0) and $FePO_4$ NPs fertilized soils (NPs) had no differences either between each other or with the other conditions. Alkaline phosphatase though, showed significant differences with the highest value in TSP, the lower in T0 and an intermediate value in NPs.

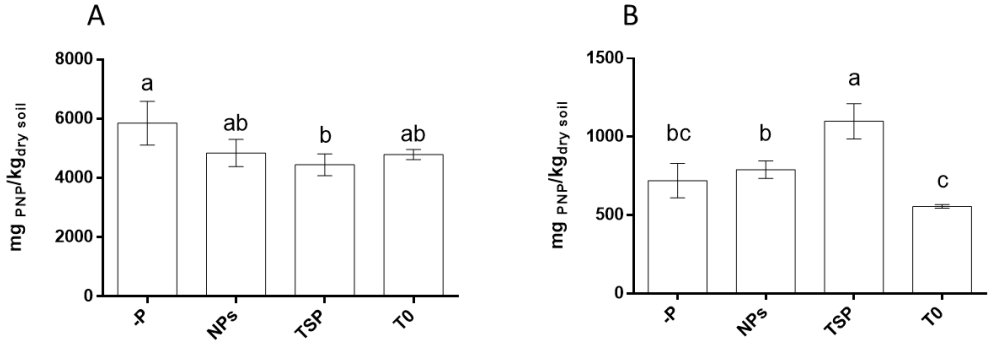

Figure 8.10. Acid (A) and alkaline (B) phosphomonoesterases of rhizospheric Romola soils after 28 days of cucumber growth in pots). Soil where plants were grown without P (-P); soil where plants were grown with $FePO_4$ NPs as source of P (NPs); soils where plants were grown with triple superphosphate as source of P (TSP). Untreated soil at zero-time of the experiment (T0). Data are means ± SD of two independent experiments with three biological replicates each one (One-way ANOVA with Turkey's test, $p<0.05$). Significant differences are indicated by different letters.

8.2.2.2 Arylsulfatase

Arylsulphatase did not show much significant differences among all the conditions analysed (Fig. 8.11). Only -P arylsulfatase activiry was significantly higher than T0. Plus, absolute values were very low for this enzyme activity. Therefore, it is reasonable to assess that the treatments very slightly affected arylsulphatase.

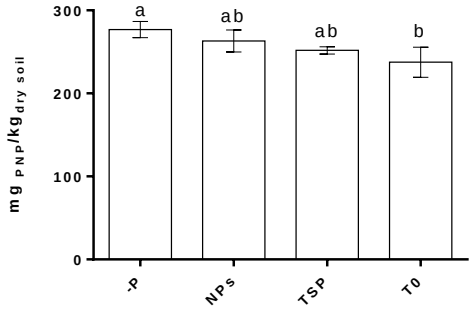

Figure 8.11. Arylsulfatase of rhizospheric Romola soils after 28 days of cucumber growth in pots). Soil where plants were grown without P (-P); soil where plants were grown with $FePO_4$ NPs as source of P (NPs); soils where plants were grown with triple superphosphate as source of P (TSP). Untreated soil at the zero-time of the experiment (T0). Data are means ± SD of two independent experiments with three biological replicates each one (One-way ANOVA with Turkey's test, $p<0.05$). Significant differences are indicated by different letters.

8.2.2.3 β-Glucosydase

β-Glucosydase activity showed no significant differences among the different rhizospheric soil conditions (Fig. 8.12), although there can be slight differences considering T0 samples.

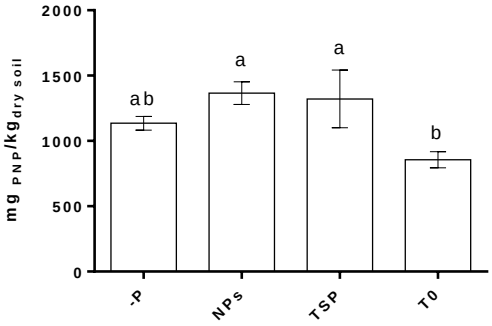

Figure 812. β-Glucosydase activity of rhizospheric Romola soils after 28 days of cucumber growth in pots). Soil where plants were grown without P (-P); soil where plants were grown with $FePO_4$ NPs as source of P (NPs); soils where plants were grown with triple superphosphate as source of P (TSP). Untreated soil at the zero-time of the experiment (T0). Data are means ± SD of two independent experiments with three biological replicates each one (One-way ANOVA with Turkey's test, $p<0.05$). Significant differences are indicated by different letters.

8.2.2.4 Protease

Concerning protease activity, TSP rhizospheric soil showed values as low as T0 samples (Fig. 8.13). Data of -P and NPs rhizospheric soils had the highest values of protease activity, that account for roughly the double of the other two conditions.

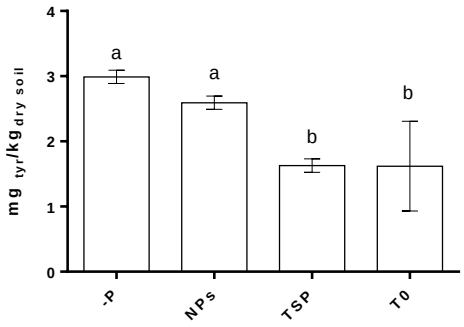

Figure 8.13. Protease activity of rhizospheric Romola soils after 28 days of cucumber growth in pots). Soil where plants were grown without P (-P); soil where plants were grown with $FePO_4$ NPs as source of P (NPs); soils where plants were grown with triple superphosphate as source of P (TSP). Data are means ± SD of two independent experiments with three biological replicates each one (One-way ANOVA with Turkey's test, $p<0.05$). Significant differences are indicated by different letters.

8.2.3 DGGE pattern analysis of rhizospheric soil microbial communities

In order to evaluate the different behaviour of soil microbiome in pot during -P, added $FePO_4$ NPs and with triple superphosphate, DGGE pattern analysis could give a general view on the similarity of microbial communities among the differently treated soil

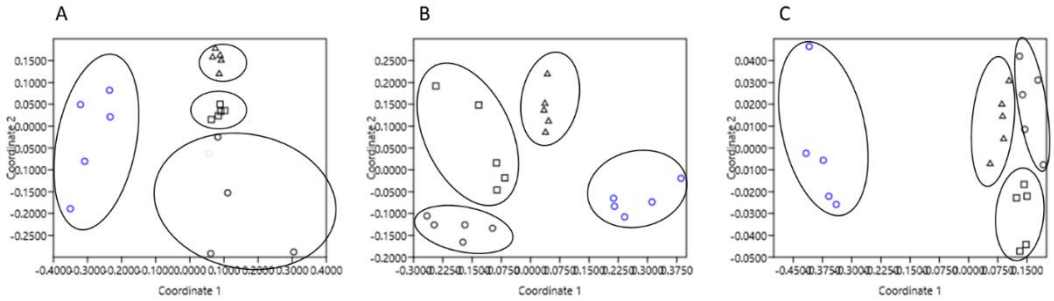

Figure 8.14. Two-dimensional plots of nMDS analyses of quantitative matrixes from DGGE gel patterns for Archaea 16S rDNA (A), Bacteria 16S rDNA (B) and Fungi 18S rDNA (C). Blue circles represent the time zero (T0) soil samples, black circles represent P deficient soil samples (-P), squares represent $FePO_4$ NPs fertilized soil samples (NPs), triangles represent triple superphosphate fertilized soil samples (TSP). Circles were drawn by the author to guide the reader into the interpretation of the graph and to evidence the four clustered groups. Stress values of NMDS analysis were A= 0,06969; B= 0,1162; C= 0,08118

samples. NMDS analysis of DGGE gel pattern showed that, on the contrary of what

observed in the case of bare soil samples, microbial communities were different among all the conditions (Fig. 8.14). For Archea (Fig. 8.14 A) Bacteria (Fig. 8.14 B), and Fungi (Fig. 8.14 C), NMDS displayed that T0 samples (blue circles) clusterized and represent the most different group of samples. Conversely, $FePO_4$ NPs fertilized soils (squares) and triple superphosphate ones (triangles) are the two conditions that had the highest similarity. So, each group is different from the others but the most similar to each other are $FePO_4$ NPs fertilized and triple superphosphate fertilized soils, as confirmed by one-way ANOSIM statistics (Table 9).

Conditions	**DGGE gel**	One-way ANOSIM	
T0; -P; NPs; TSP		R	*P*
	Fungi 18S	0.8553	0.0001
	Bacteria 16 S	0.9317	0.0001
	Archaea 16 S	0.7653	0.0001

Table 9. One-way ANOSIM global test based on Bray-Curtis similarity index of Bacteria 16S, Fungi 18S and Archaea 16S rDNA-DGGE profiles. Values presented are the R-value (R) and the P statistic (P) of significance (Clarke, 1993). R=0 means samples are not different. R=1 means sample are different. R=0,75 means samples are different but overlapping.

9. DISCUSSION

In plant nutrition, nanofertilizers represent a promising tool to increase NUE – which is remarkably low especially for P – being more reactive and, perhaps, more available to plants. The use of nanofertilizers would limit the dispersion in the environment that normally affects conventional fertilizers when applied in the soil (Marchiol et al., 2020) (Marchiol et al., 2020). Nevertheless, little is known about their effects on plants, soil microbial community and rhizosphere, since scientific literature reports a very restricted number of experiments focused on the impact on plant-soil system of nanofertilizers (Achari & Kowshik, 2018; Fu et al., 2020; Marchiol et al., 2020). A continuous and batch-method syntheses of $FePO_4$ nanoparticles (NPs) have been developed, producing a concentrated stable solution with NPs around 100 nm of diameter (Sega et al., 2019). The so synthesized $FePO_4$ NPs were proven to be a source of nutrient when supplied to maize and cucumber plants grown in hydroponic and can represent a more available source in comparison to bulk $FePO_4$ (Sega et al., 2020).
The present doctoral project was focused on investigating the impact of $FePO_4$ NPs, used as a novel nano-fertilizer, in the whole plant-soil system. In particular, we evaluated a) their potential into promoting plant growth; b) the early transcriptomic responses of two different plant models to $FePO_4$ NPs c) their effect on the soil environment by focusing on the structure and function of microbial community.

SECTION I

In the first part of the study, cucumber and maize plants were cultivated in hydroponics with $FePO_4$ NPs as source of P or Fe in comparison to bulk $FePO_4$. Synthesis of NPs was done several times during the work, obtaining results similar to the ones obtained by Sega et al. (2019) (Fig. 4.1). The morpho-physiological parameters of cucumber plants fed with $FePO_4$ NPs as source of P were similar to those of control plants (ionic forms of the salts) (Figure 4.2), whereas in maize this behaviour was observed when $FePO_4$ NPs were used as source of Fe (Figure 4.6). These results were consistent with those obtained by Sega et. al. (2020), remarking that $FePO_4$ NPs were used more efficiently than bulk as source of P from cucumber and as source of Fe from maize. This difference in the performance of NPs could be due to the fact that cucumber and maize are a strategy I and strategy II plants respectively, for Fe acquisition.

In order to dissect the molecular events taking place after a short period of contact between roots of hydroponically grown cucumber and maize seedlings with the different form of $FePO_4$ (NPs or bulk) a series of microarray analyses were performed. Differentially expressed transcripts were identified comparing the root transcriptional profiles of plants treated with NPs or bulk as P and Fe source with that of plants grown without the corresponding nutrient. First investigations showed that cucumber and maize responded specifically to the form of $FePO_4$ (NPs or bulk) with a very low number of transcripts commonly modulated (Figure 4.10).
In cucumber, MapMan pathway analysis showed that seedlings grown in contact with $FePO_4$ NPs mostly modulated transcripts belonging to the categories "*RNA*

regulation", "*transport*" and "*stress*" (Figure 4.12) in respect to bulk. It has been evidenced that molecular responses of rice to silver nanoparticles (Ag-NPs) were primarily associated to oxidative stress response and can accelerate the production and detoxification of ROS (Mirzajani et al., 2014). Vannini et al (2013) showed that either Ag-NPs or $AgNO_3$ can cause changes in the proteome related to oxidative responses in *Eruca sativa* roots, however, only AgNPs caused the modulation of proteins related to the endoplasmic reticulum and vacuole, suggesting that the two forms of Ag triggered a different response pathway (Vannini et al., 2013). Metal-based nanomaterials are the most investigated, with contrasting reports on plants responses (Hossain et al., 2020). Some metal nanomaterials were reported to induce the biosynthesis of signal molecules, such as ABA, regulating stress responses (Wang et al., 2020). Nevertheless, generally the responses of plants to metal NPs vary with the nature of the material, plant species, and stage of growth (Aslani et al., 2014). Anyway, transcriptomic specific patterns were identified in *Arabidopsis* after the exposure to different NPs (TiO-, Ag-NPs and multi walled carbon nanotubes) that could be distinguished by those related to other stressors and defined a set of NP-differentially expressed genes (Sanchez et al. 2015). Concerning the capability of plants to absorb nutrient, it has been shown that both Fe_2O_3 NPs and Fe^{3+} could be used as Fe source and induce the expression of Fe-regulated genes in *Citrus maxima*, but Fe^{3+} treatments induced caused damage to plant roots (Hu et al. 2017). These findings support the idea that the treatment with NPs could trigger a different pattern of transcriptomic responses that is dependent on the nano-size and not only on the chemical nature of the material.

Focusing on cucumber, the analysis of transcripts specifically modulated by the treatment with NPs and bulk when supplied as P source evidenced that the two nutritional forms differentially impaired genes linked to cell wall metabolism. Wu et al. (2019) showed that expansins regulate the root elongation and root hair formation in different plant species under P shortage. Our dataset showed the upregulation of an expansin like A1 transcript in the comparison -P+bulk *vs* -P (Cucsa.099360.1, FC 2.02, Appendix I) suggesting that this kind of responses to the shortage were enhanced by bulk. On the contrary, the NPs caused the downregulation of two transcripts encoding another expansin A (Cucsa.355990.1, FC 2.03,) and of a glucan synthase-like 4 (callose synthase). Expansins regulate the root elongation and root hair formation in different plant species under P shortage (Wu et al., 2019) whilst callose synthase can play a role in deposition of callose observed under P deficiency in the meristem and elongation zone of primary roots (Müller et al., 2015), which in turn interferes with symplastic cell-to-cell communication. Anyway, the supply of both P sources negatively regulated the root hair formation as suggested by the repression of root hair defective transcripts (Cucsa.352750.1, FC -2.37 for -P+NPs *vs* -P, and Cucsa.006340.1, FC -2.13 for -P+bulk *vs* -P). Furthermore, it was reported that root hair defective 6-like (RSL) transcripts were positively expressed under P deficiency in *Brachypodium distachyon* controlling the root hair formation (Kim and Dolan, 2016). Concerning the regulation of transcription, our analyses showed that NPs and bulk exerted a specific modulation of the transcripts encoding transcription factors (TFs) belonging to WRKY, NAC, bHLH and MYB-like families (Appendix I). Several WRKY genes were induced under P deficiency in *Arabidopsis* and are involved in the regulation of the responses to the starvation (Bakshi & Oelmüller, 2014). Anyway, both P sources positively regulated the expression of two transcripts encoding a protein showing homology to AtWRKY20

(Cucsa.042320.1, FC 2.26 for -P+NPs *vs* -P, Cucsa.042330.2, FC -2.37 for -P+bulk *vs* -P). We observed a downregulation of NAC transcripts both in -P+NPs *vs* -P and -P+buk *vs* -P comparisons. In particular, in the first comparison the transcript (Cucsa.081320.1, FC -2.22) encodes for a protein showing homology to AtNAC90, whilst in the second the downregulated transcript encodes a protein homologous to AtNAC82 (Cucsa.100920.5, FC -2.13). It was reported that AtNAC82 is involved into the switch between root hair and non-hair cells in responses to various stress conditions (Wang et al. 2020). Interestingly, we recorded the negative regulation of nicotianamine synthase transcripts (Cucsa.090660.1, FC -2.83 and Cucsa.092390.1, FC -2.21) only in the comparison -P+NPs *vs* -P. Both transcripts encode proteins with homology to AtNAS4 which play a role in the response to Fe deficiency and in distribution of the micronutrient (Koen et al., 2013). On the basis of this, results suggested that the treatment with NPs can also improve the Fe nutrition under P starvation. Transcripts linked to the cell wall metabolism were specifically modulated by also when $FePO_4$ NPs or bulk were supplied as Fe source. In particular, we detected a positive modulation of a transcript for pectin lyase (Cucsa.027780.1, FC 2.28) whilst two genes encoding expansins were positively and negatively regulated (Cucsa.099320.1, FC -2.62; Cucsa.302600.1, FC 3.00) in the -Fe+NPs *vs* -Fe comparison. In the case of -Fe+bulk *vs* -Fe pectate lyase transcripts were repressed (Cucsa.038070.1, FC -3.97; Cucsa.100530.1, FC -2.13) and no expansin genes resulted modulated. Taken together, these transcriptional changes suggested that the treatment with NPs can induced changes in cell wall metabolism associated to the development of lateral roots. In fact, it was hypothesized that expansins and pectate lyases are involved in lateral root formation (Somssich et al. 2016).

In maize, a higher number of specifically modulated transcripts by the form of $FePO_4$ were detected in NPs treatment as source of P (456 transcripts, Figure 4.10 C) than bulk ones (101 transcripts, Figure 4.10 C). This behaviour cannot be explained simply on the basis on the different number of transcripts that could be detected by the maize and cucumber chips (about 20% less in cucumber than maize). Furthermore, the number of modulated transcripts is more less similar in the case of Fe nutrition in the two plants. We can therefore infer that maize is more responsive to the different form of P source. Several of these transcripts are related to *stress responses* and *cell wall metabolism*, as described above for cucumber. Among these specifically modulated transcripts, we identified genes encoding TFs of the WRKY, MYB and bHLH families (Appendix I) and can be involved in the regulation of the root responses to the treatment. Moreover, it was demonstrated that P deficiency can trigger a transcriptomic response in maize which involves the modulation of members of this TF families and abiotic stress-related genes (Ma et al., 2020). Therefore, these findings support the different response to the two forms as source of P ($FePO_4$ bulk or NPs), even though both forms were an efficient source of P for maize.
Considering the modulation of transcripts involved in cell wall metabolism, the treatments with NPs proved to exert a stronger effect than bulk. In fact, five transcripts for expansins (GRMZM2G059785_T01, FC 2.90; GRMZM2G342246_T01, FC 2,92; GRMZM2G474194_T01, FC 4.38; AC234190.1_FGT001, FC 2.53; GRMZM2G127029_T01, FC 2.27) were upregulated in -P+NPs *vs* -P and only one (GRMZM2G401983_T01, FC 2.74) in -P+bulk *vs* -P. In the case of pectin lyases, three

and one transcripts were upregulated and downregulated respectively by NPs (GRMZM2G412207_T01, FC-2.87; GRMZM2G002034_T01, FC 2.40; GRMZM2G037431_T01, FC 3.15; GRMZM2G435380_T01, FC 5.90), whilst bulk did not affect genes encoding this class of enzymes. These results suggested that NPs could strongly affect the cell wall metabolism than bulk when used in maize as P source.

Transcripts linked to ethylene responses (GRMZM2G085964_T01, FC 2.22; GRMZM2G381441_T01, FC 3.00; AC210616.4_FGT005, FC -3.89; GRMZM2G040481_T01, FC -2.82) were modulated by the treatment with NPs but not by the bulk treatment. Ethylene is an important hormone involved in root growth through an interaction with auxin by stimulating the auxin biosynthesis and translocations into the root elongation zone (Růžička et al., 2007). EIN3 is an essential regulator in the ethylene signalling pathway, whose expression in Arabidopsis is induced by ethylene (Dolgikh et al. 2019). EIN3 binds to promoters of ERF genes and stimulates their transcription in an ethylene-dependent manner (Růžička et al., 2007). These ERF TFs regulate the expression of many downstream genes and ERFs are the last TFs elements of a signal cascade which trigger ethylene response (Chen et al. 2005), such as NAC TFs (Dolgikh et al. 2019). We found that a NAC transcript among the transcripts specifically modulated by the treatment with NPs (GRMZM2G062009_T01, FC 4.83). The presence of these TFs could indicate an early transcriptomic response of maize seedlings to $FePO_4$ NPs through the ethylene pathway. Syu et al. (2014) suggested a role of AgNPs acting as inhibitors of ethylene perception and interferer of its biosynthesis. Our results suggest that ethylene signalling pathway could be a target of $FePO_4$ NPs perception.

Maize plants supplied with NPs and bulk as Fe source presented a lower effect on the cell wall-related transcripts (Figure 4.12) in respect to what observed in cucumber. Moreover, $FePO_4$ NPs as source of Fe did not trigger a so wide transcriptomic responses as found when used as source of P. In -Fe+NPs *vs* -Fe a positive modulation of transcripts related to cell wall metabolism (Figure 4.12 C) was limited to a transcript encoding a pectin lyase (GRMZM2G177940_T01, FC 2,58) in response to the NPs treatment, while in the case of bulk cell wall-related transcripts were not affected, further supporting the idea of an impairing cell wall modulation mechanisms depending on the form of $FePO_4$.

A list of transcripts commonly modulated by $FePO_4$ NPs irrespective their utilization as source of P and Fe was obtained. In cucumber (Table 4) it is interesting to notice that 7 out of 8 transcripts showed an opposite modulation among P or Fe: $FePO_4$ NPs trigger downregulation when used as source of P, whereas upregulation when used as source of Fe. The opposite verse of the modulation of most of these transcripts (Table 4) could be related to the antagonism existent between Fe and P, found to basically modulate the Fe responses depending on the P availability (Ward et al., 2008) which can depend on the form of $FePO_4$. In particular, some of these transcripts seems to be involved in Fe acquisition and distribution. In fact, two transcripts encoding GTP cyclohydrolase II (Cucsa.398260.2 and Cucsa.398260.1) can be linked to the riboflavin biosynthesis putatively involved in the responses to Fe deficiency (Herz et al. 2000). Furthermore, two transcripts (Cucsa.090660.1 and Cucsa.092390.1) encoding proteins with homology to AtNAS4 could play a role in Fe homeostasis by contributing to long

distance circulation in phloem and can act as a sensor for Fe availability as described for *Arabidopsis* (Koen et al., 2013).
In maize 9 transcripts were modulated both in -P+NPs *vs* -P and -Fe+NPs *vs* -Fe comparison (Table 6). Interestingly, among these transcripts, 7 were positively modulated by NPs independently from the nutrient thus suggesting that in this species the transcriptional modulation could be more linked to the nano-sized nature of the material. This hypothesis is supported by the induction of two transcripts encoding wound responsive proteins (GRMZM2G106393_T01, WIP3) and GRMZM2G106511_T01 (WIP4). Among WIP family in *Arabidopsis*, WIP 3, 4 and 5 are not constitutionally expressed but might respond to specific developmental and environmental signals such as biotic or abiotic stress (Yu et al., 2018). Furthermore, an H^+-ATPase transcript (GRMZM2G148374_T01) is upregulated in both conditions. The activity of plasma membrane H^+-ATPases is involved in P acquisition (Shen et al., 2006; Tomasi et al., 2009). Interestingly, it was reported that the *AtAH2* was induced by Fe nanoparticles in *Arabidopsis* promoting stomatal opening (Kim et al. 2015). Moreover, H^+-ATPases can contribute to signalling events in response to diverse environmental stress, but also to plant immune responses (Elmore & Coaker, 2011). Taken together, these observations produce evidence that $FePO_4$ NPs could trigger several stress responses in maize, related to biotic or abiotic cues. Therefore, other than providing nutrients, $FePO_4$ NPs could also stimulate plant growth increasing the ability of plant to remodeling the cell wall and concurring to the basal protection from biotic and abiotic stress, as found for various other nanomaterials (Aslani et al., 2014).

SECTION II

One matter of concern about the use of NPs as fertilizers can be their influence on the soil environment (Gardea-Torresdey et al., 2014). The first part of the work was focused on highlighting the effects of the application of $FePO_4$ on the soil toward the microbial community structure and metabolic activity. To get insight in this matter, we provided $FePO_4$ NPs to two different bare soils to investigate about possible toxic effects. The soils were a sandy (Romola) and a silty (Cesa) one, whose characteristics are listed in Table 7. BioTox™ test (Šimek et al., 2017) (Fig. 6.1) and CO_2 respiration test (Fig. 6.2) were performed. We did not observe any toxic effect in response to the treatment with $FePO_4$ NPs on both soils. Furthermore, NPs treatment had no overall considerable effects on soil enzyme activities (Figures 6.3-6.6) or on the structure of soil microbial community, as assessed by NMDS analyses of DGGE profiles (Figures 6.7; 6.8). Moreover, as revealed by Anosim analyses (Table 8) "time" factor in sampling influenced the differences into the microbial community structure in an undistinguishable manner from the "treatment" factor. Our results are in contrast with other found in literature. It was shown that ZnO NPs could inhibit *B. cinerea* and *P. expansum* growth, thus revealing antifungal activity (He et al., 2011). Ben-Moshe et al. (2013) reported that CuO and Fe_3O_4 NPs affected the soil bacterial community composition within 24 hours after the treatment, even though Fe_3O_4 NPs had lower toxicity to soil bacterial communities. Basing on these evidences, the authors suggested the dependency of toxicity on the nanoparticle type and concentration. Asadishad et al. (2018) investigated the effect on the soil microbial community of different metal NPs and

reported contrasting results: Ag NPs inhibited most of the enzyme activities tested, while ZnO and CuO NPs tended to enhance some enzyme activities, but in all the cases some variations in the microbial community structure were observed. Considering the variety of nanomaterials, the use of nanocompounds in agriculture implies an evaluation of their impact on soil biology through an accurate case by case analyses without generalization. While metal-based nanoparticles were reviewed to have various negative effects on beneficial interactions between soil-microbes and plant-microbes (Ameen et al., 2021), our results encouraged an application of $FePO_4$ NPs as fertilizers in soil without negative effects.

A comparison between $FePO_4$ NPs and triple superphosphate (TSP) was done in terms of Olsen-extractable P in order to assess the availability of the element. The results showed very slight differences among the treatments ($FePO_4$ NPs and TSP) in Cesa soil (Fig. 6.9 B), which had the highest value of basal available P (8 ppm) (Table 7). Conversely, in Romola soil, which had the lowest value of basal available P (3 ppm) (Table 7), $FePO_4$ NPs provided less Olsen-extractable P during the whole incubation time than TSP (Fig. 6.9 A). It has been shown that some soil characteristics as P-buffer capacity, pH, and Fe oxide content can influence the extractability of Olsen-P (Recena et al., 2016). Soil solution pH, in particular, is critical in determining the potential availability of P, and Meyer et al. (2020) reported a decrease in P availability with decreasing pH, probably due to Al-/Fe-P precipitation. The same authors also suggested that a non-calcareous soil with pH around 7 could report higher P availability, as the magnitude of the precipitation of Ca-P minerals is low. Our data reported that in Cesa the form of fertilizer was not determinant for P availability. Soil characteristics influencing P availability are likely related to P sorption (Kristoffersen et al., 2020), which in case of Cesa might determine the efficacy of different fertilizers. However, these results need to be further interpreted in a view of their effect on plant growth (see the next section).

SECTION III

Romola was the poorest soil in terms of available P (3 ppm) therefore it was chosen to ensure a growth in a low available P environment. Cucumber plants were cultivated in pot in a growth chamber, to allow constant conditions for the whole cultivation period. Results of physiological parameters (dry weight, leaves area, SPAD, root analyses) (Figures 8.1-8.5) revealed that cucumber plants cultivated in soil with $FePO_4$ NPs used as P fertilizer grew without any phenotypical difference with plants treated with a conventional fertilizer such as TSP. Conversely, the plants grown in soil without the addition of external P sources presented a stunted growth and at leaf level symptoms of P deficiency (Fig. 8.4).

The availability of P in Romola soil after 28 days of cucumber growth (Fig. 8.9) was higher when treated with TSP in respect than NPs, similarly of what observed in Romola bare soil available P (Fig. 6.8 A) On the other hand, the fertilization efficacy in terms of biomass yield was not different depending on the two fertilizers used. Interestingly, ICP-MS analysis revealed that P concentration in both shoot and root (Fig. 8.6) was higher in plants grown with TSP than in plants grown with NPs. These results overlapped and suggest the potential of NPs to be less detectable by Olsen method, as

the form of P is one of the major factors affecting P availability in soil (Ben-Moshe et al., 2013). Rui et al., 2016 showed how both Fe_2O_3 NPs and Fe-EDTA used as Fe fertilizer could enhance the growth of peanut plants in soil without differences in physiological parameters. Moreover, the authors showed that Fe_2O_3 NPs treatment provided less Fe than Fe-EDTA in peanut tissues. Yang et al. (2020) reported that foliar fertilization with Fe_2O_3 NPs leaded to a lower Fe concentration in plant tissues in respect of Fe-EDTA, while no differences were observed between Fe_2O_3 NPs and Fe-EDTA after application on soil, despite in both cases plants could grow better in presence NPs. Concerning the nutrient concentration in the plant after the treatment with NPs, these findings are concordant with the ones we obtained in this work, suggesting the tendency of a nanosized fertilizer applied to the soil to be less detectable by methods assessing the availability of certain nutrients. This could be because NPs in the soil undergo several transformations, such as adsorption onto soil particles and aggregation (Manika & Ajittvarma, 2017), thus increasing P-buffering capacity (Weeks & Hettiarachchi, 2019). The wide variability of NPs chemical properties renders them difficult to detect in a complex matrix as soil is (Rodrigues et al., 2016). As already mentioned, NPs possess peculiar properties affecting the rate of dissolution and movement. Even if less detectable in soil, small size could favour the bioavailability of the nano-packed nutrients (Stone et al., 2010; Yusefi-Tanha et al., 2020; Zhu et al., 2012) absorbed onto soil particles or plant roots.

To evaluate the impact of $FePO_4$ NPs on the rhizosphere microbiota, analysis on enzyme activities and on microbial community in the soil after the cultivation of *C. sativus* plants in presence of NPs and TSP were conducted. Enzymes are essential to the cycling of organic matter in soil and their role is critical to the availability of nutrients to both microorganisms and plants. Soil enzyme activity represent the ability of soils to perform biogeochemical reactions (Nannipieri et al., 2018), and their activity incorporated both actively secreted enzymes and extracellular soil particles-adsorbed enzymes. Acid and alkaline phosphatases are monitored as index of P cycling (Adetunji et al., 2017) and pH changes in soil (Dick et al., 2000). Secretion of acid phosphatase is one of the responses of plants to P-deficient conditions (Vance et al., 2003). Acid phosphatases secretion is mostly of plant origin, while alkaline phosphatases are produced by microorganisms, so acid phosphatase is mostly dependent on plant nutritional status (Gianfreda & Ruggiero, 2006) and alkaline phosphatase on the microbial metabolism (Tarafdar & Claassen, 1988). We identified differences in acid phosphatase between soils in which grew P deficient plants (-P) and TSP fertilized (Fig. 8.10 A) denoting a response to P paucity in P deficient plants and an optimal P status of the plant when fertilized with TSP. Alkaline phosphatase (Fig. 8.10 B) was significantly higher in TSP than in -P and NPs. This could be due to the higher production of acid phosphatase in -P and NPs – whose secretion is regulated by acidic pH – and to the competition between alkaline and acid phosphatases production (Adetunji et al., 2017). Moreover, Olsen P is generally correlated with alakaline phosphatase (Margalef et al., 2017). Arylsulphatase and β-glucosydase are related to sulphur and carbon cycling respectively (Adetunji et al. 2017). These enzyme activities did not show significant variations with respect to P availability (Figures 8.11; 8.12), suggesting that these processes were not linked to P availability. Proteases are among the main enzymes involved in the mineralization of soil organic matter and critical into organic N cycling (Cenciani

et al., 2008), and they can be related both to microorganisms and plant proteolytic activity (Vranova et al., 2013). Protease activity showed higher values for -P and NPs rhizospheric soils whereas the lowest values were reported in the case of TSP and T0 rhizospheric soils (Fig. 8.13). Protease activity can be induced by protein supply but also by several low-molecular weight organic compounds, such as plant hormones, so the crosstalk with carbon availability is crucial (Adetunji et al., 2017). There are discordant results in literature regarding the effects of nano-compounds on enzyme activity. The increase of certain enzymatic activity in soil fertilized with slow release nanofertilizers has been reported, despite protease was not investigated (Teng et al., 2018). Protease was found to increase after 15 days in soils treated with nano-TiO_2 and nano-ZnO and such an increase was accompanied to a higher relative abundance of *Streptomyces* (Ge et al., 2012). Conversely, Du et al. (2011) reported a decrease of soil protease in presence of ZnO and TiO_2 NPs. However, several studies demonstrated that the active secretion of plant hormones and root exudates increased soil enzyme activity (Brzostek et al., 2013; Renella et al., 2007, 2011), and P deficiency stimulates the excretion of root exudates and hormones such as ethylene, which is also responsible of the increase of acid phosphatase (Li et al., 2011). It is unlikely that $FePO_4$ NPs selected significantly more proteolytic bacteria as in the case of the experiment of Ge et al. (2012), since here we found that there was not a great variation in the microbial community structure between TSP and NPs fertilized soils (Fig. 8.14, Tab. 9). NPs and TSP soils after plant cultivation reported highest similarity in microbial community structure in comparison to time zero and -P conditions, indicating slight difference in microbial community structure due to the form of P fertilizer. Therefore, the form of P fertilizer is unlikely to operate a great selection between microbial species, but it could be responsible to a remodulation of the microbial biomass and consequentially different plant response. Ge et al. (2014) demonstrated that different NPs could either stimulate or inhibit soil enzyme activity in an experiment conducted with soybean plants, depending on the peculiar properties of the NPs. These findings suggest that $FePO_4$ NPs, providing less available P directly on the soil (Fig. 8.9) could stimulate plants to actively solubilize P from the NPs which aggregated or adsorbed onto soil particles, which would turn into a stimulated secretion of extracellular plant protease and an indirect stimulation of the microorganisms to produce protease, as well as in P deficiency, but with no deficiency in P acquisition.

10. CONCLUSION

Treatment with $FePO_4$ NPs in roots of maize and cucumber were shown to cause a constitutive activation of stress responses and can trigger a different pattern of transcripts dependent on the nano-size and not only on the nutrient. Non-nano (bulk) and NPs forms can regulate the expression of different transcripts related to cell wall modulation in cucumber roots, probably with an impact on lateral roots formation, denoting an effect of the form on nutrient uptake. Transcription factors were also observed to be involved into $FePO_4$ NPs responses. Moreover, treatment with NPs could reflect on an improved Fe nutrition under P starvation. In maize, ethylene pathway could participate in the signaling of $FePO_4$ NPs when used as source of P. The evidence of a set of transcripts modulated by the form of $FePO_4$ irrespective by the nutritional state in both cucumber and maize support the hypothesis that nano form has a specific signaling in the case of $FePO_4$.

Due to the high variability of the physic-chemical properties of nano materials in respect of their non-nano counterparts, the effect of any nano-compound applied on the soil during agricultural practices necessitates an accurate case by case evaluation. Concerning the application of $FePO_4$ NPs on the soil as fertilizer, our results indicated that the soil microbial community was not significantly affected by the treatment in both the bare soils used, and therefore suggested their utilization in an environmental-friendly manner. Moreover, P availability depending on the size of a compound used as fertilizer was shown to be influenced by the type of soil. However, the extractability of P through Olsen method could be not sensitive enough to denote the efficacy of $FePO_4$ NPs as fertilizer on plants. Despite the concentration of P in the plants was higher after the treatment with TSP than with NPs, plant biomass yield was not significantly different. Therefore, even if less detectable in soil, nano-size could favour the bioavailability in soil, and in the case of $FePO_4$ by increasing the P-buffering capacity. This in turn, could allow plants to uptake nutrient continuously and in sufficient concentration.

In soil-plant system, very slight difference in microbial community structure due to the form of P fertilizer were observed. However, we shown that rhizosphere microbial community responded differently with $FePO_4$ NPs or with TSP, particularly in the case of alkaline phosphatases which were more secreted by plant roots after the treatment with TSP in respect of NPs. This could indicate that an acidification of the rhizosphere was still occurring, selecting the type of phosphatase present in the rhizosphere environment depending on the pH of the soil solution. Moreover, proteases were more represented after the treatment with NPs than with TSP and could be linked to the higher coupled metabolism of microorganisms and plants in the rhizosphere. This could indicate that the process of solubilization of NPs was always in progress, requiring a higher metabolism rate of microbiome, because of the slow-release nature of $FePO_4$ NPs.

In conclusion, in this work we showed that $FePO_4$ NPs can be applied to the soil without any negative effect for the environment, enhancing plant growth and providing P and might stimulate the soil microbial metabolic activity. This novel fertilizer has

the potential to rationalize the chemical inputs in agriculture, and eventually increasing NUE in plants in a sustainable manner.

REFERENCES

Achari, G. A., & Kowshik, M. (2018). Recent Developments on Nanotechnology in Agriculture: Plant Mineral Nutrition, Health, and Interactions with Soil Microflora. In Journal of Agricultural and Food Chemistry (Vol. 66, Issue 33, pp. 8647–8661). American Chemical Society. https://doi.org/10.1021/acs.jafc.8b00691

Adetunji, A. T., Lewu, F. B., Mulidzi, R., & Ncube, B. (2017). The biological activities of β-glucosidase, phosphatase and urease as soil quality indicators: a review. In Journal of Soil Science and Plant Nutrition (Vol. 17, Issue 3).

Álvarez-Fernández, A., Orera, I., Abadía, J., & Abadía, A. (2007). Determination of Synthetic Ferric Chelates Used as Fertilizers by Liquid Chromatography-Electrospray/Mass Spectrometry in Agricultural Matrices. Journal of the American Society for Mass Spectrometry, 18(1), 37–47. https://doi.org/10.1016/j.jasms.2006.08.018

Asadishad, B., Chahal, S., Akbari, A., Cianciarelli, V., Azodi, M., Ghoshal, S., & Tufenkji, N. (2018). Amendment of Agricultural Soil with Metal Nanoparticles: Effects on Soil Enzyme Activity and Microbial Community Composition. Environmental Science and Technology, 52(4), 1908–1918. https://doi.org/10.1021/acs.est.7b05389

Aslani, F., Bagheri, S., Muhd Julkapli, N., Juraimi, A. S., Hashemi, F. S. G., & Baghdadi, A. (2014). Effects of engineered nanomaterials on plants growth: An overview. In Scientific World Journal (Vol. 2014). Hindawi Publishing Corporation. https://doi.org/10.1155/2014/641759

Fuad Ameena, Khawla Alsamhary, Jamila A. Alabdullatif, Saleh ALNadhari (2021). A review on metal-based nanoparticles and their toxicity to beneficial soil bacteria and fungi. Ecotoxicology and Environmental Safety 213 (2021) 112027. https://doi.org/10.1016/j.ecoenv.2021.112027

Bakshi, M., & Oelmüller, R. (2014). Wrky transcription factors jack of many trades in plants. Plant Signaling and Behavior, 9(FEB). https://doi.org/10.4161/psb.27700

Baligar, V. C., & Fageria, N. K. (2015). Nutrient Use Efficiency in Plants: An Overview. In Nutrient Use Efficiency: From Basics to Advance (pp. 1–14). Springer India. https://doi.org/10.1007/978-81-322-2169-2_2

Baligar, V. C., Fageria, N. K., & He, Z. L. (2001). Nutrient use efficiency in plants. Communications in Soil Science and Plant Analysis, 32(7–8), 921–950. https://doi.org/10.1081/CSS-100104098

Bari Rajendra, Pant Bikram Datt, Stitt Mark , Scheible Wolf-Rüdiger (2006). PHO2, MicroRNA399, and PHR1 Define a Phosphate-Signaling Pathway in Plants. Plant Physiology,July 2006, Vol. 141, pp. 988–999. DOI: https://doi.org/10.1104/pp.106.079707

Beasley, J. T., Bonneau, J. P., & Johnson, A. A. T. (2017). Characterisation of the nicotianamine aminotransferase and deoxymugineic acid synthase genes essential to

Strategy II iron uptake in bread wheat (Triticum aestivum L.). PLoS ONE, 12(5). https://doi.org/10.1371/journal.pone.0177061

Ben-Moshe, T., Frenk, S., Dror, I., Minz, D., & Berkowitz, B. (2013). Effects of metal oxide nanoparticles on soil properties. Chemosphere, 90(2), 640–646. https://doi.org/10.1016/j.chemosphere.2012.09.018

Berendsen, R. L., Pieterse, C. M. J., & Bakker, P. A. H. M. (2012). The rhizosphere microbiome and plant health. In Trends in Plant Science (Vol. 17, Issue 8, pp. 478–486). https://doi.org/10.1016/j.tplants.2012.04.001

Branscheid Anja, Sieh Daniela, Pant Bikram Datt, May Patrick, Devers Emanuel A, Elkrog Anders, Schauser Leif, Scheible Wolf-Rüdiger, Krajinski Franziska (2010). Expression pattern suggests a role of MiR399 in the regulation of the cellular response to local Pi increase during arbuscular mycorrhizal symbiosis. Mol Plant Microbe Interact. 2010 Jul;23(7):915-26. doi: 10.1094/MPMI-23-7-0915.

Brzostek, E. R., Greco, A., Drake, J. E., & Finzi, A. C. (2013). Root carbon inputs to the rhizo-sphere stimulate extracellular enzyme activity and increase nitrogen availability in temperate forest soils. Biogeochemistry, 115(1–3), 65–76. https://doi.org/10.1007/s10533-012-9818-9

Cabugao, K. G., Timm, C. M., Carrell, A. A., Childs, J., Lu, T. Y. S., Pelletier, D. A., Weston, D. J., & Norby, R. J. (2017). Root and rhizosphere bacterial phosphatase activity varies with tree species and soil phosphorus availability in puerto rico tropical forest. Frontiers in Plant Science, 8. https://doi.org/10.3389/fpls.2017.01834

Carstensen, A., Herdean, A., Schmidt, S. B., Sharma, A., Spetea, C., Pribil, M., & Husted, S. (2018). The impacts of phosphorus deficiency on the photosynthetic electron transport chain1[OPEN]. Plant Physiology, 177(1), 271–284. https://doi.org/10.1104/PP.17.01624

Cenciani, K. S., Freitas, S., Auxiliadora, S., Critter, M., & Airoldi, C. (2008). MICROBIAL EN-ZYMATIC ACTIVITY AND THERMAL EFFECT IN A TROPICAL SOIL TREATED WITH ORGANIC MATERIALS. In Sci. Agric (Issue 6).

Chen, J., Lü, S., Zhang, Z., Zhao, X., Li, X., Ning, P., & Liu, M. (2018). Environmentally friendly fertilizers: A review of materials used and their effects on the environment. Science of the Total Environment, 613–614, 829–839. https://doi.org/10.1016/j.scitotenv.2017.09.186

Chen, Y. F., Etheridge, N., & Schaller, G. E. (2005). Ethylene signal transduction. In Annals of Botany (Vol. 95, Issue 6, pp. 901–915). https://doi.org/10.1093/aob/mci100

Christian, P., von der Kammer, F., Baalousha, M., & Hofmann, T. (2008). Nanoparticles: Structure, properties, preparation and behaviour in environmental media. In Ecotoxicology (Vol. 17, Issue 5, pp. 326–343). https://doi.org/10.1007/s10646-008-0213-1

Colombo, C., Palumbo, G., He, J. Z., Pinton, R., & Cesco, S. (2014). Review on iron availability in soil: Interaction of Fe minerals, plants, and microbes. In Journal of Soils

and Sediments (Vol. 14, Issue 3, pp. 538–548). https://doi.org/10.1007/s11368-013-0814-z

Dick, W. A., Cheng, L., & Wang, P. (2000). Soil acid and alkaline phosphatase activity as pH ad-justment indicators. www.elsevier.com/locate/soilbio

Degryse, F., & McLaughlin, M. J. (2014). Phosphorus Diffusion from Fertilizer: Visualization, Chemical Measurements, and Modeling. Soil Science Society of America Journal, 78(3), 832–842. https://doi.org/10.2136/sssaj2013.07.0293

Dolgikh, V. A., Pukhovaya, E. M., & Zemlyanskaya, E. v. (2019). Shaping Ethylene Response: The Role of EIN3/EIL1 Transcription Factors. In Frontiers in Plant Science (Vol. 10). Frontiers Media S.A. https://doi.org/10.3389/fpls.2019.01030

Du, W., Sun, Y., Ji, R., Zhu, J., Wu, J., & Guo, H. (2011). TiO2 and ZnO nanoparticles negatively affect wheat growth and soil enzyme activities in agricultural soil. Journal of Environmental Moni-toring, 13(4), 822–828. https://doi.org/10.1039/c0em00611d

Duhan, J. S., Kumar, R., Kumar, N., Kaur, P., Nehra, K., & Duhan, S. (2017). Nanotechnology: The new perspective in precision agriculture. In Biotechnology Reports (Vol. 15, pp. 11–23). Elsevier B.V. https://doi.org/10.1016/j.btre.2017.03.002

Eeva J. VAINIO, & Jarkko HANTULA. (2000). Direct analysis of wood-inhabiting fungi using denaturing gradient gel electrophoresis of ampli®ed ribosomal DNA. Mycol. Res. , 104(8), 927–936.

Elmore, J. M., & Coaker, G. (2011). The role of the plasma membrane H+-ATPase in plant-microbe interactions. In Molecular Plant (Vol. 4, Issue 3, pp. 416–427). Oxford University Press. https://doi.org/10.1093/mp/ssq083

FAO and IWMI. (2018). More people, more food, worse water? a global review of water pollution from agriculture.

Felske, A., Wolterink, A., van Lis, R., & Akkermans, A. D. L. (1998). Phylogeny of the Main Bacterial 16S rRNA Sequences in Drentse A Grassland Soils (The Netherlands). In APPLIED AND ENVIRONMENTAL MICROBIOLOGY (Vol. 64, Issue 3). http://aem.asm.org/

Fraceto, L. F., Grillo, R., de Medeiros, G. A., Scognamiglio, V., Rea, G., & Bartolucci, C. (2016). Nanotechnology in agriculture: Which innovation potential does it have? Frontiers in Environmental Science, 4(MAR). https://doi.org/10.3389/fenvs.2016.00020

Fu, L., Wang, Z., Dhankher, O. P., & Xing, B. (2020). Nanotechnology as a new sustainable approach for controlling crop diseases and increasing agricultural production. In Journal of Experimental Botany (Vol. 71, Issue 2, pp. 507–519). Oxford University Press. https://doi.org/10.1093/jxb/erz314

García-Sánchez, S., Bernales, I., & Cristobal, S. (2015). Early response to nanoparticles in the Arabidopsis transcriptome compromises plant defence and root-hair development through salicylic acid signalling. BMC Genomics, 16(1). https://doi.org/10.1186/s12864-015-1530-4

Gardea-Torresdey, J. L., Rico, C. M., & White, J. C. (2014). Trophic transfer, transformation, and impact of engineered nanomaterials in terrestrial environments. Environmental Science and Technology, 48(5), 2526–2540. https://doi.org/10.1021/es4050665

Ge, Y., Priester, J. H., van de Werfhorst, L. C., Walker, S. L., Nisbet, R. M., An, Y. J., Schimel, J. P., Gardea-Torresdey, J. L., & Holden, P. A. (2014). Soybean plants modify metal oxide nanoparti-cle effects on soil bacterial communities. Environmental Science and Technology, 48(22), 13489–13496. https://doi.org/10.1021/es5031646

Ge, Y., Schimel, J. P., & Holdena, P. A. (2012). Identification of soil bacteria susceptible to TiO2 and ZnO nanoparticles. Applied and Environmental Microbiology, 78(18), 6749–6758. https://doi.org/10.1128/AEM.00941-12

Gianfreda, L., & Ruggiero, P. (2006). *Nucleic Acid and Proteins in Soil. Chapter 12. Enzyme Activities in Soil*. Nucleic Acids and Proteins in Soil (pp.257-311). DOI:10.1007/3-540-29449-X_12

Guozhong Cao. (2004). Nanostructures & nanomaterials: synthesis, properties & applications.

Hackenberg M., Shi B. J., Gustafson P., Langridge P. (2013). Characterization of phosphorus-regulated miR399 and miR827 and their isomirs in barley under phosphorus-sufficient and phosphorus-deficient. BMC Plant Biology2013,13:214. DOI:10.1186/1471-2229-13-214

Hammer, D. A. T., Ryan, P. D., Hammer, Ø., & Harper, D. A. T. (2001). Past: Paleontological Statistics Software Package for Education and Data Analysis. In Palaeontologia Electronica (Vol. 4, Issue 1). http://palaeo-electronica.orghttp://palaeo-electronica.org/2001_1/past/issue1_01.htm.

Handy, R. D., von der Kammer, F., Lead, J. R., Hassellöv, M., Owen, R., & Crane, M. (2008). The ecotoxicology and chemistry of manufactured nanoparticles. In Ecotoxicology (Vol. 17, Issue 4, pp. 287–314). https://doi.org/10.1007/s10646-008-0199-8

Hasan, M. M., Hasan, M. M., Teixeira da Silva, J. A., & Li, X. (2016). Regulation of phosphorus uptake and utilization: Transitioning from current knowledge to practical strategies. In Cellular and Molecular Biology Letters (Vol. 21, Issue 1). BioMed Central Ltd. https://doi.org/10.1186/s11658-016-0008-y

Hawkesford, M. J., Kopriva, S., & de Kok, L. J. (Luit J.). (n.d.). Nutrient use efficiency in plants : concepts and approaches.

He, L., Liu, Y., Mustapha, A., & Lin, M. (2011). Antifungal activity of zinc oxide nanoparticles against Botrytis cinerea and Penicillium expansum. Microbiological Research, 166(3), 207–215. https://doi.org/10.1016/j.micres.2010.03.003

Herz, S., Eberhardt, S., & Bacher, A. (2000). Biosynthesis of riboflavin in plants. The ribA gene of Arabidopsis thaliana species a bifunctional GTP cyclohydrolase II/3,4-dihydroxy-2-butanone 4-phosphate synthase. www.elsevier.com/locate/phytochem

Hossain, Z., Yasmeen, F., & Komatsu, S. (2020). Nanoparticles: Synthesis, morpho-physiological effects, and proteomic responses of crop plants. In International Journal of Molecular Sciences (Vol. 21, Issue 9). MDPI AG. https://doi.org/10.3390/ijms21093056

Hsieh, E. J., & Waters, B. M. (2016). Alkaline stress and iron deficiency regulate iron uptake and riboflavin synthesis gene expression differently in root and leaf tissue: Implications for iron deficiency chlorosis. Journal of Experimental Botany, 67(19), 5671–5685. https://doi.org/10.1093/jxb/erw328

Hu, J., Guo, H., Li, J., Gan, Q., Wang, Y., & Xing, B. (2017). Comparative impacts of iron oxide nanoparticles and ferric ions on the growth of Citrus maxima. Environmental Pollution, 221, 199–208. https://doi.org/10.1016/j.envpol.2016.11.064

Huang, C. Y., Shirley, N., Genc, Y., Shi, B., & Langridge, P. (2011). Phosphate utilization efficiency correlates with expression of low-affinity phosphate transporters and noncoding RNA, IPS1, in Barley. Plant Physiology, 156(3), 1217–1229. https://doi.org/10.1104/pp.111.178459

Jiang, C., Gao, X., Liao, L., Harberd, N. P., & Fu, X. (2007). Phosphate starvation root architecture and anthocyanin accumulation responses are modulated by the gibberellin-DELLA signaling pathway in Arabidopsis. Plant Physiology, 145(4), 1460–1470. https://doi.org/10.1104/pp.107.103788

Kah, M., Kookana, R. S., Gogos, A., & Bucheli, T. D. (2018). A critical evaluation of nanopesticides and nanofertilizers against their conventional analogues. Nature Nanotechnology, 13(8), 677–684. https://doi.org/10.1038/s41565-018-0131-1

Kappler, A., & Straub, K. L. (2018). Geomicrobiological cycling of iron. In Molecular Geomicrobiology (Vol. 59, pp. 85–108). Walter de Gruyter GmbH. https://doi.org/10.2138/rmg.2005.59.5

Khan, I., Saeed, K., & Khan, I. (2019). Nanoparticles: Properties, applications and toxicities. In Arabian Journal of Chemistry (Vol. 12, Issue 7, pp. 908–931). Elsevier B.V. https://doi.org/10.1016/j.arabjc.2017.05.011

Kim, C. M., & Dolan, L. (2016). ROOT HAIR DEFECTIVE SIX-LIKE Class I Genes Promote Root Hair Development in the Grass Brachypodium distachyon. PLoS Genetics, 12(8). https://doi.org/10.1371/journal.pgen.1006211

Kim, J. H., Oh, Y., Yoon, H., Hwang, I., & Chang, Y. S. (2015). Iron nanoparticle-induced activation of plasma membrane H+-ATPase promotes stomatal opening in Arabidopsis thaliana. Environmental Science and Technology, 49(2), 1113–1119. https://doi.org/10.1021/es504375t

Kobayashi, T., & Nishizawa, N. K. (2012). Iron uptake, translocation, and regulation in higher plants. In Annual Review of Plant Biology (Vol. 63, pp. 131–152). https://doi.org/10.1146/annurev-arplant-042811-105522

Koen, E., Besson-Bard, A., Duc, C., Astier, J., Gravot, A., Richaud, P., Lamotte, O., Boucherez, J., Gaymard, F., & Wendehenne, D. (2013a). Arabidopsis thaliana

nicotianamine synthase 4 is required for proper response to iron deficiency and to cadmium exposure. Plant Science, 209, 1–11. https://doi.org/10.1016/j.plantsci.2013.04.006

Koen, E., Besson-Bard, A., Duc, C., Astier, J., Gravot, A., Richaud, P., Lamotte, O., Boucherez, J., Gaymard, F., & Wendehenne, D. (2013b). Arabidopsis thaliana nicotianamine synthase 4 is required for proper response to iron deficiency and to cadmium exposure. Plant Science, 209, 1–11. https://doi.org/10.1016/j.plantsci.2013.04.006

Kristoffersen, A. Ø., Krogstad, T., & Øgaard, A. F. (2020). Prediction of available phosphorus in soil: Combined use for crop production and water quality protection. *Journal of Environmental Quality*, *49*(6), 1575–1584. https://doi.org/10.1002/jeq2.20165

Kummu, M., de Moel, H., Porkka, M., Siebert, S., Varis, O., & Ward, P. J. (2012). Lost food, wasted resources: Global food supply chain losses and their impacts on freshwater, cropland, and fertiliser use. Science of the Total Environment, 438, 477–489. https://doi.org/10.1016/j.scitotenv.2012.08.092

Ladd, J. N., & Butler, J. H. A. (1972). SHORT-TERM ASSAYS OF SOIL PROTEOLYTIC ENZYME ACTIVITIES USING PROTEINS AND DIPEPTIDE DERIVATIVES AS SUBSTRATES. In SoilBiol. Biochem (Vol. 4). Pergamon Press.

Lappalainen, J., Juvonen, Ri., Vaajasaarl, K., & Karp, M. (1999). PIh S0045-6535(98)00352-X A NEW FLASH METHOD FOR MEASURING THE TOXICITY OF SOLID AND COLORED SAMPLES. In Chemosphere (Vol. 38, Issue 5).

Lauer, M. J., Blevins, D. G., & Sierzputowska-Gracz, H. (1989). 31P-Nuclear Magnetic Resonance Determination of Phosphate Compartmentation in Leaves of Reproductive Soybeans (Glycine max L.) as Affected by Phosphate Nutrition'. In Plant Physiol (Vol. 89). https://plantphysiol.org

Lauer, M. J., Pallardy, S. G., Blevins, D. G., & Randall, D. D. (1989). Whole Leaf Carbon Exchange Characteristics of Phosphate Deficient Soybeans (Glycine max L. ". In Plant Physiol (Vol. 91). https://plantphysiol.org

Li, Y. S., Gao, Y., Tian, Q. Y., Shi, F. L., Li, L. H., & Zhang, W. H. (2011). Stimulation of root ac-id phosphatase by phosphorus deficiency is regulated by ethylene in Medicago falcata. Environmen-tal and Experimental Botany, 71(1), 114–120. https://doi.org/10.1016/j.envexpbot.2010.11.007

Li, T., Lü, S., Ji, Y., Qi, T., & Liu, M. (2018). A biodegradable Fe-fertilizer with high mechanical property and sustainable release for potential agriculture and horticulture applications. New Journal of Chemistry, 42(23), 19129–19136. https://doi.org/10.1039/c8nj04381g

Liang, G., Zhang, H., Li, Y., Pu, M., Yang, Y., Li, C., Lu, C., Xu, P., & Yu, D. (2020). FER-LIKE FE DEFICIENCY-INDUCED TRANSCRIPTION FACTOR (OsFIT) interacts with OsIRO2 to regulate iron homeostasis. https://doi.org/10.1101/2020.03.06.981126

Lin, D., & Xing, B. (2008). Root uptake and phytotoxicity of ZnO nanoparticles. Environmental Science and Technology, 42(15), 5580–5585. https://doi.org/10.1021/es800422x

Liu, R., & Lal, R. (2015). Potentials of engineered nanoparticles as fertilizers for increasing agronomic productions. In Science of the Total Environment (Vol. 514, pp. 131–139). Elsevier B.V. https://doi.org/10.1016/j.scitotenv.2015.01.104

Lohila, A., Aurela, M., Regina, K., & Laurila, T. (2003). Soil and total ecosystem respiration in agricultural fields: effect of soil and crop type. In and Soil (Vol. 251, Issue 2).

Lucena, J. J. (2003). Fe chelates for remediation of Fe chlorosis in strategy I plants. Journal of Plant Nutrition, 26(10–11), 1969–1984. https://doi.org/10.1081/PLN-120024257

Ma, N., Dong, L., Lü, W., Lü, J., Meng, Q., & Liu, P. (2020). Transcriptome analysis of maize seedling roots in response to nitrogen-, phosphorus-, and potassium deficiency. Plant and Soil, 447(1–2), 637–658. https://doi.org/10.1007/s11104-019-04385-3

Manika, M., & Ajittvarma, K. (2017). Soil Biology Nanoscience and Plant-Soil Systems. ISBN 978-3-319-46833-4. https://doi.org/10.1007/978-3-319-46835-8

Marchiol, L., Iafisco, M., Fellet, G., & Adamiano, A. (2020). Nanotechnology support the next agricultural revolution: Perspectives to enhancement of nutrient use efficiency. In Advances in Agronomy (1st ed.). Elsevier Inc. https://doi.org/10.1016/bs.agron.2019.12.001

Margalef, O., Sardans, J., Fernández-Martínez, M., Molowny-Horas, R., Janssens, I. A., Ciais, P., Goll, D., Richter, A., Obersteiner, M., Asensio, D., & Peñuelas, J. (2017). Global patterns of phos-phatase activity in natural soils. Scientific Reports, 7(1). https://doi.org/10.1038/s41598-017-01418-8

Marschner, H., & Rsmheld, V. (1994). Strategies of plants for acquisition of iron. In Plant and Soil (Vol. 165). Kluwer Academic Publishers.

Marschner, P. (2011). Marschner's Mineral Nutrition of Higher Plants Third Edition. https://doi.org/10.1016/B978-0-12-384905-2.X0001-5

Meyer, G., Bell, M. J., Doolette, C. L., Brunetti, G., Zhang, Y., Lombi, E., & Kopittke, P. M. (2020). Plant-Available Phosphorus in Highly Concentrated Fertilizer Bands: Effects of Soil Type, Phosphorus Form, and Coapplied Potassium. *Journal of Agricultural and Food Chemistry*, *68*(29), 7571–7580. https://doi.org/10.1021/acs.jafc.0c01287

Mirzajani, F., Askari, H., Hamzelou, S., Schober, Y., Römpp, A., Ghassempour, A., & Spengler, B. (2014). Proteomics study of silver nanoparticles toxicity on Oryza sativa L. Ecotoxicology and Environmental Safety, 108, 335–339. https://doi.org/10.1016/j.ecoenv.2014.07.013

Monreal, C. M., Derosa, M., Mallubhotla, S. C., Bindraban, P. S., & Dimkpa, C. (2016). Nanotechnologies for increasing the crop use efficiency of fertilizer-micronutrients. In

Biology and Fertility of Soils (Vol. 52, Issue 3, pp. 423–437). Springer Verlag. https://doi.org/10.1007/s00374-015-1073-5

Mori Satoshi. (1999). Iron acquisition by plants. 2(Current Opinion in Plant Biology), 250–253.

Morrissey, J., & Guerinot, M. lou. (2009). Iron uptake and transport in plants: The good, the bad, and the ionome. Chemical Reviews, 109(10), 4553–4567. https://doi.org/10.1021/cr900112r

Mosse Barbara. (1972). Plant growht responses to vescicular-arbuscolar mycorrhiza. The New Phytologist Vol. 72, No. 1 (Jan., 1973), pp. 127-136

Mudahar, M. S., & Hignett, T. P. (1985). ENERGY EFFICIENCY IN NITROGEN FERTILIZER PRODUCTION. In Energy in Agriculture (Vol. 4).

Müller, J., Toev, T., Heisters, M., Teller, J., Moore, K. L., Hause, G., Dinesh, D. C., Bürstenbinder, K., & Abel, S. (2015). Iron-Dependent Callose Deposition Adjusts Root Meristem Maintenance to Phosphate Availability. Developmental Cell, 33(2), 216–230. https://doi.org/10.1016/j.devcel.2015.02.007

Nannipieri, P, Ascher, J., Ceccherini, M. T., Landi, L., Pietramellara, G., & Renella, G. (2003). Microbial diversity and soil functions. https://doi.org/10.1046/j.1365-2389.2003.00556.x

Nannipieri, P., Ascher-Jenull, J., Ceccherini, M. T., Pietramellara, G., Renella, G., & Scholter, M. (2020). Beyond microbial diversity for predicting soil functions: A mini review. In Pedosphere (Vol. 30, Issue 1, pp. 5–17). Soil Science Society of China. https://doi.org/10.1016/S1002-0160(19)60824-6

Nannipieri, Paolo, Trasar-Cepeda, C., & Dick, R. P. (2018). Soil enzyme activity: a brief history and biochemistry as a basis for appropriate interpretations and meta-analysis. Biology and Fertility of Soils, 54(1), 11–19. https://doi.org/10.1007/s00374-017-1245-6

Enrique Navarro, Anders Baun, Renata Behra, Nanna B. Hartmann, Juliane Filser, Ai-Jun Miao, Antonietta Quigg, Peter H. Santschi, Laura Sigg (2008). Environmental be-havior and ecotoxicity of engineerednanoparticles to algae, plants, and fungi. Ecotox-icology (2008) 17:372–386. DOI 10.1007/s10646-008-0214-0

Norwegian Pollution Control Authority, E.J. Joner, T. Hartnik, & C.E. Amundsen. (2008). Environmental fate and ecotoxicity of engineered nanoparticles: Nanoparticles and the environment.

Olsen, S. R., & Sommers, L. E. (1982). Determination of available phosphorus. In "Method of Soil Analysis", vol. 2 ed. A. L. Page, R. H. Miller, and D. R. Keeney, 403. Madison, WI: American Society of Agronomy.

Oyewole, O. A., Inselsbacher, E., & Näsholm, T. (2014). Direct estimation of mass flow and diffusion of nitrogen compounds in solution and soil. New Phytologist, 201(3), 1056–1064. https://doi.org/10.1111/nph.12553

Pachapur, V., Brar, S. K., Verma, M., & Surampalli, R. Y. (2015). Nano-ecotoxicology of natural and engineered nanomaterials for animals and humans. In Nanomaterials in the Environment (pp. 421–438). American Society of Civil Engineers (ASCE). https://doi.org/10.1061/9780784414088.ch16

Pastorelli, R., & Landi, S. (2009). Changes in active microbial soil communities in agricultural managments: From anthropic to natural. LIFE+SelPiBio View project 42° Congresso Nazionale della Società Italiana di Scienza del Suolo "Il suolo a servizio degli ecosistemi" View project. https://www.researchgate.net/publication/265278417

Pastorelli, R., Paletto, A., Agnelli, A. E., Lagomarsino, A., & de Meo, I. (2020). Microbial communities associated with decomposing deadwood of downy birch in a natural forest in Khibiny Mountains (Kola Peninsula, Russian Federation). Forest Ecology and Management, 455. https://doi.org/10.1016/j.foreco.2019.117643

Penn, C. J., & Camberato, J. J. (2019). A critical review on soil chemical processes that control how soil ph affects phosphorus availability to plants. Agriculture (Switzerland), 9(6). https://doi.org/10.3390/agriculture9060120

Péret, B., Desnos, T., Jost, R., Kanno, S., Berkowitz, O., & Nussaume, L. (2014). Root architecture responses: In search of phosphate. Plant Physiology, 166(4), 1713–1723. https://doi.org/10.1104/pp.114.244541

Pérez-de-Luque, A. (2017). Interaction of nanomaterials with plants: What do we need for real applications in agriculture? Frontiers in Environmental Science, 5(APR). https://doi.org/10.3389/fenvs.2017.00012

Pérez-Labrada, F., Benavides-Mendoza, A., Juárez-Maldonado, A., Solís-Gaona, S., & González-Morales, S. (2020). Organic acids combined with Fe-chelate improves ferric nutrition in tomato grown in calcisol soil. Journal of Soil Science and Plant Nutrition, 20(2), 673–683. https://doi.org/10.1007/s42729-019-00155-3

Pushnik, J. C., & Miller, G. W. (1989). Iron regulation of chloroplast photosynthetic function: Mediation of ps i development. Journal of Plant Nutrition, 12(4), 407–421. https://doi.org/10.1080/01904168909363962

Raliya, R., Saharan, V., Dimkpa, C., & Biswas, P. (2018). Nanofertilizer for Precision and Sustainable Agriculture: Current State and Future Perspectives. In Journal of Agricultural and Food Chemistry (Vol. 66, Issue 26, pp. 6487–6503). American Chemical Society. https://doi.org/10.1021/acs.jafc.7b02178

Ramette, A. (2007). Multivariate analyses in microbial ecology. In FEMS Microbiology Ecology (Vol. 62, Issue 2, pp. 142–160). https://doi.org/10.1111/j.1574-6941.2007.00375.x

Rana, S., & Kalaichelvan, P. T. (2013). Ecotoxicity of Nanoparticles. ISRN Toxicology, 2013, 1–11. https://doi.org/10.1155/2013/574648

Ray Paresh Chandra, Yu Hongtau & Fu Peter P. (2009). Toxicity and Environmental Risks of Nanomaterials: Challenges and Future Needs, Journal of Environmental Science and Health Part C, 27:1, 1-35, DOI: 10.1080/10590500802708267

Recena, R., Díaz, I., del Campillo, M. C., Torrent, J., & Delgado, A. (2016). Calculation of threshold Olsen P values for fertilizer response from soil properties. Agronomy for Sustainable Development, 36(4). https://doi.org/10.1007/s13593-016-0387-5

Renella, G., Landi, L., Garcia Mina, J. M., Giagnoni, L., & Nannipieri, P. (2011). Microbial and hy-drolase activity after release of indoleacetic acid and ethylene-polyamine precursors by a model root surface. Applied Soil Ecology, 47(2), 106–110. https://doi.org/10.1016/j.apsoil.2010.11.009

Renella, G., Landi, L., Valori, F., & Nannipieri, P. (2007). Microbial and hydrolase activity after re-lease of low molecular weight organic compounds by a model root surface in a clayey and a sandy soil. Applied Soil Ecology, 36(2–3), 124–129. https://doi.org/10.1016/j.apsoil.2007.01.001

Richard P. Feynman. (1960). There's plenty of room at the bottom. Engineering and Science, 23, 22–36.

Roberts, T. L., & Johnston, A. E. (2015). Phosphorus use efficiency and management in agriculture. Resources, Conservation and Recycling, 105, 275–281. https://doi.org/10.1016/j.resconrec.2015.09.013

Rodrigues, S. M., Trindade, T., Duarte, A. C., Pereira, E., Koopmans, G. F., & Römkens, P. F. A. M. (2016). A framework to measure the availability of engineered nanoparticles in soils: Trends in soil tests and analytical tools. In TrAC - Trends in Analytical Chemistry (Vol. 75, pp. 129–140). Elsevier B.V. https://doi.org/10.1016/j.trac.2015.07.003

Romheld, V., & Marschner, H. (1986). Evidence for a Specific Uptake System for Iron Phytosiderophores in Roots of Grasses'. In Plant Physiol (Vol. 80).

Rui, M., Ma, C., Hao, Y., Guo, J., Rui, Y., Tang, X., Zhao, Q., Fan, X., Zhang, Z., Hou, T., & Zhu, S. (2016). Iron oxide nanoparticles as a potential iron fertilizer for peanut (Arachis hypogaea). Fron-tiers in Plant Science, 7(June2016). https://doi.org/10.3389/fpls.2016.00815

Růžička, K., Ljung, K., Vanneste, S., Podhorská, R., Beeckman, T., Friml, J., & Benková, E. (2007). Ethylene regulates root growth through effects on auxin biosynthesis and transport-dependent auxin distribution. Plant Cell, 19(7), 2197–2212. https://doi.org/10.1105/tpc.107.052126

Samreen, S., & Kausar, S. (2019). Phosphorus Fertilizer: The Original and Commercial Sources. In Phosphorus - Recovery and Recycling. IntechOpen. https://doi.org/10.5772/intechopen.82240

Santi, C., Zamboni, A., Varanini, Z., & Pandolfini, T. (2017). Growth stimulatory effects and genome-wide transcriptional changes produced by protein hydrolysates in maize seedlings. Frontiers in Plant Science, 8. https://doi.org/10.3389/fpls.2017.00433

Santi, S., Cesco, S., Varanini, Z., & Pinton, R. (2005). Two plasma membrane H+-ATPase genes are differentially expressed in iron-deficient cucumber plants. Plant

Physiology and Biochemistry, 43(3), 287–292. https://doi.org/10.1016/j.plaphy.2005.02.007

Schinner, Franz., Ohlinger, Richard., Kandeler, Ellen., & Margesin, Rosa. (1996). Methods in Soil Biology. Springer Berlin Heidelberg.

Sega, D., Baldan, B., Zamboni, A., & Varanini, Z. (2020). FePO4 NPs Are an Efficient Nutritional Source for Plants: Combination of Nano-Material Properties and Metabolic Responses to Nutritional Deficiencies. Frontiers in Plant Science, 11. https://doi.org/10.3389/fpls.2020.586470

Sega, D., Ciuffreda, G., Mariotto, G., Baldan, B., Zamboni, A., & Varanini, Z. (2019). FePO4 nanoparticles produced by an industrially scalable continuous-flow method are an available form of P and Fe for cucumber and maize plants. Scientific Reports, 9(1), 11252. https://doi.org/10.1038/s41598-019-47492-y

Shen, H., Chen, J., Wang, Z., Yang, C., Sasaki, T., Yamamoto, Y., Matsumoto, H., & Yan, X. (2006). Root plasma membrane H+-ATPase is involved in the adaptation of soybean to phosphorus starvation. Journal of Experimental Botany, 57(6), 1353–1362. https://doi.org/10.1093/jxb/erj111

Shen, J, Rengel, Z., Tang, C., & Zhang, F. (2003). Role of phosphorus nutrition in development of cluster roots and release of carboxylates in soil-grown Lupinus albus. In Plant and Soil (Vol. 248).

Shen, Jianbo, Yuan, L., Zhang, J., Li, H., Bai, Z., Chen, X., Zhang, W., & Zhang, F. (2011). Phosphorus dynamics: From soil to plant. Plant Physiology, 156(3), 997–1005. https://doi.org/10.1104/pp.111.175232

Šimek, M., Elhottová, D., Mench, M., Giagnoni, L., Nannipieri, P., & Renella, G. (2017). Greenhouse gas emissions from a Cu-contaminated soil remediated by in situ stabilization and phytomanaged by a mixed stand of poplar, willows, and false indigobush. International Journal of Phytoremediation, 19(11), 976–984. https://doi.org/10.1080/15226514.2016.1267706

Somssich, M., Khan, G. A., & Staffan, S. P. (2016). Cell wall heterogeneity in root development of arabidopsis. In Frontiers in Plant Science (Vol. 7, Issue AUG2016). Frontiers Research Foundation. https://doi.org/10.3389/fpls.2016.01242

Stone, V., Nowack, B., Baun, A., van den Brink, N., von der Kammer, F., Dusinska, M., Handy, R., Hankin, S., Hassellöv, M., Joner, E., & Fernandes, T. F. (2010). Nanomaterials for environmental studies: Classification, reference material issues, and strategies for physico-chemical characterisa-tion. Science of the Total Environment, 408(7), 1745–1754. https://doi.org/10.1016/j.scitotenv.2009.10.035

Su, Y., Ashworth, V. E. T. M., Geitner, N. K., Wiesner, M. R., Ginnan, N., Rolshausen, P., Roper, C., & Jassby, D. (2020). Delivery, Fate, and Mobility of Silver Nanoparticles in Citrus Trees. ACS Nano, 14(3), 2966–2981. https://doi.org/10.1021/acsnano.9b07733

Subramanian, K. S., Manikandan, A., Thirunavukkarasu, M., & Rahale, C. S. (2015). Nano-fertilizers for balanced crop nutrition. In Nanotechnologies in Food and

Agriculture (pp. 69–80). Springer International Publishing. https://doi.org/10.1007/978-3-319-14024-7_3

Motofumi Suzuki, Atsumi Urabe, Sayaka Sasaki, Ryo Tsugawa, Satoshi Nishio, Haruka Mukaiyama,Yoshiko Murata, Hiroshi Masuda, May Sann Aung, Akane Mera, Masaki Takeuchi, Keijo Fukushima, Michika Kanaki, Kaori Kobayashi, Yuichi Chiba, Binod Babu Shrestha,Hiromi Nakanishi, Takehiro Watanabe, Atsushi Nakayama, Hiromichi Fujino, Takanori Kobayashi, Keiji Tanino, Naoko K. Nishizawa & Kosuke Namba (2021). Development of a mugineic acid familyphytosiderophore analog as an iron fertilizer. NATURE COMMUNICATION (2021) 12:1558| https://doi.org/10.1038/s41467-021-21837

Syers, J. K. (John K., Johnston, A. E., Curtin, Denis., & Food and Agriculture Organization of the United Nations. (2008). Efficiency of soil and fertilizer phosphorus use : reconciling changing concepts of soil phosphorus behaviour with agronomic information. Food and Agriculture Organization of the United Nations.

Syers, J. K., Johnston, A. E., & Curtin. (2008). Improving the efficiency of soil and fertilizer phosphorus use in. FAO Fertilizer and Plant Nutrition Bulletin 18. FAO (2008).

Syu, Y. yu, Hung, J. H., Chen, J. C., & Chuang, H. wen. (2014). Impacts of size and shape of silver nanoparticles on Arabidopsis plant growth and gene expression. Plant Physiology and Biochemistry, 83, 57–64. https://doi.org/10.1016/j.plaphy.2014.07.010

Tarafdar, J. C., & Claassen, N. (1988). Organic phosphorus compounds as a phosphorus source for higher plants through the activity of phosphatases produced by plant roots and microorganisms. In Biol Fertil Soils (Vol. 5).

Teng, Q., Zhang, D., Niu, X., & Jiang, C. (2018). Influences of application of slow-release Nano-fertilizer on green pepper growth, soil nutrients and enzyme activity. IOP Conference Series: Earth and Environmental Science, 208(1). https://doi.org/10.1088/1755-1315/208/1/012014

Tomasi, N., Kretzschmar, T., Espen, L., Weisskopf, L., Fuglsang, A. T., Palmgren, M. G., Neumann, G., Varanini, Z., Pinton, R., Martinoia, E., & Cesco, S. (2009). Plasma membrane H+-ATPase-dependent citrate exudation from cluster roots of phosphate-deficient white lupin. Plant, Cell and Environment, 32(5), 465–475. https://doi.org/10.1111/j.1365-3040.2009.01938.x

Vance, C. P., Uhde-Stone, C., & Allan, D. L. (2003). Phosphorus acquisition and use: critical adaptations by plants for securing a nonrenewable resource (Vol. 55108). www.newphytologist.com

Vannini, C., Domingo, G., Onelli, E., Prinsi, B., Marsoni, M., Espen, L., & Bracale, M. (2013). Morphological and Proteomic Responses of Eruca sativa Exposed to Silver Nanoparticles or Silver Nitrate. PLoS ONE, 8(7). https://doi.org/10.1371/journal.pone.0068752

Versaw, W. K., & Harrison, M. J. (2002). A chloroplast phosphate transporter, PHT2;1, influences allocation of phosphate within the plant and phosphate-starvation responses. Plant Cell, 14(8), 1751–1766. https://doi.org/10.1105/tpc.002220

Vorwieger, A., Gryczka, C., Czihal, A., Douchkov, D., Tiedemann, J., Mock, H. P., Jakoby, M., Weisshaar, B., Saalbach, I., & Bäumlein, H. (2007). Iron assimilation and transcription factor controlled synthesis of riboflavin in plants. Planta, 226(1), 147–158. https://doi.org/10.1007/s00425-006-0476-9.

Vranova, V., Rejsek, K., & Formanek, P. (2013). Proteolytic activity in soil: A review. In Applied Soil Ecology (Vol. 70, pp. 23–32). https://doi.org/10.1016/j.apsoil.2013.04.003

Walters Robin G., Ibrahim Douglas G., Horton Peter, Kruger Nicholas J. (2004). A Mutant of Arabidopsis Lacking the Triose-Phosphate/Phosphate Translocator Reveals Metabolic Regulation of Starch Breakdown in the Light. Plant Physiology, June 2004, Vol. 135, pp. 891–906. DOI: 10.1104/pp.104.040469.

Wang, F., Itai, R. N., Nozoye, T., Kobayashi, T., Nishizawa, N. K., & Nakanishi, H. (2020). The bHLH protein OsIRO3 is critical for plant survival and iron (Fe) homeostasis in rice (Oryza sativa L.) under Fe-deficient conditions. Soil Science and Plant Nutrition, 66(4), 579–592. https://doi.org/10.1080/00380768.2020.1783966

Wang, H. Y., Klatte, M., Jakoby, M., Bäumlein, H., Weisshaar, B., & Bauer, P. (2007). Iron deficiency-mediated stress regulation of four subgroup Ib BHLH genes in Arabidopsis thaliana. Planta, 226(4), 897–908. https://doi.org/10.1007/s00425-007-0535-x

Wang, W., Ryu, K. H., Bruex, A., Barron, C., & Schiefelbein, J. (2020). Molecular basis for a cell fate switch in response to impaired ribosome biogenesis in the Arabidopsis root epidermis. Plant Cell, 32(7), 2402–2423. https://doi.org/10.1105/tpc.19.00773

Wang, Z., Yue, L., Dhankher, O. P., & Xing, B. (2020). Nano-enabled improvements of growth and nutritional quality in food plants driven by rhizosphere processes. In Environment International (Vol. 142). Elsevier Ltd. https://doi.org/10.1016/j.envint.2020.105831

Ward, J. T., Lahner, B., Yakubova, E., Salt, D. E., & Raghothama, K. G. (2008). The effect of iron on the primary root elongation of Arabidopsis during phosphate deficiency. Plant Physiology, 147(3), 1181–1191. https://doi.org/10.1104/pp.108.118562

Watanabe, T., Kimura, M., & Asakawa, S. (2006). Community structure of methanogenic archaea in paddy field soil under double cropping (rice-wheat). Soil Biology and Biochemistry, 38(6), 1264–1274. https://doi.org/10.1016/j.soilbio.2005.09.020

Weeks, J. J., & Hettiarachchi, G. M. (2019). A Review of the Latest in Phosphorus Fertilizer Tech-nology: Possibilities and Pragmatism. Journal of Environmental Quality, 48(5), 1300–1313. https://doi.org/10.2134/jeq2019.02.0067

Wu, W., Zhu, S., Chen, Q., Lin, Y., Tian, J., & Liang, C. (2019). Cell wall proteins play critical roles in plant adaptation to phosphorus deficiency. In International Journal of

Molecular Sciences (Vol. 20, Issue 21). MDPI AG. https://doi.org/10.3390/ijms20215259

Yang, X., Alidoust, D., & Wang, C. (2020). Effects of iron oxide nanoparticles on the mineral com-position and growth of soybean (Glycine max L.) plants. Acta Physiologiae Plantarum, 42(8). https://doi.org/10.1007/s11738-020-03104-1

Yusefi-Tanha, E., Fallah, S., Rostamnejadi, A., & Pokhrel, L. R. (2020). Zinc oxide nanoparticles (ZnONPs) as a novel nanofertilizer: Influence on seed yield and antioxidant defense system in soil grown soybean (Glycine max cv. Kowsar). *Science of the Total Environment*, *738*. https://doi.org/10.1016/j.scitotenv.2020.140240

Yu, L., Wang, Y., Liu, Y., Li, N., Yan, J., & Luo, L. (2018). Wound-induced polypeptides improve resistance against Pseudomonas syringae pv. tomato DC3000 in Arabidopsis. Biochemical and Biophysical Research Communications, 504(1), 149–156. https://doi.org/10.1016/j.bbrc.2018.08.147

Zanin, L., Venuti, S., Zamboni, A., Varanini, Z., Tomasi, N., & Pinton, R. (2017). Transcriptional and physiological analyses of Fe deficiency response in maize reveal the presence of Strategy I components and Fe/P interactions. BMC Genomics, 18(1). https://doi.org/10.1186/s12864-016-3478-4

Zhu, Z. J., Wang, H., Yan, B., Zheng, H., Jiang, Y., Miranda, O. R., Rotello, V. M., Xing, B., & Vachet, R. W. (2012). Effect of surface charge on the uptake and distribution of gold nanoparticles in four plant species. Environmental Science and Technology, 46(22), 12391–12398. https://doi.org/10.1021/es301977w

Zwart, C. G., & Bok, J. (2004). Protocol DGGE.

AKNOWLEDGEMENTS

First, I would like to thank my supervisor, Prof. Zeno Varanini, who constantly guided me during this project and along the construction of my scientific path; Dr. Anita Zamboni, who patiently taught me experimental design, data analysis and for providing her knowledge during the writing of this thesis. I also would like to thank Prof. Giancarlo Renella, to host me in his lab at the University of Florence and guided me through the design and analysis of the soil experiments, and Dr. Laura Giagnoni for her help and mentoring during these experiments; Dr. Roberta Pastorelli for hosting me at CREA-AA and taught and follow me during the DGGE analysis.

A special thanks goes to Dr. Davide Sega, who contributed to most of the experiments and explained me most of the things. Plus, for his friendship.

Thank you to all the people who shared the laboratory with us, even those who came for short time, and for all the doctors and students who rapidly became friends, especially Paolo, Mauro and the whole "five brothers" group (they have never been just "five", so to name them all would require a lot of space).

I would also like to thank all my friends, Stefania, Pacis, Margherita, and the others who share my life in Verona. Also, the other friends who remained in Pisa, Luca, Jacopo, Andrea, Gaia, Marco, or a little more distant such as Olivia. Thanks also to Paloma for the nice time spent together. All of my friends have been fundamental, I would never have reached this goal without their support.

Last, but not least, I would like to thank my parents who always believed in me, even though sometimes I did not.

APPENDIX I.

Differentially modulated transcripts in cucumber.

Transcripts			Fold Change per condition			
Transcript name	gene ontology	Description	-P+NPs vs -P	-P+bulk vs -P	-Fe+NPs vs -Fe	-Fe+bulk vs -Fe
Cucsa.237530.1	AT5G41750.1	Disease resistance protein (TIR-NBS-LRR class) family	-2,68			
Cucsa.120050.1			-2,02			
Cucsa.365740.1	AT2G36800.1	don-glucosyltransferase 1	-4,88			
Cucsa.081320.1	AT5G22380.1	NAC domain containing protein 90	-2,22			
Cucsa.093360.1	AT2G24230.1	Leucine-rich repeat protein kinase family protein	-2,27			
Cucsa.133230.1	AT1G70330.1	equilibrative nucleotide transporter 1	-2,70		4,58	
Cucsa.051320.1			2,10			
Cucsa.398260.3	AT5G64300.1	GTP cyclohydrolase II	-3,06			
Cucsa.181070.1			2,31			
Cucsa.090660.1	AT1G56430.1	nicotianamine synthase 4	-2,83		7,16	
Cucsa.189500.1	AT1G59960.1	NAD(P)-linked oxidoreductase superfamily protein	-2,06			
Cucsa.346050.4	AT5G53390.1	O-acyltransferase (WSD1-like) family protein	-3,18			
Cucsa.316590.1	AT5G07870.1	HXXXD-type acyl-transferase family protein	-2,84			
Cucsa.377410.1	AT2G02040.1	peptide transporter 2	-2,03			
Cucsa.092390.1	AT1G56430.1	nicotianamine synthase 4	-2,21		9,01	
Cucsa.166810.1	AT5G44440.1	FAD-binding Berberine family protein	-3,46		11,09	
Cucsa.090590.1			-2,36			
Cucsa.286280.1	AT1G23350.1	Plant invertase/pectin methylesterase inhibitor superfamily protein	-2,19			
Cucsa.170810.1	AT2G23970.1	Class I glutamine amidotransferase-like superfamily protein	-2,54			
Cucsa.016540.1	AT1G69560.1	myb domain protein 105	2,25			
Cucsa.398260.1	AT5G64300.1	GTP cyclohydrolase II	-2,89		3,37	
Cucsa.342250.1	AT1G75160.1	Protein of unknown function (DUF620)	2,07			
Cucsa.052560.1	AT1G43760.1	DNAse I-like superfamily protein	-2,32			
Cucsa.038890.1			-2,15			
Cucsa.121580.1	AT1G68390.1	Core-2/I-branching beta-1.6-N-acetylglucosaminyltransferase family protein	5,23		3,39	
Cucsa.338660.1	AT5G36930.1	Disease resistance protein (TIR-NBS-LRR class) family	4,12			
Cucsa.352750.1	AT4G33880.1	ROOT HAIR DEFECTIVE 6-LIKE 2	-2,36			
Cucsa.069720.1	AT2G45470.1	FASCICLIN-like arabinogalactan protein 8	-2,28			
Cucsa.207030.1	AT1G08080.1	alpha carbonic anhydrase 7	-2,12			
Cucsa.010890.1	AT2G39690.1	Protein of unknown function. DUF547	2,01			
Cucsa.178310.1	AT1G04520.1	plasmodesmata-located protein 2	2,11			
Cucsa.057380.1	AT5G58150.1	Leucine-rich repeat protein kinase family protein	-2,10			
Cucsa.359740.1			2,77			

Cucsa.200410.1	AT5G228900.1	C2H2 and C2HC zinc fingers superfamily protein	-2,40			
Cucsa.185020.1	AT4G01410.1	Late embryogenesis abundant (LEA) hydroxyproline-rich glycoprotein family	-4,91			
Cucsa.043630.1	AT4G21410.1	cysteine-rich RLK (RECEPTOR-like protein kinase) 29	-2,40			
Cucsa.122680.6	AT3G149800.1	Acyl-CoA N-acyltransferase with RING/FYVE/PHD-type zinc finger protein	-2,11			
Cucsa.095840.1			2,39			
Cucsa.340620.1	AT1G02305.1	Cysteine proteinases superfamily protein	2,10			
Cucsa.107080.1	AT1G641600.1	Disease resistance-responsive (dirigent-like protein) family protein	2,01			
Cucsa.301770.1			-2,03			
Cucsa.132990.1			-5,27			
Cucsa.048300.5	AT2G347300.2	myosin heavy chain-related	-2,25			
Cucsa.081340.1			2,18			
Cucsa.058230.1	AT3G145700.1	glucan synthase-like 4	-2,00			
Cucsa.051180.1	AT5G269200.1	Cam-binding protein 60-like G	-2,29			
Cucsa.118570.2	AT1G543100.2	S-adenosyl-L-methionine-dependent methyltransferases superfamily protein	2,24			
Cucsa.256010.1			-2,55			
Cucsa.106870.1	AT5G634700.2	nuclear factor Y. subunit C4	-2,01			
Cucsa.057670.1	AT1G786800.1	gamma-glutamyl hydrolase 2	-2,60			
Cucsa.091300.1	AT1G550200.1	lipoxygenase 1	-2,54			
Cucsa.366840.1			-2,09			
Cucsa.322910.1	AT4G357783.1	ROTUNDIFOLIA like 6	-3,22			
Cucsa.249050.1	AT3G079700.1	Pectin lyase-like superfamily protein	3,62			
Cucsa.158540.1	AT3G478700.1	LOB domain-containing protein 27	-2,80			
Cucsa.257230.1	AT1G290000.1	Heavy metal transport/detoxification superfamily protein	2,02			
Cucsa.240260.1	AT5G190400.1	isopentenyltransferase 5	-2,21			
Cucsa.047360.1			-3,13			
Cucsa.044240.1	AT1G657700.1	ascorbic acid mannose pathway regulator 1	-3,22			
Cucsa.355990.1	AT3G459700.1	expansin-like A1	-2,04			
Cucsa.241420.1			-2,15			
Cucsa.065340.1	AT5G128900.1	UDP-Glycosyltransferase superfamily protein	2,09			
Cucsa.015150.1	AT2G025200.1	RNA-directed DNA polymerase (reverse transcriptase)-related family protein	2,17			
Cucsa.053460.1	AT1G061500.1	basic helix-loop-helix (bHLH) DNA-binding superfamily protein	-2,03			
Cucsa.398260.2	AT5G643000.1	GTP cyclohydrolase II	-2,55		3,28	
Cucsa.083360.1	AT1G083500.2	Endomembrane protein 70 protein family	-2,02			
Cucsa.042320.1	AT4G266400.2	WRKY family transcription factor family protein	2,26			
Cucsa.398980.1	AT1G487200.1			-4,31		
Cucsa.106380.1	AT5G664000.1	Dehydrin family protein		-4,06		
Cucsa.247520.1				-3,98	-2,10	
Cucsa.373220.1	AT5G288810.1	Domain of unknown function (DUF1985)		-3,76		
Cucsa.058330.1	AT3G217900.1	UDP-Glycosyltransferase superfamily protein		-3,64		
Cucsa.191200.1	AT2G154900.1	UDP-glycosyltransferase 73B4		-3,63		

Cucsa.253130.2	AT5G276900.1	Heavy metal transport/detoxification superfamily protein		-3,61		
Cucsa.341810.1	AT4G217600.1	beta-glucosidase 47		-3,48		
Cucsa.375450.1				-3,47		
Cucsa.139570.1				-3,45		
Cucsa.126230.1				-3,39		
Cucsa.068340.1	AT3G569600.1	phosphatidyl inositol monophosphate 5 kinase 4		-3,09		
Cucsa.183420.3	AT5G268300.1	Threonyl-tRNA synthetase		-2,97		
Cucsa.109340.1	AT2G214700.1	SUMO-activating enzyme 2		-2,95		
Cucsa.289230.1	AT5G526005.1	Defensin-like (DEFL) family protein		-2,92		
Cucsa.280880.1	AT1G688800.1	TCP domain protein 12		-2,78		
Cucsa.284490.1	AT2G036300.1	suppressor SRP40-like protein		-2,77		
Cucsa.085620.3	AT3G540700.1	Ankyrin repeat family protein		-2,69		
Cucsa.140570.1				-2,68		
Cucsa.299630.1	AT4G330800.1	AGC (cAMP-dependent. cGMP-dependent and protein kinase C) kinase family protein		-2,61		
Cucsa.235670.1				-2,46		
Cucsa.327790.2	AT1G265200.1	Cobalamin biosynthesis CobW-like protein		-2,46		
Cucsa.156990.1	AT5G140400.1	phosphate transporter 3;1		-2,44		
Cucsa.125010.1	AT5G038100.1	GDSL-like Lipase/Acylhydrolase family protein		-2,38		
Cucsa.152610.1	AT1G555700.1	SKU5 similar 12		-2,28		
Cucsa.032300.1	AT4G277900.1	Calcium-binding EF hand family protein		-2,19		
Cucsa.387860.1				-2,19		
Cucsa.094890.1	AT3G483400.1	Cysteine proteinases superfamily protein		-2,19		
Cucsa.027780.1	AT3G598500.1	Pectin lyase-like superfamily protein		-2,16	2,28	
Cucsa.006340.1	AT1G664700.1	ROOT HAIR DEFECTIVE6		-2,13		
Cucsa.384740.1	AT1G050100.1	ethylene-forming enzyme		-2,13		
Cucsa.042760.5	AT3G202900.2	EPS15 homology domain 1		-2,13		
Cucsa.100920.5	AT5G093300.2	NAC domain containing protein 82		-2,13		
Cucsa.127510.1				-2,09		
Cucsa.088940.1	AT3G622300.1	F-box family protein		-2,08		-2,88
Cucsa.394580.4	AT3G263800.1	Melibiase family protein		-2,08		
Cucsa.251680.2	AT2G450100.1	PLAC8 family protein		-2,07	-2,21	
Cucsa.312970.1	AT4G179400.1	Tetratricopeptide repeat (TPR)-like superfamily protein		-2,05		
Cucsa.119400.1				-2,05		
Cucsa.240430.1	AT1G437600.1	DNAse I-like superfamily protein		-2,04		-2,32
Cucsa.135640.1	AT4G003500.1	MATE efflux family protein		-2,03		
Cucsa.207300.1	AT3G452900.1	Seven transmembrane MLO family protein		-2,02		
Cucsa.109410.1	AT4G391500.2	DNAJ heat shock N-terminal domain-containing protein		-2,01		
Cucsa.319800.1	AT5G224100.1	root hair specific 18		-2,00	2,64	
Cucsa.099360.1	AT3G459700.1	expansin-like A1		2,02		
Cucsa.011110.1	AT1G599700.1	Matrixin family protein		2,03		

Cucsa.197530.2	AT5G62740.1	SPFH/Band 7/PHB domain-containing membrane-associated protein family		2,03		
Cucsa.391100.1	ATCG01090.1	NADPH dehydrogenases		2,05		
Cucsa.364720.1	AT2G16970.1	Major facilitator superfamily protein		2,06		
Cucsa.011640.1	AT4G24270.1	EMBRYO DEFECTIVE 140		2,07		
Cucsa.107150.1	AT4G23720.1	Protein of unknown function (DUF1191)		2,08		
Cucsa.244190.1	AT1G25275.3	Thionin-like protein		2,08		
Cucsa.244380.1				2,11		
Cucsa.038790.1	AT2G25710.1	holocarboxylase synthase 1		2,11		
Cucsa.096600.2	AT3G15660.2	glutaredoxin 4		2,13		
Cucsa.362150.1	AT3G59540.1	Ribosomal L38e protein family		2,14		
Cucsa.126790.1	AT4G21020.1	proteins d		2,15		
Cucsa.347510.1	ATCG00270.1	photosystem II reaction center protein D		2,18		
Cucsa.184540.1	AT3G22600.1	Bifunctional inhibitor/lipid-transfer protein/seed storage 2S albumin superfamily protein		2,20		
Cucsa.354560.1				2,25		
Cucsa.057820.1	AT4G16580.1	Protein phosphatase 2C family protein		2,26		
Cucsa.105710.1	AT5G25280.2	serine-rich protein-related		2,28		
Cucsa.369470.2	AT1G74700.1	tRNAse Z1		2,31		
Cucsa.129110.1	AT5G51150.1	Mitochondrial import inner membrane translocase subunit Tim17/Tim22/Tim23 family protein		2,32		
Cucsa.115550.1	AT3G26140.1	Cellulase (glycosyl hydrolase family 5) protein		2,33		
Cucsa.042330.2	AT4G26640.2	WRKY family transcription factor family protein		2,37		
Cucsa.218330.1	AT5G09530.1	hydroxyproline-rich glycoprotein family protein		2,40		
Cucsa.186210.1				2,41		
Cucsa.158430.1	AT5G39900.1	Small GTP-binding protein		2,43		
Cucsa.092300.1				2,46		
Cucsa.240180.1				2,53		
Cucsa.197530.3	AT5G62740.1	SPFH/Band 7/PHB domain-containing membrane-associated protein family		2,66		
Cucsa.165550.1	AT3G09110.1	Protein of unknown function (DUF674)		2,90		
Cucsa.107330.1	AT2G19170.1	subtilisin-like serine protease 3		3,20		
Cucsa.151890.1	AT1G07050.1	CCT motif family protein		3,25		
Cucsa.369460.1	ATMG00860.1	DNA/RNA polymerases superfamily protein		3,56		
Cucsa.184050.1				3,70		
Cucsa.146940.1	AT2G29630.3	thiaminC		3,82		
Cucsa.242440.2	AT5G06620.1	SET domain protein 38			-2,43	
Cucsa.318750.5	AT1G11755.1	Undecaprenyl pyrophosphate synthetase family protein			-2,80	
Cucsa.313560.1	AT5G46940.1	Plant invertase/pectin methylesterase inhibitor superfamily protein			2,45	
Cucsa.332620.1	AT3G54070.1	Ankyrin repeat family protein			-5,41	
Cucsa.083680.1					-2,20	
Cucsa.128330.1	AT1G48930.1	glycosyl hydrolase 9C1			2,62	
Cucsa.099320.1	AT3G45960.2	expansin-like A3			-2,62	
Cucsa.128450.1	AT5G17820.1	Peroxidase superfamily protein			-2,92	

Cucsa.119960.1	AT2G17350.1				-2,15	
Cucsa.079320.1					-2,09	
Cucsa.142170.4	AT4G26410.1	Uncharacterised conserved protein UCP022280			-2,76	
Cucsa.193280.1	AT5G19790.1	related to AP2 11			-2,12	
Cucsa.342870.1	AT1G19850.1	Transcriptional factor B3 family protein / auxin-responsive factor AUX/IAA-related			-2,46	
Cucsa.152940.1	AT2G27080.2	Late embryogenesis abundant (LEA) hydroxyproline-rich gly-coprotein family			2,16	
Cucsa.397360.1	AT5G56860.1	GATA type zinc finger transcription factor family protein			-6,47	
Cucsa.322110.2	AT2G35530.1	basic region/leucine zipper transcription factor 16			-2,90	
Cucsa.395510.1	AT1G10140.1	Uncharacterised conserved protein UCP031279			-2,13	
Cucsa.173620.1					-3,26	
Cucsa.048470.1	AT1G34575.1	FAD-binding Berberine family protein			-3,76	
Cucsa.182020.1	AT1G09030.1	nuclear factor Y. subunit B4			11,35	
Cucsa.182040.1	AT1G09030.1	nuclear factor Y. subunit B4			6,99	
Cucsa.175530.1	AT5G60020.1	laccase 17			-2,75	
Cucsa.147030.1	AT5G58750.1	NAD(P)-binding Rossmann-fold superfamily protein			2,01	
Cucsa.190600.1	AT1G61560.1	Seven transmembrane MLO family protein			-2,10	
Cucsa.140240.1	AT5G48850.1	Tetratricopeptide repeat (TPR)-like superfamily protein			-3,08	
Cucsa.104530.1	AT5G65090.1	DNAse I-like superfamily protein			-2,31	
Cucsa.169290.1	AT2G37170.1	plasma membrane intrinsic protein 2			8,19	
Cucsa.362420.1	AT2G44540.1	glycosyl hydrolase 9B9			-3,96	
Cucsa.136680.1					-2,36	
Cucsa.308720.1					-2,02	
Cucsa.368350.1	AT5G05500.1	Pollen Ole e 1 allergen and extensin family protein			2,37	
Cucsa.253070.1	AT5G49030.3	tRNA synthetase class I (I. L. M and V) family protein			-2,52	
Cucsa.045850.1	AT1G11260.1	sugar transporter 1			-2,94	
Cucsa.129070.2	AT5G17165.1				5,42	
Cucsa.184710.1	AT3G43660.1	Vacuolar iron transporter (VIT) family protein			4,83	
Cucsa.045370.1	AT4G28556.1	PAK-box/P21-Rho-binding family protein			3,45	
Cucsa.012980.1	AT1G78090.1	trehalose-6-phosphate phosphatase			3,10	
Cucsa.131920.1	AT2G26695.1	Ran BP2/NZF zinc finger-like superfamily protein			7,00	
Cucsa.026530.1	AT4G09940.1	P-loop containing nucleoside triphosphate hydrolases super-family protein			-2,52	
Cucsa.254980.4	AT5G43600.1	ureidoglycolate amidohydrolase			-2,20	
Cucsa.195220.1					-4,04	
Cucsa.206840.1					-2,62	
Cucsa.162210.1	AT5G25480.1	DNA methyltransferase-2			-2,30	
Cucsa.102230.1					-2,95	
Cucsa.357630.1					-2,06	
Cucsa.134680.1	AT1G30870.1	Peroxidase superfamily protein			2,13	
Cucsa.204430.1	AT2G01050.1	zinc ion binding;nucleic acid binding			-2,79	
Cucsa.116320.2	AT3G24500.1	multiprotein bridging factor 1C			-2,99	

Cucsa.167050.1	AT3G10710.1	root hair specific 12			2,79	
Cucsa.175680.1	AT2G37730.1	Protein of unknown function (DUF604)			2,35	
Cucsa.078340.1	AT3G07070.1	Protein kinase superfamily protein			2,63	
Cucsa.318500.1					-3,95	
Cucsa.089740.1	AT4G25810.1	xyloglucan endotransglycosylase 6			4,12	
Cucsa.096820.1	AT4G02170.1				2,36	
Cucsa.302600.1	AT1G12560.1	expansin A7			3,00	
Cucsa.239280.1	ATMG01250.1	RNA-directed DNA polymerase (reverse transcriptase)			-2,18	
Cucsa.326860.1	AT4G28850.1	xyloglucan endotransglucosylase/hydrolase 26			2,84	
Cucsa.356340.1	AT1G65480.1	PEBP (phosphatidylethanolamine-binding protein) family protein			-3,00	
Cucsa.026880.2	AT5G53130.1	cyclic nucleotide gated channel 1			-2,80	
Cucsa.038100.1	AT5G06860.1	polygalacturonase inhibiting protein 1			26,67	
Cucsa.148490.1	AT3G21690.1	MATE efflux family protein			-2,64	
Cucsa.090340.1	AT3G05858.1				-5,97	
Cucsa.269430.1	AT1G77120.1	alcohol dehydrogenase 1			2,24	
Cucsa.335780.1					-2,41	
Cucsa.089390.3	AT2G18850.1	SET domain-containing protein			-2,30	
Cucsa.077220.1	AT3G13690.1	Protein kinase protein with adenine nucleotide alpha hydrolases-like domain			2,02	
Cucsa.378870.1	AT3G09925.1	Pollen Ole e 1 allergen and extensin family protein			2,32	
Cucsa.193040.1	AT5G59100.1	Subtilisin-like serine endopeptidase family protein			-2,53	
Cucsa.129070.1	AT5G17165.1				5,72	
Cucsa.273890.1	ATMG00860.1	DNA/RNA polymerases superfamily protein			-4,11	
Cucsa.192090.1					-3,90	
Cucsa.192160.1	AT5G06900.1	cytochrome P450. family 93. subfamily D. polypeptide 1			2,76	
Cucsa.000220.1					-2,42	
Cucsa.098090.1	AT5G11010.2	Pre-mRNA cleavage complex II protein family			-2,08	
Cucsa.151690.1	AT5G01320.1	Thiamine pyrophosphate dependent pyruvate decarboxylase family protein				-2,16
Cucsa.275620.1	AT3G21000.1	Gag-Pol-related retrotransposon family protein				-2,30
Cucsa.399380.1	AT3G24255.1	RNA-directed DNA polymerase (reverse transcriptase)-related family protein				-3,03
Cucsa.352760.1						-2,46
Cucsa.206900.1	AT1G76750.1	Protein of unknown function (DUF1278)				-3,14
Cucsa.113190.1	AT5G61120.1					-2,28
Cucsa.042220.1	AT2G38920.1	SPX (SYG1/Pho81/XPR1) domain-containing protein / zinc finger (C3HC4-type RING finger) protein-related				-2,16
Cucsa.240610.1	AT5G26730.1	Fasciclin-like arabinogalactan family protein				-2,44
Cucsa.107320.1						-2,50
Cucsa.004210.1	AT1G64260.1	MuDR family transposase				-3,87
Cucsa.133330.1	AT3G22910.1	ATPase E1-E2 type family protein / haloacid dehalogenase-like hydrolase family protein				-2,41
Cucsa.100530.1	AT3G07820.1	Pectin lyase-like superfamily protein				-2,13
Cucsa.029900.1						-2,05
Cucsa.085850.1						-5,14

Cucsa.061280.1	AT3G29750.1	Eukaryotic aspartyl protease family protein				-2,23
Cucsa.053670.1	AT1G07090.1	Protein of unknown function (DUF640)				-2,87
Cucsa.123520.1						-2,33
Cucsa.254250.2	AT5G19530.1	S-adenosyl-L-methionine-dependent methyltransferases superfamily protein				-3,28
Cucsa.172940.1	AT1G21430.1	Flavin-binding monooxygenase family protein				-3,59
Cucsa.368920.1						-3,41
Cucsa.106730.1	AT4G11400.1	ARID/BRIGHT DNA-binding domain;ELM2 domain protein				2,05
Cucsa.040320.1	AT3G24255.1	RNA-directed DNA polymerase (reverse transcriptase)-related family protein				-2,10
Cucsa.224470.1	AT3G10840.1	alpha/beta-Hydrolases superfamily protein				-3,20
Cucsa.218500.1						-2,03
Cucsa.113750.1	AT4G29035.1	Plant self-incompatibility protein S1 family				-2,54
Cucsa.259530.1						-2,26
Cucsa.042130.1	AT1G55870.1	Polynucleotidyl transferase. ribonuclease H-like superfamily protein				-2,56
Cucsa.303970.1						-2,06
Cucsa.105730.1	AT1G80550.1	Pentatricopeptide repeat (PPR) superfamily protein				-2,06
Cucsa.048980.1	AT3G12720.1	myb domain protein 67				-2,04
Cucsa.101970.1						-2,43
Cucsa.117050.1	AT5G56970.1	cytokinin oxidase 3				-2,83
Cucsa.130070.2	AT3G08880.1					-2,38
Cucsa.101440.1						-2,18
Cucsa.254460.1	AT3G22640.1	cupin family protein				-2,37
Cucsa.038070.1	AT2G43890.1	Pectin lyase-like superfamily protein				-3,97
Cucsa.157390.1	AT5G63450.1	cytochrome P450. family 94. subfamily B. polypeptide 1				-2,66
Cucsa.326860.2						-3,70
Cucsa.089610.1	AT1G73050.1	Glucose-methanol-choline (GMC) oxidoreductase family protein				-3,59
Cucsa.066810.1	AT3G09270.1	glutathione S-transferase TAU 8				-3,27
Cucsa.096330.1	AT3G15850.1	fatty acid desaturase 5				-2,11
Cucsa.051360.1	AT3G25270.1	Ribonuclease H-like superfamily protein				-2,31
Cucsa.392540.1	ATMG01410.1	open reading frame 204				-2,39
Cucsa.069230.1						-2,29
Cucsa.184870.1						-3,41
Cucsa.201340.1						-3,37
Cucsa.385200.1	AT4G33790.1	Jojoba acyl CoA reductase-related male sterility protein				-2,06
Cucsa.122170.1	AT1G75240.1	homeobox protein 33				-2,49
Cucsa.200370.1	AT3G44880.1	Pheophorbide a oxygenase family protein with Rieske [2Fe-2S] domain				-2,15
Cucsa.089420.1						-2,23

APPENDIX II.

Differentially modulated transcripts in maize.

Transcripts			**Fold Change per condition**			
Transcript name	**gene ontology**	**Description**	**-P+NPs vs -P**	**-P+bulk vs -P**	**-Fe+NPs vs -Fe**	**-Fe+bulk vs -Fe**
GRMZM2G471240_T01	AT2G26560.1	phospholipase A 2A	-16,18			
GRMZM2G040263_T01	AT1G48480.1	receptor-like kinase 1	-15,97			
AC177831.3_FGT004			-11,56			
GRMZM2G036631_T01	AT5G05365.1	Heavy metal transport/detoxification superfamily protein	-10,88			10,24
GRMZM2G412436_T01	AT3G53040.1	late embryogenesis abundant protein, putative / LEA protein, putative	-9,84			
GRMZM2G088312_T01	AT2G34610.1		-7,34			
GRMZM2G020761_T01	AT2G46950.1	cytochrome P450, family 709, subfamily B, polypeptide 2	-6,88			
GRMZM2G039383_T01	AT3G18280.1	Bifunctional inhibitor/lipid-transfer protein/seed storage 2S albumin superfamily protein	-6,87			
GRMZM2G063126_T01	AT2G27510.1	ferredoxin 3	-6,42			
GRMZM2G174192_T01	AT5G49690.1	UDP-Glycosyltransferase superfamily protein	-6,40			
GRMZM2G056369_T01	AT3G21720.1	isocitrate lyase	-6,15			
GRMZM2G019686_T01	AT5G24860.1	flowering promoting factor 1	-5,30			
GRMZM2G010468_T01	AT2G30490.1	cinnamate-4-hydroxylase	-5,26			
GRMZM2G464676_T01			-5,22			
GRMZM2G028252_T01			-5,02			
GRMZM2G703582_T01	AT3G21420.1	2-oxoglutarate (2OG) and Fe(II)-dependent oxygenase superfamily protein	-4,99			
GRMZM2G159831_T01	AT5G20100.1		-4,96			
GRMZM2G048549_T01	AT4G38810.2	Calcium-binding EF-hand family protein	-4,72			

GRMZM2G090568_T01	AT4G35090.1	catalase 2	-4,71			
GRMZM2G368890_T01	AT2G02130.1	low-molecular-weight cysteine-rich 68	-4,71			
GRMZM2G039312_T01	AT2G36026.1	Ovate family protein	-4,69			
GRMZM2G026980_T01	AT4G25810.1	xyloglucan endotransglycosylase 6	-4,55			
GRMZM2G125196_T01	AT3G03080.1	Zinc-binding dehydrogenase family protein	-4,49			5,40
GRMZM2G020423_T01			-4,35			
GRMZM2G115388_T01	AT5G57520.1	zinc finger protein 2	-4,30			
GRMZM2G058491_T01	AT1G64110.2	P-loop containing nucleoside triphosphate hydrolases superfamily protein	-4,28			
GRMZM2G326270_T01	AT2G41250.1	Haloacid dehalogenase-like hydrolase (HAD) superfamily protein	-4,23			
GRMZM2G063287_T01	AT2G18340.2	late embryogenesis abundant domain-containing protein / LEA domain-containing protein	-4,22			
GRMZM2G178356_T01	AT5G46240.1	potassium channel in Arabidopsis thaliana 1	-4,13			
GRMZM2G080054_T01	AT2G20180.1	phytochrome interacting factor 3-like 5	-4,04			
GRMZM2G019626_T01			-3,95			
GRMZM2G324956_T01	AT1G53540.1	HSP20-like chaperones superfamily protein	-3,93			
GRMZM5G870592_T01	AT4G18770.1	myb domain protein 98	-3,90			
GRMZM2G417684_T01	AT1G43722.1		-3,89			
AC210616.4_FGT005	AT5G65100.1	Ethylene insensitive 3 family protein	-3,89			
GRMZM2G093291_T01	AT5G27270.1	Tetratricopeptide repeat (TPR)-like superfamily protein	-3,86			
GRMZM2G455321_T01	AT1G17610.1	Disease resistance protein (TIR-NBS class)	-3,78			
GRMZM2G022837_T01	AT1G18870.1	isochorismate synthase 2	-3,69			
GRMZM2G169943_T01	AT5G01670.1	NAD(P)-linked oxidoreductase superfamily protein	-3,62			
GRMZM2G167758_T01	AT5G04830.2	Nuclear transport factor 2 (NTF2) family protein	-3,61			
GRMZM2G052869_T01			-3,59			
GRMZM2G125571_T01			-3,58			
GRMZM2G092780_T01	AT3G26570.2	phosphate transporter 2;1	-3,57			
GRMZM2G333033_T01	AT3G10130.1	SOUL heme-binding family protein	-3,52			

GRMZM5G801307_T01			-3,46		2,47	
GRMZM2G050915_T01	AT5G02540.1	NAD(P)-binding Rossmann-fold superfamily protein	-3,45			
GRMZM2G082434_T01	AT5G09220.1	amino acid permease 2	-3,42			
GRMZM2G024871_T01	AT3G23230.1	Integrase-type DNA-binding superfamily protein	-3,41			
GRMZM2G075330_T01	AT3G10130.1	SOUL heme-binding family protein	-3,39			
GRMZM5G807267_T01	AT3G52720.1	alpha carbonic anhydrase 1	-3,34			
GRMZM2G033515_T01	AT1G65930.1	cytosolic NADP+-dependent isocitrate dehydrogenase	-3,32			
GRMZM2G074040_T01	AT3G10130.1	SOUL heme-binding family protein	-3,30			
GRMZM5G818776_T01	AT4G00120.1	basic helix-loop-helix (bHLH) DNA-binding superfamily protein	-3,29			
GRMZM2G034469_T01	AT5G57345.1		-3,29			
GRMZM2G103771_T01	AT4G16160.1	Mitochondrial import inner membrane translocase sub-unit Tim17/Tim22/Tim23 family protein	-3,27			
GRMZM2G113844_T01	AT1G19250.1	flavin-dependent monooxygenase 1	-3,25			
GRMZM2G129713_T01			-3,23			
GRMZM5G875046_T01			-3,21			
GRMZM2G037685_T01	AT3G60890.2	protein binding	-3,20			
GRMZM2G156748_T01			-3,19			
GRMZM5G884801_T01			-3,15			
GRMZM2G402708_T01	AT3G54510.2	Early-responsive to dehydration stress protein (ERD4)	-3,14			
GRMZM2G371375_T01	AT5G44310.2	Late embryogenesis abundant protein (LEA) family protein	-3,13			
AC207309.3_FGT010			-3,10			
GRMZM2G152447_T01	AT1G14700.1	purple acid phosphatase 3	-3,09			
GRMZM2G501775_T01	AT2G46400.1	WRKY DNA-binding protein 46	-3,07			
GRMZM2G070500_T01	AT5G64700.1	nodulin MtN21 /EamA-like transporter family protein	-3,06			
GRMZM2G405272_T01			-3,06			
GRMZM2G418776_T01	AT3G06720.1	importin alpha isoform 1	-3,06			
GRMZM2G410352_T01			-3,03			

GRMZM2G173865_T01			-3,03			
GRMZM2G361475_T01	AT1G71695.1	Peroxidase superfamily protein	-3,01		2,00	
GRMZM2G045720_T01	AT3G26618.1	eukaryotic release factor 1-3	-2,98			
GRMZM2G331316_T01			-2,98			
GRMZM2G179270_T01	AT2G19130.1	S-locus lectin protein kinase family protein	-2,97			
GRMZM2G029096_T01	AT5G49700.1	Predicted AT-hook DNA-binding family protein	-2,96			
GRMZM2G060991_T01	AT2G46370.4	Auxin-responsive GH3 family protein	-2,96			
AC202911.3_FGT002			-2,94			
GRMZM2G026143_T01			-2,93			
GRMZM2G112908_T01	AT5G58560.1	Phosphatidate cytidylyltransferase family protein	-2,93			
GRMZM2G099064_T01	AT2G24960.1		-2,93			
GRMZM2G055143_T01			-2,92			
GRMZM2G122614_T01	AT4G30080.1	auxin response factor 16	-2,89			
GRMZM5G836308_T01	AT2G33520.1		-2,89			
GRMZM2G412207_T01	AT4G13710.1	Pectin lyase-like superfamily protein	-2,87			
GRMZM2G703968_T01			-2,87			
GRMZM2G042920_T01	AT4G36930.1	basic helix-loop-helix (bHLH) DNA-binding superfamily protein	-2,87			
GRMZM2G353266_T01			-2,87			
GRMZM2G059465_T01	AT4G35160.1	O-methyltransferase family protein	-2,86			
GRMZM2G094892_T01	AT3G21330.1	basic helix-loop-helix (bHLH) DNA-binding superfamily protein	-2,86			
GRMZM2G323413_T01			-2,86			
GRMZM2G120151_T01	AT5G60970.1	TEOSINTE BRANCHED 1, cycloidea and PCF transcription factor 5	-2,85			
GRMZM2G033612_T01	AT3G13960.1	growth-regulating factor 5	-2,85			
GRMZM2G419328_T01	AT5G01180.1	peptide transporter 5	-2,83			
GRMZM2G040481_T01	AT5G65100.1	Ethylene insensitive 3 family protein	-2,83			
GRMZM2G081571_T01	AT1G30910.1	Molybdenum cofactor sulfurase family protein	-2,82			

GRMZM2G025611_T01	AT3G53720.1	cation/H+ exchanger 20	-2,80			
GRMZM2G156398_T01	AT1G78955.1	camelliol C synthase 1	-2,78			
GRMZM2G055699_T01	AT1G02850.2	beta glucosidase 11	-2,77			
GRMZM2G059836_T01	AT1G22990.1	Heavy metal transport/detoxification superfamily protein	-2,77			
GRMZM2G428040_T01	AT5G42290.1	transcription activator-related	-2,77			
GRMZM2G043336_T01			-2,77			
GRMZM2G090697_T01			-2,76			
GRMZM2G438080_T01			-2,76			
GRMZM2G162527_T01	AT2G37540.1	NAD(P)-binding Rossmann-fold superfamily protein	-2,76			
GRMZM2G127457_T01			-2,75			
GRMZM2G552793_T01			-2,74			
GRMZM2G059397_T01	AT2G23810.1	tetraspanin8	-2,73			
GRMZM2G703903_T01			-2,72			
GRMZM2G077181_T01	AT3G57520.1	seed imbibition 2	-2,72			
GRMZM2G180082_T01	AT5G36110.1	cytochrome P450, family 716, subfamily A, polypeptide 1	-2,70			
AC208564.3_FGT004	AT2G03710.3	K-box region and MADS-box transcription factor family protein	-2,70			
AC186147.3_FGT008	AT4G37690.1	Galactosyl transferase GMA12/MNN10 family protein	-2,70			
GRMZM2G035268_T01	AT2G24270.4	aldehyde dehydrogenase 11A3	-2,70			
GRMZM2G143426_T01			-2,70			
GRMZM2G019742_T01	AT5G45890.1	senescence-associated gene 12	-2,69			
GRMZM2G087870_T01	AT4G05320.4	polyubiquitin 10	-2,68			
GRMZM2G157822_T01	AT1G17580.1	myosin 1	-2,68			
GRMZM2G020996_T01	AT5G60250.1	zinc finger (C3HC4-type RING finger) family protein	-2,68			
GRMZM2G106950_T01	AT5G48220.1	Aldolase-type TIM barrel family protein	-2,67			
GRMZM2G348125_T01	AT2G39050.1	hydroxyproline-rich glycoprotein family protein	-2,67			
GRMZM2G169005_T01	AT1G01800.1	NAD(P)-binding Rossmann-fold superfamily protein	-2,66			

GRMZM2G004748_T01	AT4G25960.1	P-glycoprotein 2	-2,66			
GRMZM2G164182_T01	AT1G08080.1	alpha carbonic anhydrase 7	-2,63			
GRMZM2G027187_T01	AT5G51600.1	Microtubule associated protein (MAP65/ASE1) family protein	-2,61			
GRMZM2G086210_T01	AT1G12570.1	Glucose-methanol-choline (GMC) oxidoreductase family protein	-2,61			
GRMZM2G127336_T01	AT5G23960.1	terpene synthase 21	-2,61			
GRMZM2G131489_T01	AT1G76570.1	Chlorophyll A-B binding family protein	-2,59			
GRMZM2G035821_T01	AT3G12920.1	SBP (S-ribonuclease binding protein) family protein	-2,58			
GRMZM2G180160_T01	AT1G21230.1	wall associated kinase 5	-2,57			
GRMZM5G817436_T01	AT5G01180.1	peptide transporter 5	-2,57			
GRMZM2G159678_T01	AT4G34215.1	Domain of unknown function (DUF303)	-2,57			
GRMZM2G416808_T01	AT2G24960.1		-2,56			
GRMZM5G867893_T01			-2,56			
GRMZM2G118770_T01	AT2G19900.1	NADP-malic enzyme 1	-2,56			
GRMZM2G060394_T01	AT1G20140.1	SKP1-like 4	-2,55			
GRMZM2G134251_T01	AT1G05590.1	beta-hexosaminidase 2	-2,54			
GRMZM2G165867_T01			-2,54			
GRMZM2G031719_T01			-2,54			-2,53
AC199517.4_FGT006			-2,53			
GRMZM2G462641_T01			-2,53			
GRMZM2G171315_T01			-2,52			
GRMZM2G105069_T01			-2,52			
GRMZM5G860137_T01	AT5G47720.2	Thiolase family protein	-2,51			
GRMZM2G478779_T01	AT3G12110.1	actin-11	-2,51			
GRMZM2G000411_T01			-2,51			
GRMZM2G168956_T01	AT1G25450.1	3-ketoacyl-CoA synthase 5	-2,51			
GRMZM5G820832_T01			-2,51			

GRMZM2G042407_T01	AT5G66350.1	Lateral root primordium (LRP) protein-related	-2,51			
GRMZM2G049675_T01	AT1G47480.1	alpha/beta-Hydrolases superfamily protein	-2,49			
AC183928.4_FGT001			-2,49			
GRMZM2G420882_T01	AT2G19130.1	S-locus lectin protein kinase family protein	-2,49			
GRMZM2G149869_T01	AT1G49435.1	low-molecular-weight cysteine-rich 16	-2,48			
GRMZM2G020492_T01	AT1G50830.1	Aminotransferase-like, plant mobile domain family protein	-2,48			
GRMZM2G056335_T01	AT2G36750.1	UDP-glucosyl transferase 73C1	-2,48			
GRMZM2G304687_T01			-2,48			
GRMZM2G338661_T01	AT1G12790.1		-2,47			
GRMZM2G497976_T01			-2,47			
GRMZM2G143210_T01	AT1G53490.1	RING/U-box superfamily protein	-2,47			
GRMZM2G331701_T01	AT4G10250.1	HSP20-like chaperones superfamily protein	-2,47			
GRMZM2G095209_T01	AT1G16260.2	Wall-associated kinase family protein	-2,46			
GRMZM2G460958_T01	AT4G40070.1	RING/U-box superfamily protein	-2,45			
GRMZM2G063824_T01	AT4G36670.1	Major facilitator superfamily protein	-2,45			
GRMZM2G171707_T01	AT2G05710.1	aconitase 3	-2,45			
GRMZM2G475683_T01	AT2G46690.1	SAUR-like auxin-responsive protein family	-2,45			
AC214244.4_FGT003			-2,42			
GRMZM2G543070_T01			-2,42			
GRMZM2G110881_T01	AT5G58490.1	NAD(P)-binding Rossmann-fold superfamily protein	-2,42			
GRMZM2G152287_T01			-2,41			
GRMZM2G468929_T01	AT2G07050.1	cycloartenol synthase 1	-2,39			
GRMZM2G103137_T01	AT1G29120.5	Hydrolase-like protein family	-2,39			
GRMZM2G091044_T01	AT4G17900.1	PLATZ transcription factor family protein	-2,39			
GRMZM2G408881_T01	AT5G17760.1	P-loop containing nucleoside triphosphate hydrolases superfamily protein	-2,38			
GRMZM2G156451_T01	AT1G29500.1	SAUR-like auxin-responsive protein family	-2,38			

GRMZM2G143373_T01	AT5G50600.1	hydroxysteroid dehydrogenase 1	-2,37			
AC193745.3_FGT002			-2,37			
GRMZM2G154316_T01	AT1G07970.1		-2,37			
GRMZM2G085218_T01	AT3G21150.1	B-box 32	-2,36			
GRMZM2G173674_T01	AT5G17530.3	phosphoglucosamine mutase family protein	-2,36			
GRMZM2G365754_T01			-2,35			
GRMZM2G106807_T01	AT3G50940.1	P-loop containing nucleoside triphosphate hydrolases superfamily protein	-2,34			
GRMZM2G317895_T01			-2,34			
GRMZM2G704490_T01			-2,34			
GRMZM2G111136_T01	AT1G02065.1	squamosa promoter binding protein-like 8	-2,34			
GRMZM2G043695_T01	AT3G16520.3	UDP-glucosyl transferase 88A1	-2,34			
AC233850.1_FGT003	AT5G46940.1	Plant invertase/pectin methylesterase inhibitor superfamily protein	-2,33			
GRMZM2G408038_T01	AT3G10450.1	serine carboxypeptidase-like 7	-2,33			
GRMZM2G102183_T01	AT5G03860.2	malate synthase	-2,32			
GRMZM2G396527_T01	AT2G46680.1	homeobox 7	-2,32			
GRMZM2G062245_T01			-2,32			
AC200298.4_FGT001	AT3G56891.1	Heavy metal transport/detoxification superfamily protein	-2,31			
GRMZM2G148176_T01	AT3G18080.1	B-S glucosidase 44	-2,30			
GRMZM2G168829_T01	AT4G05320.2	polyubiquitin 10	-2,29			
AC216705.3_FGT002			-2,29			
GRMZM2G401009_T01	AT3G18773.1	RING/U-box superfamily protein	-2,28			
GRMZM2G085577_T01	AT3G46970.1	alpha-glucan phosphorylase 2	-2,28			
AC217415.3_FGT004	AT1G54740.1	Protein of unknown function (DUF3049)	-2,28			
GRMZM2G422240_T01	AT5G59720.1	heat shock protein 18.2	-2,28			
GRMZM2G343972_T01	AT5G60710.1	Zinc finger (C3HC4-type RING finger) family protein	-2,27			
GRMZM2G114866_T01			-2,26			

GRMZM2G364566_T01	AT3G62300.1	DOMAIN OF UNKNOWN FUNCTION 724 7	-2,26			
GRMZM2G175406_T01			-2,25			
GRMZM2G123860_T01	AT4G02290.1	glycosyl hydrolase 9B13	-2,25			
GRMZM2G497978_T01			-2,24			
GRMZM2G134182_T01	AT1G71480.1	Nuclear transport factor 2 (NTF2) family protein	-2,24			3,18
GRMZM2G087769_T01	AT4G22530.1	S-adenosyl-L-methionine-dependent methyltransferases superfamily protein	-2,24			
GRMZM5G834518_T01	AT3G47420.1	phosphate starvation-induced gene 3	-2,24			
AC186287.7_FGT005	AT5G58003.1	C-terminal domain phosphatase-like 4	-2,23			
GRMZM2G093725_T01	AT2G37590.1	DNA binding with one finger 2.4	-2,23			
GRMZM2G006287_T01	AT1G78160.1	pumilio 7	-2,23			
GRMZM2G143625_T01	AT3G02610.1	Plant stearoyl-acyl-carrier-protein desaturase family protein	-2,23			
GRMZM2G329791_T01			-2,23			
AF546188.1_FGT007			-2,22			
GRMZM2G413170_T01	AT4G02550.1		-2,22			
GRMZM2G089812_T01	AT5G63470.2	nuclear factor Y, subunit C4	-2,22			
GRMZM2G446047_T01	AT5G02390.1	Protein of unknown function (DUF3741)	-2,22			
GRMZM2G085049_T01	AT3G07880.1	Immunoglobulin E-set superfamily protein	-2,22			
GRMZM2G396248_T01	AT2G27690.1	cytochrome P450, family 94, subfamily C, polypeptide 1	-2,22			
GRMZM2G125378_T01	AT1G60170.1	pre-mRNA processing ribonucleoprotein binding region-containing protein	-2,22			
GRMZM2G165726_T01	AT5G24130.1		-2,21			
GRMZM2G071688_T01	AT1G23070.1	Protein of unknown function (DUF300)	-2,21			
GRMZM2G077415_T01	AT2G22780.1	peroxisomal NAD-malate dehydrogenase 1	-2,21			
GRMZM2G362960_T01	AT5G39530.1	Protein of unknown function (DUF1997)	-2,21			
GRMZM2G347655_T01	AT4G19130.1	Replication factor-A protein 1-related	-2,20			
GRMZM2G312732_T01			-2,19			
GRMZM5G884408_T01			-2,19			

GRMZM2G417835_T01	AT3G56710.1	sigma factor binding protein 1	-2,19			
GRMZM2G414668_T01			-2,19			
GRMZM2G141607_T01	AT3G50560.1	NAD(P)-binding Rossmann-fold superfamily protein	-2,18			
GRMZM2G319307_T01	AT3G47090.1	Leucine-rich repeat protein kinase family protein	-2,18			
GRMZM2G031057_T01	AT3G09050.1		-2,18			
GRMZM2G163407_T01			-2,17			
GRMZM2G051256_T01	AT2G47460.1	myb domain protein 12	-2,17			
GRMZM2G478160_T01	AT2G44310.1	Calcium-binding EF-hand family protein	-2,16			
GRMZM2G059620_T01			-2,16			
GRMZM2G031125_T01	AT5G24910.1	cytochrome P450, family 714, subfamily A, polypeptide 1	-2,15			
GRMZM2G005107_T01	AT3G12800.1	short-chain dehydrogenase-reductase B	-2,15			
GRMZM2G375975_T01	AT1G73670.1	MAP kinase 15	-2,15			
GRMZM2G095397_T01	AT4G24210.1	F-box family protein	-2,15			
GRMZM2G093405_T01	AT1G17100.1	SOUL heme-binding family protein	-2,15			
GRMZM2G469380_T01	AT2G39050.1	hydroxyproline-rich glycoprotein family protein	-2,15			
GRMZM2G017351_T01	AT5G19010.1	mitogen-activated protein kinase 16	-2,15			
GRMZM2G404688_T01			-2,15			
GRMZM2G024468_T01	AT3G47600.1	myb domain protein 94	-2,14			
GRMZM2G403590_T01	AT5G57520.1	zinc finger protein 2	-2,14			
GRMZM2G340297_T01			-2,13			
GRMZM2G450822_T01			-2,13			
GRMZM2G381691_T01	AT5G24930.1	CONSTANS-like 4	-2,13			
GRMZM2G121878_T01	AT5G14740.2	carbonic anhydrase 2	-2,12			
GRMZM2G123774_T01			-2,12			
GRMZM2G082264_T01	AT5G16560.1	Homeodomain-like superfamily protein	-2,11			
GRMZM2G118403_T01			-2,11			

GRMZM5G846506_T01	AT2G38300.1	myb-like HTH transcriptional regulator family protein	-2,11			
GRMZM2G069365_T01	AT4G24660.1	homeobox protein 22	-2,10			
GRMZM2G084005_T01	AT3G48510.1		-2,10			
GRMZM2G095807_T01	AT3G16520.3	UDP-glucosyl transferase 88A1	-2,10			
GRMZM2G140317_T01			-2,10			
GRMZM2G158232_T01	AT1G53540.1	HSP20-like chaperones superfamily protein	-2,10			
GRMZM2G330684_T01	AT5G60710.1	Zinc finger (C3HC4-type RING finger) family protein	-2,09			
GRMZM5G830365_T01	AT1G12980.1	Integrase-type DNA-binding superfamily protein	-2,08			
GRMZM2G101125_T01	AT2G41190.1	Transmembrane amino acid transporter family protein	-2,08			
GRMZM2G143046_T01	AT1G48000.1	myb domain protein 112	-2,08			
GRMZM2G078324_T01	AT2G23670.1	homolog of Synechocystis YCF37	-2,08			
GRMZM2G071307_T01			-2,08			
GRMZM2G169535_T01			-2,07			
GRMZM2G403669_T01			-2,06			
GRMZM2G089466_T01	AT4G32600.1	RING/U-box superfamily protein	-2,06			
GRMZM2G131961_T01	AT5G65210.2	bZIP transcription factor family protein	-2,06			
GRMZM5G848857_T01			-2,05			
AC209213.4_FGT002			-2,05			
GRMZM2G100747_T01	AT1G75050.1	Pathogenesis-related thaumatin superfamily protein	-2,05			
GRMZM2G158029_T01	AT5G08490.1	Tetratricopeptide repeat (TPR)-like superfamily protein	-2,05			
GRMZM2G462750_T01	AT5G42470.1		-2,04			
GRMZM5G888620_T01	AT2G15480.2	UDP-glucosyl transferase 73B5	-2,04			
GRMZM2G381283_T01	AT4G24700.1		-2,03			
AC225716.2_FGT006	AT5G45890.1	senescence-associated gene 12	-2,03			
GRMZM2G042356_T01	AT3G51520.1	diacylglycerol acyltransferase family	-2,03			
GRMZM2G087435_T01	AT1G05385.1	photosystem II 11 kDa protein-related	-2,03			

GRMZM5G834532_T01			-2,03			
GRMZM2G417945_T01	AT4G15480.1	UDP-Glycosyltransferase superfamily protein	-2,03			
GRMZM2G122850_T01	AT4G14040.1	selenium-binding protein 2	-2,02			
GRMZM2G409104_T01	AT5G10840.1	Endomembrane protein 70 protein family	-2,02			
GRMZM2G109787_T01	AT1G14790.1	RNA-dependent RNA polymerase 1	-2,02			
AC212354.3_FGT002			-2,02			
GRMZM2G032266_T01	AT1G62780.1		-2,02			
GRMZM2G019106_T01	AT2G35530.1	basic region/leucine zipper transcription factor 16	-2,02			
GRMZM2G391833_T01	AT5G19930.1	Protein of unknown function DUF92, transmembrane	-2,01			
GRMZM5G835987_T01	AT3G57910.1	D111/G-patch domain-containing protein	-2,01			
GRMZM2G166186_T01			-2,01			
AC184764.3_FGT006			-2,01			
GRMZM2G168479_T01			-2,01			
GRMZM5G851051_T01	AT1G70760.1	inorganic carbon transport protein-related	-2,00			
GRMZM2G461825_T01			2,00			
AC215907.3_FGT003			2,01			
GRMZM2G072578_T01	AT2G06925.1	Phospholipase A2 family protein	2,01			
GRMZM2G106393_T01	AT4G10265.1	Wound-responsive family protein	2,02		3,29	
GRMZM2G132693_T01	AT3G02550.1	LOB domain-containing protein 41	2,02			
GRMZM2G380889_T01	AT3G08970.1	DNAJ heat shock N-terminal domain-containing protein	2,02			
GRMZM2G035712_T01			2,02			
GRMZM2G091560_T01	AT1G48520.1	GLU-ADT subunit B	2,03			
GRMZM2G107026_T01			2,03			
GRMZM2G437490_T01	AT5G50380.1	exocyst subunit exo70 family protein F1	2,04			
GRMZM2G031216_T01			2,04			
GRMZM2G326222_T01	AT3G03670.1	Peroxidase superfamily protein	2,04			

AC210598.3_FGT003	AT5G44070.1	phytochelatin synthase 1 (PCS1)	2,04			
GRMZM5G873779_T01	AT1G63900.2	E3 Ubiquitin ligase family protein	2,04			
GRMZM2G351921_T01	AT3G50950.1	HOPZ-ACTIVATED RESISTANCE 1	2,05			
GRMZM2G172159_T01			2,05			
GRMZM2G040689_T01	AT3G22142.1	Bifunctional inhibitor/lipid-transfer protein/seed storage 2S albumin superfamily protein	2,05			
GRMZM2G020131_T01	AT2G46330.1	arabinogalactan protein 16	2,05			
GRMZM2G039280_T01	AT4G02680.1	ETO1-like 1	2,06			
GRMZM2G443885_T01	AT5G05340.1	Peroxidase superfamily protein	2,06			
AC204687.3_FGT001			2,07			
GRMZM2G023921_T01	AT1G80450.1	VQ motif-containing protein	2,07			
GRMZM2G059392_T01	AT3G53450.1	Putative lysine decarboxylase family protein	2,08			
GRMZM5G805906_T01			2,09			
GRMZM2G058814_T01			2,09			
GRMZM2G702379_T01			2,10			
GRMZM2G080825_T01	AT3G05390.1		2,11			
GRMZM2G407869_T01	AT5G19770.1	tubulin alpha-3	2,11			
GRMZM2G093408_T01	AT2G34160.1	Alba DNA/RNA-binding protein	2,13			
GRMZM2G081928_T01	AT4G25980.1	Peroxidase superfamily protein	2,13			
GRMZM2G170307_T01	AT4G13830.2	DNAJ-like 20	2,14			
GRMZM2G177218_T01	AT5G57500.1	Galactosyltransferase family protein	2,14			
AC213834.3_FGT005			2,14			
GRMZM2G101390_T01	AT2G39300.1		2,14			
GRMZM2G031477_T01	AT1G79480.1	Carbohydrate-binding X8 domain superfamily protein	2,14			
AC212449.4_FGT004	AT1G47230.1	CYCLIN A3;4	2,15			
GRMZM2G445478_T01	AT1G70160.1		2,15			
GRMZM2G021410_T01	AT5G21950.1	alpha/beta-Hydrolases superfamily protein	2,15			

GRMZM2G356355_T01	AT3G07470.1	Protein of unknown function, DUF538	2,15			
GRMZM2G028766_T01	AT1G04850.1	ubiquitin-associated (UBA)/TS-N domain-containing protein	2,15			
GRMZM5G830585_T01			2,16			
GRMZM2G180168_T01	AT1G01030.1	AP2/B3-like transcriptional factor family protein	2,17			
GRMZM2G425729_T01	AT2G01300.1		2,17			
GRMZM2G011636_T01	AT1G11890.1	Synaptobrevin family protein	2,17		3,41	
GRMZM2G358711_T01	AT4G28890.1	RING/U-box superfamily protein	2,18			
GRMZM2G410338_T01	AT4G12520.1	Bifunctional inhibitor/lipid-transfer protein/seed storage 2S albumin superfamily protein	2,18			
GRMZM2G451300_T01	AT5G10530.1	Concanavalin A-like lectin protein kinase family protein	2,19			
GRMZM5G829897_T01	AT5G45920.1	SGNH hydrolase-type esterase superfamily protein	2,19		2,11	
GRMZM2G107204_T01			2,19			
GRMZM2G147221_T01			2,20			
AC185586.4_FGT003			2,21			
AC210168.4_FGT003	AT2G28790.1	Pathogenesis-related thaumatin superfamily protein	2,21			
GRMZM2G138727_T01			2,21			
GRMZM2G057841_T01			2,21			
GRMZM2G022686_T01	AT2G47460.1	myb domain protein 12	2,22			
GRMZM2G085964_T01	AT3G16770.1	ethylene-responsive element binding protein	2,22			
AC205057.3_FGT004	AT2G06510.1	replication protein A 1A	2,22			
GRMZM2G054745_T01	AT1G77930.2	Chaperone DnaJ-domain superfamily protein	2,23			
GRMZM5G822028_T01			2,24			
GRMZM2G336824_T01	AT4G35160.1	O-methyltransferase family protein	2,25			
GRMZM2G148896_T01	AT5G32470.1	Haem oxygenase-like, multi-helical	2,25			
GRMZM2G082118_T01	AT2G44340.1	VQ motif-containing protein	2,25			
GRMZM5G879116_T01	AT1G05370.1	Sec14p-like phosphatidylinositol transfer family protein	2,26			
GRMZM2G442658_T01	AT1G77120.1	alcohol dehydrogenase 1	2,27			

GRMZM2G133394_T01	AT1G79720.1	Eukaryotic aspartyl protease family protein	2,27			
GRMZM2G102550_T01	AT4G36810.1	geranylgeranyl pyrophosphate synthase 1	2,27			
GRMZM2G127029_T01	AT1G12560.1	expansin A7	2,27			
GRMZM2G120463_T01			2,31			
GRMZM5G819222_T01	AT5G13140.1	Pollen Ole e 1 allergen and extensin family protein	2,31			
GRMZM2G435684_T01	AT4G37860.1	SPT2 chromatin protein	2,31			
GRMZM2G088865_T01	AT1G16810.2		2,32			
GRMZM2G353957_T01	AT5G04870.1	calcium dependent protein kinase 1	2,32			
GRMZM2G386597_T01			2,33			
GRMZM2G167829_T01	AT4G37780.1	myb domain protein 87	2,35			
GRMZM2G095452_T01	AT1G79960.1	ovate family protein 14	2,35			
GRMZM2G038622_T01	AT3G58000.1	VQ motif-containing protein	2,35			
GRMZM2G396927_T01	AT3G25690.2	Hydroxyproline-rich glycoprotein family protein	2,36			
GRMZM2G123492_T01			2,36			
AC185587.3_FGT003	AT1G65880.1	benzoyloxyglucosinolate 1	2,36			
GRMZM2G047656_T01	AT5G67400.1	root hair specific 19	2,38			
GRMZM2G138303_T01	AT3G26782.1	Tetratricopeptide repeat (TPR)-like superfamily protein	2,38			
GRMZM2G363971_T01			2,39			
GRMZM2G002034_T01	AT1G60590.1	Pectin lyase-like superfamily protein	2,40			
GRMZM2G035890_T01			2,41			
GRMZM2G177755_T01			2,41			
GRMZM2G703261_T01	AT3G45100.2	UDP-Glycosyltransferase superfamily protein	2,42			
GRMZM5G881088_T01	AT2G32830.1	phosphate transporter 1;5	2,42			
GRMZM2G437481_T01	AT1G05805.1	basic helix-loop-helix (bHLH) DNA-binding superfamily protein	2,42			
GRMZM2G306143_T01	AT4G10550.1	Subtilase family protein	2,47			
GRMZM2G405280_T01			2,48			

GRMZM2G048850_T01	AT3G60530.1	GATA transcription factor 4	2,49			
GRMZM2G496350_T01			2,50			
GRMZM2G028179_T01			2,51			
GRMZM2G001497_T01	AT4G19970.1		2,52			
GRMZM2G136353_T01	AT1G28440.1	HAESA-like 1	2,52			
AC234190.1_FGT001	AT4G01630.1	expansin A17	2,53			
GRMZM2G389789_T01	AT1G67530.2	ARM repeat superfamily protein	2,53			
GRMZM2G486933_T01			2,53			
AC207260.3_FGT004			2,55			
GRMZM2G453296_T01	AT1G09160.1	Protein phosphatase 2C family protein	2,56			
GRMZM2G168073_T01	AT5G58400.1	Peroxidase superfamily protein	2,58			
GRMZM2G450501_T01	AT4G02380.1	senescence-associated gene 21	2,58			
GRMZM2G406313_T01	AT4G12520.1	Bifunctional inhibitor/lipid-transfer protein/seed storage 2S albumin superfamily protein	2,58			
GRMZM2G026020_T01	AT1G11800.1	endonuclease/exonuclease/phosphatase family protein	2,59			
GRMZM2G063473_T01	AT5G57930.2	Arabidopsis thaliana protein of unknown function (DUF794)	2,60			
AC212287.4_FGT002			2,61			
AC233899.1_FGT002	AT1G72210.1	basic helix-loop-helix (bHLH) DNA-binding superfamily protein	2,61			
GRMZM2G322129_T01	AT3G06880.1	Transducin/WD40 repeat-like superfamily protein	2,61			
GRMZM2G098279_T01			2,61			
GRMZM2G149700_T01			2,62			
GRMZM2G413135_T01	AT4G37420.1	Domain of unknown function (DUF23)	2,62			
GRMZM2G002976_T01			2,64			
GRMZM2G048175_T01	AT5G13140.1	Pollen Ole e 1 allergen and extensin family protein	2,65			
GRMZM2G113165_T01	AT1G08080.1	alpha carbonic anhydrase 7	2,66			
GRMZM2G387341_T01			2,68			
AC194670.2_FGT001	AT1G76150.1	enoyl-CoA hydratase 2	2,69			

GRMZM2G024680_T01	AT1G19180.1	jasmonate-zim-domain protein 1	2,69			
GRMZM2G701392_T01			2,74			
GRMZM2G316362_T01	AT1G43800.1	Plant stearoyl-acyl-carrier-protein desaturase family protein	2,74			
GRMZM5G873767_T01	AT5G45910.1	GDSL-like Lipase/Acylhydrolase superfamily protein	2,75			
GRMZM2G085068_T01	AT2G44440.1	Emsy N Terminus (ENT) domain-containing protein	2,76			
GRMZM2G124011_T01	AT4G25480.1	dehydration response element B1A	2,76			
GRMZM2G117347_T01	AT5G42680.1	Protein of unknown function, DUF617	2,76			
GRMZM2G106511_T01	AT4G10270.1	Wound-responsive family protein	2,83		3,18	
GRMZM2G325038_T01	AT2G38250.1	Homeodomain-like superfamily protein	2,83			
AC211749.4_FGT007			2,85			
GRMZM2G118312_T01	AT2G03220.1	fucosyltransferase 1	2,87			
GRMZM2G058622_T01	AT2G32300.1	uclacyanin 1	2,89			
GRMZM2G059785_T01	AT1G65680.1	expansin B2	2,90			
GRMZM2G342246_T01	AT1G65680.1	expansin B2	2,92			
GRMZM5G899708_T01			2,93			
GRMZM2G065073_T01	AT4G39640.2	gamma-glutamyl transpeptidase 1	2,94			
GRMZM2G413711_T01	AT3G49320.1	Metal-dependent protein hydrolase	2,97			
GRMZM2G031628_T01	AT4G21760.1	beta-glucosidase 47	2,99			
GRMZM2G381441_T01	AT3G23240.1	ethylene response factor 1	3,00			
GRMZM2G024345_T01			3,03			
AC215201.3_FGT008	AT2G40435.1		3,05			
GRMZM2G393062_T01	AT4G24110.1		3,06			
GRMZM2G037431_T01	AT1G10640.1	Pectin lyase-like superfamily protein	3,15			
AC210422.3_FGT009			3,20			
GRMZM2G072089_T01	AT3G07880.1	Immunoglobulin E-set superfamily protein	3,21			
GRMZM2G025536_T01	AT2G44800.1	2-oxoglutarate (2OG) and Fe(II)-dependent oxygenase superfamily protein	3,23			

GRMZM2G053639_T01	AT2G30200.2	catalytics;transferases;[acyl-carrier-protein] S-malonyl-transferases;binding	3,24		3,12	
GRMZM2G076562_T01	AT5G17820.1	Peroxidase superfamily protein	3,30			
GRMZM2G031660_T01	AT1G61820.1	beta glucosidase 46	3,35			
GRMZM2G023811_T01			3,36			
GRMZM2G380619_T01	AT5G02880.1	ubiquitin-protein ligase 4	3,38			
GRMZM2G386170_T01	AT4G39830.1	Cupredoxin superfamily protein	3,41			
GRMZM2G148374_T01	AT3G42640.1	H(+)-ATPase 8	3,44		4,20	
GRMZM5G835672_T01			3,57			
GRMZM2G055101_T01	AT4G33840.1	Glycosyl hydrolase family 10 protein	3,67			
GRMZM2G430936_T01	AT5G24090.1	chitinase A	3,73			
GRMZM2G150327_T01	AT2G22760.1	basic helix-loop-helix (bHLH) DNA-binding superfamily protein	3,86			
GRMZM2G485356_T01			3,94			
GRMZM5G860864_T01			4,22			
GRMZM2G052935_T01	AT5G13280.1	aspartate kinase 1	4,23			
GRMZM2G474194_T01	AT1G65680.1	expansin B2	4,38			
GRMZM5G851266_T01			4,56		3,36	
GRMZM2G040630_T01	AT2G37090.1	Nucleotide-diphospho-sugar transferases superfamily protein	4,64			
GRMZM2G062009_T01	AT4G28530.1	NAC domain containing protein 74	4,83			
AC208358.3_FGT005	AT2G24070.2	Family of unknown function (DUF566)	5,07			
GRMZM2G435380_T01	AT5G14650.1	Pectin lyase-like superfamily protein	5,90			
GRMZM2G124567_T01			5,98			
GRMZM2G590027_T01			9,93			
GRMZM2G406101_T01				2,17		
GRMZM2G444393_T01	AT5G11680.1			3,06		
GRMZM2G376674_T01				2,28		
GRMZM2G045699_T01				-9,06		

GRMZM2G365815_T01	AT5G12180.1	calcium-dependent protein kinase 17		2,12		
GRMZM2G173532_T01	AT2G06510.2	replication protein A 1A		2,85		
GRMZM5G885425_T01				2,79		
GRMZM2G017365_T01				2,16		
GRMZM2G095115_T01				-2,43		
GRMZM2G110299_T01	AT4G13080.1	xyloglucan endotransglucosylase/hydrolase 1		-2,26		
GRMZM2G065635_T01	AT3G50660.1	Cytochrome P450 superfamily protein		-2,57		
GRMZM2G137502_T01	AT5G60200.1	TARGET OF MONOPTEROS 6		2,52		
GRMZM2G169095_T01	AT4G36760.1	aminopeptidase P1		2,47		
GRMZM2G041231_T01	AT4G13650.1	Pentatricopeptide repeat (PPR) superfamily protein		2,93		
GRMZM2G057768_T01	AT2G33700.1	Protein phosphatase 2C family protein		2,28		
GRMZM2G498171_T01				-2,16		
GRMZM2G351966_T01				-2,41		
GRMZM2G398825_T01	AT1G76630.2	Tetratricopeptide repeat (TPR)-like superfamily protein		-2,39		
GRMZM2G160739_T01				2,04		
GRMZM2G180612_T01	AT5G47860.1	Protein of unknown function (DUF1350)		2,15		2,11
GRMZM2G430675_T01	AT2G37010.1	non-intrinsic ABC protein 12		-2,28		-2,10
GRMZM5G842214_T01				2,18		
GRMZM2G106185_T01	AT1G14600.1	Homeodomain-like superfamily protein		2,10		
GRMZM2G102230_T01	AT3G04400.1	Ribosomal protein L14p/L23e family protein		2,53		
GRMZM5G883813_T01				2,07		
GRMZM2G400694_T01	AT3G53810.1	Concanavalin A-like lectin protein kinase family protein		2,56		
GRMZM2G426067_T01	AT5G41460.1	Protein of unknown function (DUF604)		2,69		
GRMZM2G033236_T01				-2,08		
AC208848.3_FGT005				2,55		
GRMZM2G040728_T01	AT3G56630.1	cytochrome P450, family 94, subfamily D, polypeptide 2		-2,67		

GRMZM2G485559_T01	AT5G15350.1	early nodulin-like protein 17		2,02		
GRMZM2G135228_T01				-2,35		
GRMZM2G540322_T01				-2,20		
AC148152.3_FGT008	AT3G06510.1	Glycosyl hydrolase superfamily protein		2,34		
GRMZM2G027302_T01	AT1G07090.1	Protein of unknown function (DUF640)		-2,61		
GRMZM2G429992_T01				-2,30		
GRMZM5G872279_T01				2,01		
GRMZM2G348035_T01	AT1G13980.2	sec7 domain-containing protein		2,14		
AC207254.3_FGT005				2,25		
GRMZM2G036547_T01				2,02		
GRMZM2G402156_T01	AT5G47390.1	myb-like transcription factor family protein		2,19		
GRMZM5G870100_T01				3,04		
GRMZM2G476848_T01	AT2G41905.1			2,44		
GRMZM2G141624_T01	AT5G66110.1	Heavy metal transport/detoxification superfamily protein		2,71		
GRMZM2G009413_T01	AT1G03360.1	ribosomal RNA processing 4		2,88		
GRMZM2G351023_T01	AT1G24360.1	NAD(P)-binding Rossmann-fold superfamily protein		2,39		
GRMZM2G395844_T01	AT5G14670.1	ADP-ribosylation factor A1B		2,00		
AC203237.3_FGT001				2,03		
GRMZM2G003669_T01	AT3G18690.1	MAP kinase substrate 1		-2,36		
GRMZM2G139211_T01				-7,52		
GRMZM2G103759_T01				2,80		
GRMZM2G022188_T01	AT3G15980.3	Coatomer, beta\' subunit		2,09		
GRMZM2G087766_T01	AT1G10750.1	Protein of Unknown Function (DUF239)		2,29		
GRMZM2G166430_T01	AT1G79060.1			2,07		
GRMZM2G522710_T01				2,18		
GRMZM2G139639_T01	AT5G43360.1	phosphate transporter 1;3		2,19		

GRMZM2G041308_T01	AT5G66390.1	Peroxidase superfamily protein		2,28		
GRMZM5G830839_T01	AT5G59190.1	subtilase family protein		2,15		
GRMZM2G109586_T01	AT2G21520.2	Sec14p-like phosphatidylinositol transfer family protein		2,56		
GRMZM2G554653_T01	AT3G51980.1	ARM repeat superfamily protein		2,31		
AC213896.2_FGT005	AT2G22490.2	Cyclin D2;1		2,04		
GRMZM2G076943_T01	AT4G23160.1	cysteine-rich RLK (RECEPTOR-like protein kinase) 8		-2,82		
AC187046.3_FGT009				2,32		
GRMZM2G170391_T01	AT5G45890.1	senescence-associated gene 12		2,01		
GRMZM2G357040_T01				2,12		
GRMZM2G045030_T01				2,01		
GRMZM2G063897_T01	AT2G28250.1	Protein kinase superfamily protein		-2,92		
GRMZM2G353091_T01	AT4G03000.1	RING/U-box superfamily protein		2,03		
GRMZM2G338049_T01	AT5G41980.1			-2,50		
AC208109.2_FGT004				2,02		
GRMZM2G123365_T01	AT1G28590.1	GDSL-like Lipase/Acylhydrolase superfamily protein		2,12		
GRMZM2G401983_T01	AT1G65680.1	expansin B2		2,74		
GRMZM2G117497_T01	AT4G39250.1	RAD-like 1		-2,88		
GRMZM2G374989_T01	AT1G15460.1	HCO3- transporter family		2,52		
GRMZM2G421779_T01				-2,31		
GRMZM2G700784_T01	AT3G57030.1	Calcium-dependent phosphotriesterase superfamily protein		2,85		
AC213804.4_FGT004				2,10		
GRMZM2G101020_T01	AT1G19910.1	ATPase, F0/V0 complex, subunit C protein		2,54		
AC185642.4_FGT001	AT1G16810.2			2,35		
GRMZM5G813937_T01				2,53		
GRMZM2G130358_T01	AT1G75350.1	Ribosomal protein L31		2,21		
GRMZM5G822352_T01				2,20		

GRMZM2G163709_T01	AT4G36945.1	PLC-like phosphodiesterases superfamily protein		2,66		
GRMZM2G059985_T01	AT4G38060.1			3,15		3,23
GRMZM2G179121_T01	AT4G30080.1	auxin response factor 16		2,53		
GRMZM2G071270_T01	AT5G23310.1	Fe superoxide dismutase 3		-2,31		
GRMZM2G041404_T01	AT1G54500.1	Rubredoxin-like superfamily protein		2,06		
GRMZM5G894115_T01	AT2G22410.1	SLOW GROWTH 1		2,39		
GRMZM2G003489_T01				2,56		
GRMZM2G146809_T01	AT2G02120.1	Scorpion toxin-like knottin superfamily protein		2,22		
GRMZM2G024131_T01	AT2G43820.1	UDP-glucosyltransferase 74F2		3,02		
GRMZM2G146665_T01	AT1G70370.1	polygalacturonase 2		2,12		
GRMZM5G877275_T01				-2,98		
GRMZM2G169149_T01	AT4G31800.1	WRKY DNA-binding protein 18		-2,03		
GRMZM2G008923_T01	AT5G59240.1	Ribosomal protein S8e family protein		2,01		
GRMZM2G325938_T01	AT4G33510.1	3-deoxy-d-arabino-heptulosonate 7-phosphate synthase		-3,69		
GRMZM2G540318_T01				-2,17		
GRMZM2G068557_T01	AT5G49740.1	ferric reduction oxidase 7		-2,03		
GRMZM2G370999_T01				2,75		
GRMZM2G393742_T01	AT2G16390.1	SNF2 domain-containing protein / helicase domain-containing protein		-2,12		
GRMZM2G166906_T01	AT1G12570.1	Glucose-methanol-choline (GMC) oxidoreductase family protein		2,29		
GRMZM2G491366_T01					-3,66	
GRMZM2G703077_T01	AT5G05920.1	deoxyhypusine synthase			-2,98	
GRMZM2G072488_T01	AT3G63470.1	serine carboxypeptidase-like 40			-2,82	
GRMZM2G136367_T01	AT5G64080.1	Bifunctional inhibitor/lipid-transfer protein/seed storage 2S albumin superfamily protein			-2,52	
GRMZM2G018716_T01	AT1G55120.1	beta-fructofuranosidase 5			-2,52	
GRMZM2G361968_T01	AT2G45260.1	Plant protein of unknown function (DUF641)			-2,31	
GRMZM2G001508_T01	AT4G29260.1	HAD superfamily, subfamily IIIB acid phosphatase			-2,24	

AC199873.4_FGT002					-2,24	
GRMZM2G421669_T01	AT3G47570.1	Leucine-rich repeat protein kinase family protein			-2,21	
GRMZM2G059073_T01	AT3G21070.2	NAD kinase 1			-2,15	
GRMZM2G442265_T01					-2,15	
GRMZM2G054703_T01	AT3G45400.1	exostosin family protein			-2,13	
GRMZM2G104294_T01	AT4G30210.2	P450 reductase 2			-2,07	
GRMZM2G354519_T01	AT1G56410.1	heat shock protein 70 (Hsp 70) family protein			-2,05	
GRMZM5G849919_T01					2,00	
GRMZM2G060544_T01	AT3G02550.1	LOB domain-containing protein 41			2,02	
GRMZM2G389944_T01	AT2G36800.1	don-glucosyltransferase 1			2,03	
GRMZM2G000052_T01	AT2G43020.1	polyamine oxidase 2			2,08	
GRMZM2G154721_T01	AT2G42330.2	GC-rich sequence DNA-binding factor-like protein with Tuftelin interacting domain			2,09	
GRMZM5G813627_T01	AT4G36690.1	U2 snRNP auxilliary factor, large subunit, splicing factor			2,11	
GRMZM2G035826_T01	AT1G02060.1	Tetratricopeptide repeat (TPR)-like superfamily protein			2,12	
AC196009.2_FGT008					2,12	
GRMZM5G887750_T01					2,13	
GRMZM2G175995_T01					2,13	
GRMZM2G016212_T01	AT5G66240.2	Transducin/WD40 repeat-like superfamily protein			2,14	
GRMZM2G700848_T01					2,14	
AC213800.3_FGT001					2,16	
GRMZM2G021049_T01	AT1G76190.1	SAUR-like auxin-responsive protein family			2,16	
GRMZM2G152774_T01	AT4G13870.2	Werner syndrome-like exonuclease			2,19	
GRMZM2G153456_T01	AT5G17510.1				2,20	
GRMZM2G174669_T01	AT1G01860.1	Ribosomal RNA adenine dimethylase family protein			2,21	
GRMZM2G134045_T01	AT4G17890.1	ARF-GAP domain 8			2,23	
GRMZM2G029815_T01	AT1G65920.1	Regulator of chromosome condensation (RCC1) family with FYVE zinc finger domain			2,25	

GRMZM2G061776_T01	AT4G30170.1	Peroxidase family protein			2,26	
GRMZM2G305362_T01	AT3G10040.1	sequence-specific DNA binding transcription factors			2,29	
GRMZM2G309356_T01	AT3G08800.1	ARM repeat superfamily protein			2,33	
GRMZM2G091579_T01					2,34	
GRMZM2G165930_T01	AT3G47680.1	DNA binding			2,35	
GRMZM2G021560_T01	AT1G65480.1	PEBP (phosphatidylethanolamine-binding protein) family protein			2,37	
GRMZM2G701138_T01					2,37	
GRMZM2G052288_T01	AT5G11880.1	Pyridoxal-dependent decarboxylase family protein			2,40	
GRMZM2G158831_T01	AT2G20815.1	Family of unknown function (DUF566)			2,46	
GRMZM2G098875_T01	AT5G17330.1	glutamate decarboxylase			2,47	
GRMZM2G177940_T01	AT5G19730.1	Pectin lyase-like superfamily protein			2,58	
AC209629.2_FGT007					2,60	
GRMZM2G135803_T01					2,61	
GRMZM2G114503_T01	AT1G75250.1	RAD-like 6			2,64	
GRMZM2G363805_T01					2,76	
GRMZM2G058370_T01	AT5G13250.1	RING finger protein			2,78	
GRMZM2G038677_T01	AT5G15120.1	Protein of unknown function (DUF1637)			2,87	
GRMZM2G171096_T01					2,92	
GRMZM2G027016_T01	AT1G47530.1	MATE efflux family protein			2,95	
GRMZM2G127121_T01	AT1G65480.1	PEBP (phosphatidylethanolamine-binding protein) family protein			2,96	
GRMZM2G169569_T01					3,05	
AC182413.4_FGT002					3,32	
GRMZM2G046326_T01					3,42	
GRMZM2G341771_T01	AT2G36800.1	don-glucosyltransferase 1			3,54	
GRMZM2G523462_T01					3,60	
GRMZM2G091243_T01	AT1G07870.1	Protein kinase superfamily protein			3,67	

GRMZM2G150608_T01	AT5G19280.1	kinase associated protein phosphatase			3,88	
GRMZM2G336766_T01	AT3G56850.1	ABA-responsive element binding protein 3			3,91	
GRMZM2G442148_T01	AT1G52240.1	RHO guanyl-nucleotide exchange factor 11			3,93	
GRMZM2G453581_T01	AT3G10350.1	P-loop containing nucleoside triphosphate hydrolases superfamily protein			4,07	
GRMZM2G086401_T01	AT4G16340.1	guanyl-nucleotide exchange factors;GTPase binding;GTP binding			4,10	
GRMZM5G888797_T01	AT2G27385.2	Pollen Ole e 1 allergen and extensin family protein			4,33	
GRMZM2G397927_T01	AT5G57123.1				4,44	
GRMZM2G048919_T01	AT1G15760.1	Sterile alpha motif (SAM) domain-containing protein			4,51	
GRMZM2G158117_T01	AT4G39250.1	RAD-like 1			5,51	
GRMZM2G045999_T01	AT5G11680.1				6,74	
GRMZM2G066020_T01	AT5G20900.1	jasmonate-zim-domain protein 12				-3,48
GRMZM2G041369_T01	AT1G27480.1	alpha/beta-Hydrolases superfamily protein				-2,90
GRMZM5G832125_T01						-2,74
GRMZM5G846916_T01	AT5G55180.1	O-Glycosyl hydrolases family 17 protein				-2,71
GRMZM2G017268_T01	AT1G34670.1	myb domain protein 93				-2,63
GRMZM2G016346_T01						-2,46
AC184130.4_FGT012	AT4G18470.1	negative regulator of systemic acquired resistance (SNI1)				-2,32
GRMZM2G467348_T01						-2,27
GRMZM2G333140_T01						-2,26
GRMZM5G803981_T01	AT4G15210.1	beta-amylase 5				-2,25
GRMZM5G898337_T01						-2,22
GRMZM2G131205_T01	AT1G15950.1	cinnamoyl coa reductase 1				-2,21
GRMZM2G573324_T01	AT2G22670.4	indoleacetic acid-induced protein 8				-2,21
GRMZM2G109741_T01						-2,19
GRMZM5G837621_T01						-2,16
GRMZM2G704175_T01						-2,16

GRMZM2G017008_T01	AT3G62630.1	Protein of unknown function (DUF1645)				-2,14
GRMZM2G478996_T01	AT2G22590.1	UDP-Glycosyltransferase superfamily protein				-2,13
GRMZM2G319786_T01						-2,12
GRMZM2G414114_T01	AT3G12170.1	Chaperone DnaJ-domain superfamily protein				-2,12
GRMZM2G134889_T01	AT5G60640.1	PDI-like 1-4				-2,11
GRMZM2G141704_T01	AT1G07810.1	ER-type Ca2+-ATPase 1				-2,09
GRMZM2G053711_T01	AT2G45150.1	cytidinediphosphate diacylglycerol synthase 4				-2,08
GRMZM2G015418_T01	AT1G01050.1	pyrophosphorylase 1				-2,08
GRMZM2G016655_T01	AT5G11560.1	catalytics				-2,07
GRMZM2G127050_T01	AT4G35230.1	BR-signaling kinase 1				-2,06
GRMZM2G018728_T01	AT3G56490.1	HIS triad family protein 3				-2,04
GRMZM5G892338_T01	AT5G37820.1	NOD26-like intrinsic protein 4;2				-2,03
GRMZM2G702180_T01						-2,03
GRMZM2G027683_T01	AT5G11420.1	Protein of unknown function, DUF642				-2,01
GRMZM2G426306_T01	AT2G02180.1	tobamovirus multiplication protein 3				-2,00
GRMZM5G839416_T01	AT3G19050.1	phragmoplast orienting kinesin 2				-2,00
GRMZM2G070931_T01						2,02
GRMZM2G105523_T01	AT1G56700.2	Peptidase C15, pyroglutamyl peptidase I-like				2,05
GRMZM2G339344_T01						2,05
GRMZM2G034623_T01	AT5G41761.1					2,07
GRMZM2G070079_T01						2,07
GRMZM2G013617_T01	AT5G41410.1	POX (plant homeobox) family protein				2,10
GRMZM5G850100_T01						2,11
GRMZM2G139786_T01	AT1G09310.1	Protein of unknown function, DUF538				2,11
GRMZM2G170400_T01	AT3G18000.1	S-adenosyl-L-methionine-dependent methyltransferases superfamily protein				2,12
GRMZM5G888228_T01						2,14

GRMZM2G438652_T01						2,26
GRMZM2G143460_T01	AT2G24150.1	heptahelical protein 3				2,27
GRMZM2G056896_T01						2,30
GRMZM2G076593_T01	AT5G09220.1	amino acid permease 2				2,34
GRMZM2G034958_T01	AT1G71691.2	GDSL-like Lipase/Acylhydrolase superfamily protein				2,41
GRMZM2G117742_T01	AT5G06700.1	Plant protein of unknown function (DUF828)				2,41
GRMZM2G112247_T01	AT4G35750.1	SEC14 cytosolic factor family protein / phosphoglyceride transfer family protein				2,45
GRMZM2G102811_T01	AT1G53280.1	Class I glutamine amidotransferase-like superfamily protein				2,45
GRMZM2G049464_T01	AT1G10280.1	Core-2/I-branching beta-1,6-N-acetylglucosaminyltransferase family protein				2,46
GRMZM2G160611_T01						2,48
GRMZM2G434597_T01						2,50
GRMZM2G029566_T01	AT1G12050.1	fumarylacetoacetase, putative				2,54
GRMZM2G021289_T01						2,67
GRMZM2G375602_T01	AT1G28610.2	GDSL-like Lipase/Acylhydrolase superfamily protein				2,70
GRMZM2G453919_T01						2,73
GRMZM2G137868_T01	AT2G13360.2	alanine:glyoxylate aminotransferase				2,78
GRMZM2G340130_T01	AT3G13460.1	evolutionarily conserved C-terminal region 2				2,89
GRMZM2G355752_T01	AT3G22840.1	Chlorophyll A-B binding family protein				2,99
GRMZM2G459498_T01						3,06
AC195148.3_FGT001						3,12
AC216229.3_FGT002						3,21
GRMZM2G362470_T01						3,30
GRMZM5G890604_T01	AT2G36290.1	alpha/beta-Hydrolases superfamily protein				3,35
GRMZM2G163099_T01	AT3G09590.1	CAP (Cysteine-rich secretory proteins, Antigen 5, and Pathogenesis-related 1 protein) superfamily protein				3,36
GRMZM2G701738_T01						3,40
GRMZM2G700995_T01						3,43

GRMZM2G320305_T01	AT1G20020.1	ferredoxin-NADP(+)-oxidoreductase 2				3,55
GRMZM2G018649_T01	AT2G37170.1	plasma membrane intrinsic protein 2				3,95
GRMZM2G094360_T01	AT4G29905.1					3,99
GRMZM2G365810_T01	AT5G14780.1	formate dehydrogenase				4,79

APPENDIX III.

Number and percentage of differentially modulated transcripts in each comparison in maize and cucumber

Cucumber	Modulated transcripts (n°)	% downregulated	% upregulated
-P+NPs *vs* -P	81	71.6	28.4
-P+bulk *vs* -P	92	57.7	42.3
-Fe+NPs *vs* -Fe	90	57.6	42.4
-Fe+bulk *vs* -Fe	57	98.1	1.9
Maize			
-P+NPs *vs* -P	466	63.9	36.1
-P+bulk *vs* -P	111	27.7	72.3
-Fe+NPs *vs* -Fe	81	17.9	82.1
-Fe+bulk *vs* -Fe	82	43.0	57.0

APPENDIX IV.

Table of elemental analysis performed through ICP-MS for Mg, K, Ca, Mn, Cu and Zn. Average values are listed above. Standard deviations are listed below.

	shoot			root			
	-P	**NPs**	**TSP**	**-P**	**NPs**	**TSP**	
Mg	5.7	4.9	5.6	3.8	3.1	3.6	
K	25.4	27.6	26.3	36.3	42.2	40.6	mg/g
Ca	18.5	14.4	15.3	7.1	6.7	6.7	
Mn	78.8	55.2	63.8	144.8	81.0	100.5	
Cu	11.6	7.7	8.4	19.1	17.6	19.8	µg/g
Zn	74.5	63.9	71.5	127.5	108.6	131.4	

	shoot			root			
	-P	**NPs**	**TSP**	**-P**	**NPs**	**TSP**	
Mg	1.0	1.5	1.6	0.7	0.4	0.5	
K	10.0	9.9	6.9	7.1	4.9	5.1	mg/g
Ca	6.5	6.5	6.8	0.7	0.9	0.8	
Mn	18.5	12.7	12.5	42.3	25.6	18.9	
Cu	2.7	2.9	2.9	6.2	5.9	5.0	µg/g
Zn	28.1	20.6	24.4	30.3	39.9	48.9	